

51  
12T

SYNCHRONIZATION OF OSCILLATORS  
BY INTERRUPTED WAVE TRAINS

A THESIS

Presented to  
the Faculty of the Graduate Division

by

Donald Woodrow Fraser

In Partial Fulfillment  
of the Requirements for the Degree  
Doctor of Philosophy  
in the School of Electrical Engineering

Georgia Institute of Technology

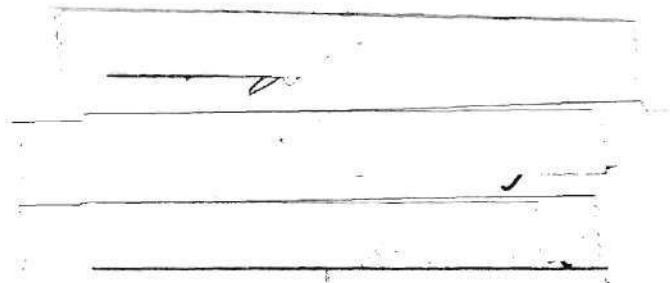
June 1955

100-100000  
427  
1-15-55



SYNCHRONIZATION OF OSCILLATORS  
BY INTERRUPTED WAVE TRAINS

Approved:

A handwritten signature is written on the first of four horizontal lines. The signature appears to be 'W. J. ...'.

Date Approved by Chairman: May 27, 1928

## A C K N O W L E D G E M E N T

I wish to express my appreciation first to the members of my family for their patience during the time the work was in progress. I should also like to thank Dr. B. J. Dasher for his suggestions and encouragement.

## TABLE OF CONTENTS

	Page
Acknowledgment . . . . .	ii
List of Tables . . . . .	v
List of Illustrations . . . . .	vi
List of Symbols . . . . .	viii
Summary . . . . .	xi
Chapter	
I. Introduction	
Synchronization of Oscillators . . . . .	1
The Problem . . . . .	3
Summary of Succeeding Chapters . . . . .	7
II. Synchronization of Oscillators by C-W Signals	
Development of Theory for Vacuum-Tube Oscillators . . . . .	9
Simplified Theories of Synchronization by C-W Signals . . . . .	18
Solutions of the Nonlinear Differential Equation of Synchronization . . . . .	23
III. Transients in Periodic Modulation and Related Topics	
Experimental Observations as Related to the Problem. . . . .	27
General Forms of Fourier Series . . . . .	41
The Complex Fourier Series in Phase Modulation . . . . .	43
Trigonometric Fourier Series in Phase Modulation . . . . .	48
Spectrum of Wave Train Modulated with Rectangular Pulse . . . . .	49
IV. Mechanism of Synchronization with Interrupted Wave Trains	
Phase Requirements in Synchronization . . . . .	53
Summary of the Chapter . . . . .	74



V. Frequency Spectrum of Synchronized Oscillator	
Phase Deviations in Disturbed Oscillator . . . . .	75
Spectrum of Rectangular Pulse F-M Wave . . . . .	81
Simultaneous Phase and Amplitude Modulation . . . . .	93
VI. Synchronization by Sidebands of Interrupted Wave Trains	
Physical Viewpoint of Sideband Synchronization . . . . .	101
Phase Deviations Occurring During Synchronization by Sidebands . . . . .	107
Frequency Spectrum of Oscillator Synchronized by Sidebands of Injected Signals . . . . .	120
VII. Experimental Procedures and Applications of the Synchronized Oscillator	
Details of Experimental Equipment . . . . .	128
Methods of Increasing the Range of Synchronization . . . . .	131
Applications of the Synchronized Oscillator . . . . .	133
Bibliography . . . . .	137
Vita . . . . .	138

## LIST OF TABLES

Table	Page
1. Width of Band of Synchronization Due to First Sideband of Interrupted Wave Train	115

## LIST OF ILLUSTRATIONS

Fig.	Page
1. Voltage Due to Shock-Excited Crystal at High-Order Overtone . .	5
2. Equipment Arrangement for Preliminary Tests of Synchronization by Interrupted Wave Trains . . . . .	5
3. Diagram of a Feedback Oscillator . . . . .	12
4. Negative Resistance Oscillator . . . . .	12
5. Voltage Relationships in a Disturbed Oscillator . . . . .	22
6. Synchronization Frequency Bands . . . . .	22
7. Block Diagram of Arrangement for Synchronization by Interrupted Wave Trains . . . . .	30
8. Interrupted Wave Train as Synchronizing Source . . . . .	30
9. Lissajou Patterns Illustrating Phase Modulation in Oscillator .	33
10. Variation of Individual Cycles of Oscillator . . . . .	35
11. Synchronizing Pattern of Interrupted Wave Train . . . . .	47
12. Phase and Frequency Deviations in Square-Wave FM . . . . .	47
13. Spectrum Behavior of Square-Wave FM . . . . .	47
14. Spectrum of a Rectangular Pulse . . . . .	52
15. Spectrum of Sine Wave Modulated by Rectangular Pulse . . . . .	52
16. Vector Triangle of Voltages . . . . .	53
17. Phase Deviations in the Synchronized Oscillator . . . . .	65
18. Modulation Frequencies Required for Synchronization . . . . .	71
19. Modulation Frequencies and Bands of Synchronization When Signal is Modulated With Square Wave . . . . .	72
20. Modulation Indices of Phase-Modulated Oscillator Voltage . . .	78

Fig.	Page
21. Interrupted Wave-Train Synchronizing Signal . . . . .	82
22. Phase and Frequency of Rectangular-Pulse FM Wave . . . . .	82
23. Frequency Spectra of Rectangular-Pulse FM Wave . . . . .	86
24. Phase Deviations of an Oscillator Synchronized by Square-Wave Modulated Wave Train . . . . .	88
25. Spectra of Oscillator with Phase Deviation of Figure 24 . . . . .	91
26. Frequency Spectra of Oscillators Synchronized by Square-Wave Interrupted Synchronized Signal . . . . .	92
27. Vector Triangles of Oscillator Voltage Illustrating Amplitude Modulation . . . . .	97
28. Forms of Oscillator Voltage Illustrating Amplitude Modulations .	97
29. Upper Half of Envelope of Voltage Synchronized Oscillator . . . .	97
30. Angular Frequencies Involved in Synchronization by First Upper Sideband . . . . .	104
31. Vector Diagram of Oscillator Voltages . . . . .	104
32. Phase Deviations of Disturbed Oscillator with Respect to Input of Angular Frequency $\omega_1$ . . . . .	111
33. Angular Frequencies Involved in Synchronization by First Side- band . . . . .	111
34. Bandwidth of Synchronization by First Sideband of Square-Wave Interrupted Wave Train . . . . .	115
35. Phase Deviations in Oscillator Synchronized by Sidebands of Injected Signal . . . . .	122
36. Spectra of Oscillator Synchronized by Sidebands of Interrupted Wave Train, Computed Values . . . . .	126
37. Spectra of Oscillator Synchronized by Sidebands, Experimental Values . . . . .	127
38. Circuit of Oscillator Used in Basic Experiments . . . . .	131
39. Spectrum of Wave Producing Desired Frequency Components . . . . .	131

## LIST OF SYMBOLS

Symbol	Definition
$a_n, b_n, c_n, d_n, A_n, B_n$	Coefficients of Fourier series.
$\beta$	A simplifying substitution in integral equations.
$e, E$	E.M.F.
$\varepsilon$	A constant of small magnitude.
$F(V)$	A function of voltage.
$\gamma$	A phase angle.
$k$ (also $x$ )	Duty cycle of interrupted wave train, ratio of duration of signal to period of modulating voltage.
$K$	A ratio of frequencies, $K = \omega_s / \omega_c$ .
$\lambda$	A coefficient, a Lagrange multiplier.
$m$	Modulation index = $\Delta\omega / \omega_m = \omega_s / \omega_m$ .
$m_1, m_2$	Slopes of phase deviation curves.
$\mu$	A generalized variable representing voltage, current, or frequency as applicable.
$n, N$	An integer (1, 2, 3, 4, .....)
$\phi$	In an oscillator, the angle between grid voltage and feedback voltage.
$\phi(t, t_0)$	A function of $t$ and $t_0$ .
$Q$	Quality factor.
$R_n$	A negative resistance.
$\theta$	In a synchronized oscillator, the angle between grid voltage and synchronizing voltage.
$\theta_0$	The terminal angle in a synchronized oscillator.



Symbol	Definition
$\Sigma$	Summation
$S(t)$	Phase deviations as a time function.
$\tau, t$	Time
$T$	A modulation period, $T = \frac{2\pi}{\omega_m}$
$V_L$	Magnitude of synchronizing voltage.
$V_g$	Magnitude of grid voltage.
$V_R$	Magnitude of feedback voltage.
$\omega$	Angular frequency, $\omega = 2\pi f$ .
$\omega_L$	Angular frequency of synchronizing voltage, $\omega_L = 2\pi f_L$ .
$\omega_o$	Angular frequency of free-running oscillator, $\omega = 2\pi f_o$ .
$\omega_s$	$\omega_s = \omega_L - \omega_o$ .
$\omega_c$	Half-width of band of synchronization due to c-w signal.
$\omega_m$	Angular frequency of modulation, $\omega_m = 2\pi f_m$ .
$\omega_{lsb}$	Half-width of band of synchronization due to first sideband of input.

## S U M M A R Y

## S U M M A R Y

The phenomenon of synchronization is well known and is demonstrated in many familiar devices. The mechanism of synchronization of vacuum-tube oscillators by c-w signals or by periodically repeated pulses has been the subject of numerous papers in the literature and several authors have arrived at substantially identical conclusions by diverse methods of analysis. Both analytical and graphical solutions have been presented and both methods are in general use in present studies of nonlinear oscillatory systems.

A form of synchronizing input which has not been discussed in available literature consists of a signal which is modulated in some periodic manner so that a voltage of significant amplitude is present during a portion of the modulation period. During the remainder of the modulation period the amplitude of this signal is assumed to be zero. Such a signal is designated as an interrupted wave train and is the subject of the study to which this paper is devoted.

Experimental tests demonstrate that when an interrupted wave train is employed as a synchronizing signal the frequency of the oscillator may be made equal to the frequency of the input signal if the latter is restricted to a narrow band centered about the natural frequency of the oscillator. This band corresponds in sense, to the "locking band" exhibited in the presence of a c-w signal but has significant differences. First, it is narrower than the corresponding band of c-w synchronized oscillators, second, it involves the presence of phase modulation, and third, it may exist around each frequency in the frequency spectrum of the input signal.



The mechanism of synchronization has been described analytically in this paper by employing a simple physical criterion for synchronization which states that, if two signals are to be of equal frequency, the net relative phase deviation must be zero if many cycles are considered. The interval of time within which this criterion has been applied is the modulation period since both experimental and analytical data indicate that the criterion of zero net phase deviation is satisfied during each modulation period when synchronization persists. If the synchronizing signal has some other frequency appearing in the spectrum of the input, this frequency must be  $f_1 \pm nf_m$  where  $f_1$  is the frequency of the input,  $f_m$  is the modulating frequency, and  $n$  is an integer. In this case the criterion of synchronization differs in that the net phase deviation must be  $2n\pi$ , where  $n$  is the order of the sideband involved.

The analysis proceeds by utilizing a known nonlinear differential equation which describe the transient behavior of the oscillator during presence of synchronizing signal. By integrating the phase variations over a complete modulation cycle there are developed transcendental equations which describe the action of the phase angle during the period. By methods of maximization it is possible to determine the limits of synchronization both by the fundamental component and by sidebands of the interrupted wave train.

Numerous curves and graphs illustrate the conditions required for synchronization and illustrate the frequency spectra appearing in the output of the oscillator. The output has been analyzed from a standpoint of phase modulation by both analytical and numerical methods

of Fourier analysis. Experimental and computed data are presented and are shown to be substantially identical. The effect of amplitude modulation resulting from the changing input signal has also been evaluated. Finally, methods of extending the range of synchronization are discussed in conjunction with suggested methods of utilizing this form of synchronized oscillator in practical applications.

## CHAPTER I

### INTRODUCTION

#### Synchronization of Oscillators

The phenomenon of synchronization is well known and the effects of a synchronizing action are observed in many familiar electrical and mechanical systems. Examples are found in pendulums which swing in unison on a common support, in dual aircraft engines which rotate in synchronized precision, and in television receivers which display stabilized video patterns. Each of these actions illustrates a form of synchronization and each points out a known or possible application of the phenomenon.

Vacuum-tube oscillators are probably the most common and numerous of the devices which employ a synchronizing process and oscillators thus controlled are utilized in a variety of equipment. The oscillators themselves differ widely in form and in type but the synchronizing action in each is usually produced by one of two types of applied signals. The first of these types appears as a series of equidistant pulses, a form of synchronizing signal which has been successfully employed in television, radar, and similar devices. The second type appears as a sinusoidal voltage which is continuous in time and constant in amplitude. This form of signal has been found adequate in many applications, and is illustrated in the synchronized oscillators which serve as amplifiers and limiters in some models of F-M receivers.

Both of these types of synchronizing signals and the methods by which they perform the synchronizing function have been studied by many individuals. Particular attention has been devoted to the second of the two types and an extensive literature appears on the subject of synchronization of oscillators by sinusoidal voltages. Several papers which are devoted to the analysis of the mechanism of synchronization by continuous waves are important in the discussion that follows in succeeding chapters and are referred to when appropriate.

It is repeated, for emphasis, that the usual synchronizing signal applied to a vacuum-tube oscillator is either in the form of equidistant pulses or of continuous sinusoidal voltages. However, although these two types do comprise the principal source of synchronizing signals, there does exist a separate and quite different form of voltage which can also satisfactorily perform the function of synchronization. This newly designated type may be unique in its application to the present study, since it is neither employed in known equipment nor discussed in available literature, but it is believed to be of significant practical value. This signal is designated as an "interrupted wave train" but its exact form is not simply defined. A detailed description of its form and the parameters involved in defining its properties belongs properly with a discussion of the action that it performs. The next section of this paper defines the problem associated with application of the signal to an oscillator and illustrates the form of voltage wave involved.



### The Problem

The subject of this study was suggested by an earlier investigation of piezoelectric quartz crystals. In the course of an experiment to determine the high-frequency response of such crystals it was observed that a shock-excited crystal could produce a short burst of sinusoidal voltage of very high frequency. A numerical example best illustrates both the experiment and the observed results.

The experimental procedure involved a "swept-frequency" technique of exciting the piezoelectric crystal. In one particular case a crystal whose fundamental frequency was 5.000 mc was subjected to a frequency-modulated voltage whose center frequency was 315 mc. This exciting voltage was "swept" at a 60-cycle rate over a narrow (314-316 mc) band and was applied, by one of various techniques, to the crystal. It was then observed that when this driving voltage passed through the center frequency of 315 mc the quartz crystal was excited at the 63rd mechanical overtone of its 5.000-mc fundamental frequency. The mechanical oscillations of the excited crystal, converted into electrical impulses at the holder terminals, produced a short burst of r-f energy whose frequency was that of the vibrations in the crystals. The form of output, derived from an observed envelope and a measured frequency, is illustrated in Figure 1. The crystal was excited twice during each period of the 60-cycle "sweep", hence the envelope was repeated each 1/120th of a second. The actual width of the envelope was never measured but was, in each case, a small fraction of the spacing between envelopes.

The important aspect of this signal was that the cycles of r-f voltage, occurring with a frequency determined by properties of the

piezoelectric crystal, might be assumed to have the excellent frequency stability usually associated with quartz crystal resonators. However, inasmuch as the signal occurred only in the form of a periodically repeated damped oscillation, no practical application was immediately evident. Later, further consideration of the potentialities of stable high-frequency voltages suggested the possibility that this signal, although not continuous in time, might be utilized as a synchronizing agent. If these voltages could be applied to a free-running oscillator whose center frequency was 315 mc and if synchronization could be effected, then direct crystal control of the oscillator would have been achieved. Inasmuch as most methods of direct crystal control are limited to frequencies much lower than 300 mc the possibility of employing a synchronizing process at or above 315 mc was considered worthy of further study.

If synchronization of an oscillator by the signal shown in Figure 1 was to be attempted, it was important first to conduct a thorough investigation of the more fundamental aspects of the method of synchronization. It was therefore decided to employ a signal of the same general form but to work at much lower frequencies and under carefully controlled conditions. This plan was implemented by the construction of a low-frequency oscillator as a test vehicle and by the utilization of signal generators and gating circuits to produce synthetically the synchronizing signal. The arrangement shown in Figure 2 was completed. This figure shows the basic units employed and the form of signal which was injected, as a possible synchronizing agent, into a free-running oscillator.

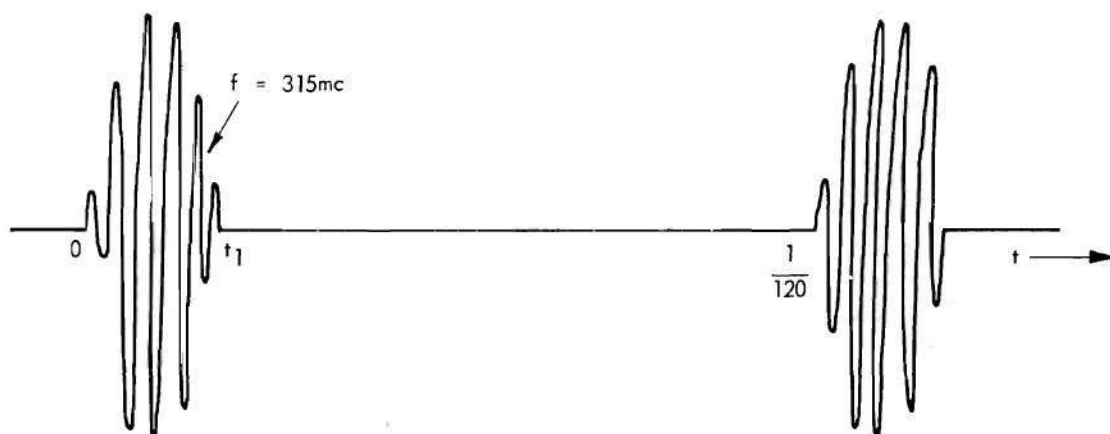


FIGURE 1. VOLTAGE DUE TO SHOCK-EXCITED CRYSTAL AT HIGH-ORDER OVERTONE.

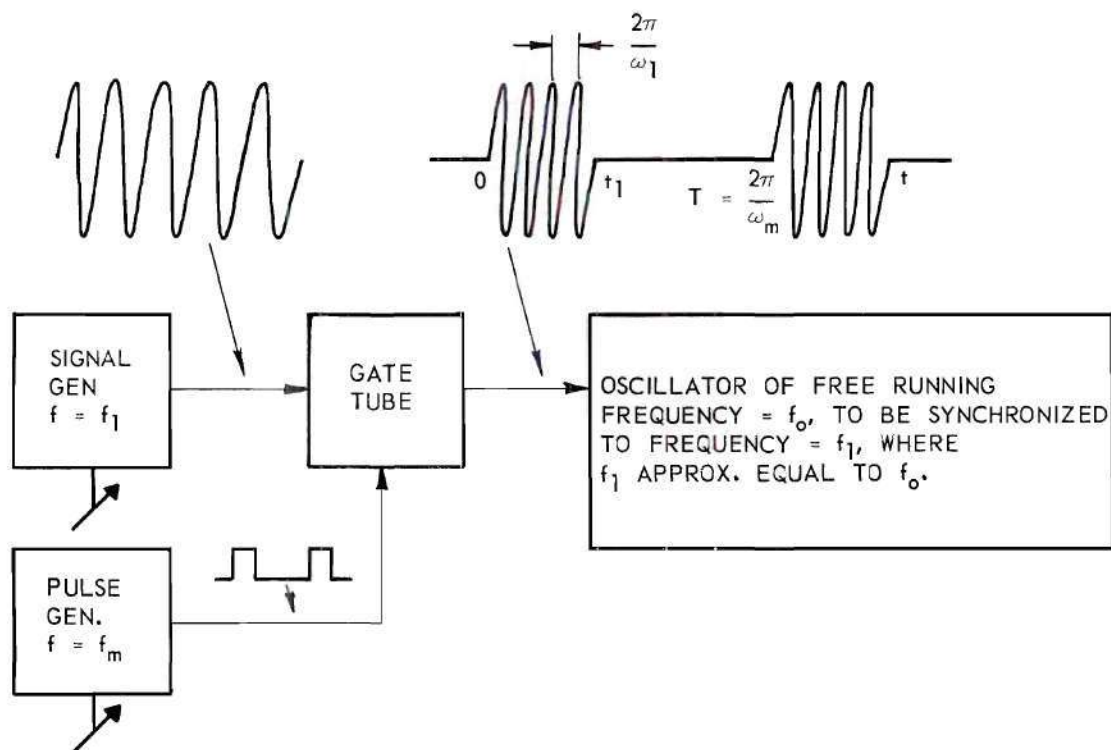


FIGURE 2. EQUIPMENT ARRANGEMENT FOR PRELIMINARY TESTS OF SYNCHRONIZATION BY INTERRUPTED WAVE TRAINS.



The output of the pulse generator shown in Figure 2 was variable in frequency and in width of pulse. The output of the signal generator was variable in frequency and in amplitude. This combination input signals to the gating circuit permitted the synthesis of a signal which was variable in basic frequency, in modulation (gating) frequency, and in duty cycle (ratio of  $t_1$  to  $T$ ). Representative numbers employed in the basic test were approximately as follows:  $f_0 = 20,000$  cps,  $f_1 = 20,200$  cps,  $f_m = 700$  cps, and duty cycle =  $1/2$ .

The results of the preliminary tests were encouraging. It was demonstrated conclusively, by the use of frequency counters, that the average frequency of the oscillator became identically equal to that of the input frequency  $f_1$  if the latter frequency remained near (but not necessarily equal to) the free-running frequency  $f_0$ . Therefore it was evident that some form of synchronizing action was present, but the mechanism by which synchronization was effected was not obvious. Further questions as to the nature of the action and the characteristics of the synchronized oscillator were raised when further studies revealed the presence of phase-modulation in the output signal.

The necessary scope of the investigation was indicated by the observations made and the data recorded in these early tests. The problem could now be defined with some completeness. It was evident that the following items, at least, required analysis:

(a) a description of the mechanism by which synchronization could be effected by an interrupted wave train,



(b) derivation of the relationships between the parameters of oscillator and synchronizing signal by which to specify the action expected to result from any given combination of parameters, and

(c) determination of the expected form of output signal derived from the synchronized oscillator.

These three items have constituted the essential problem which the investigation has sought to solve, although other considerations have arisen during the course of the study. Included are topics such as consideration of the most practical means of producing the desired synchronizing signal, determination of effects of amplitude modulation in the output signal, and investigation of means of most adequately utilizing the synchronization phenomenon. Each of these latter topics is mentioned at appropriate places in the paper, but is given minor emphasis. Primary emphasis has been directed toward an adequate discussion of the three basic topics. The manner of analysis of these topics is summarized in the next section.

#### Summary of Succeeding Chapters

The main body of this paper is preceded by two chapters whose purpose is to assemble for convenient reference several known and accepted principles which can be utilized as tools in the analysis of the synchronization phenomenon. Chapter II deals with the synchronization of oscillators by continuous waves and also includes a brief summary of, or reference to, appropriate papers from the literature. This summary is not necessarily for the purpose of providing more tools for solution of the present problem. It is included as a means of illustrating the

many and diverse methods of analysis of the process of synchronization. It also provides a convenient collection of references for the reader who is interested in examining the phenomenon more closely.

Chapter III describes some of the experimental results obtained during the course of the investigation and then develops, in brief form, several formulas and equations which are used in later chapters. General forms of Fourier series and the application of Fourier series to phase modulation are included inasmuch as these will be found to be primary tools useful in describing the output of the synchronized oscillator. The spectrum of a wave train which has been modulated by a rectangular pulse is analyzed and the results of the analysis are included. This form of spectrum is also found to be significant to the problem.

Chapters IV, V, and VI deal directly with the specific items of the problem and develop equations, curves, and spectra which explain the synchronizing action and predict the effect of a given form of input. These curves and diagrams are the primary result of the study and form definitive answers to the three specific items listed as primary topics.

Finally, Chapter VII records the experimental equipment used in various phases of the investigation and describes those experimental procedures not previously discussed. The chapter also includes comments upon methods of obtaining the desired synchronizing signals and describes means of utilizing these signals in practical and useful equipment.

## CHAPTER II

### SYNCHRONIZATION OF OSCILLATORS BY C-W SIGNALS

#### Development of Theory for Vacuum-Tube Oscillators

Important contributions to the nonlinear theory of oscillations have been made by van der Pol<sup>(1)</sup>. He pioneered in analytical studies of non-linear oscillatory systems and a nonlinear differential equation, now generally referred to as van der Pol's equation, appears in a variety of forms. It may be written as

$$\frac{d^2\mu}{dt^2} - \mathcal{E}(1 - \mu^2) \frac{d\mu}{dt} + \mu = 0 \quad (1)$$

where  $\mu$  is a generalized variable applicable to the particular characteristic under study. This equation is a fundamental one and describes a variety of systems but it is conveniently derived in the analysis of vacuum tube oscillators. In electrical systems the symbol  $\mu$  may be taken to represent either voltage or current.

Numerous methods of solution for this equation have been advanced. Van der Pol himself offered two independent solutions. These are often referred to as the method of variation of parameters and the method of equivalent linearization. Each of these methods will be described in brief detail.

The method of variation of parameters involves the separation of the second-order differential equation into two distinct first-order



differential equations, one which determines the amplitude and the other the frequency of oscillation. The analysis is begun by assuming that the voltage across the tuned circuit of an oscillator of the type shown in Figure 3, or of an oscillator of similar type, may be described as

$$v = A(t) \cos \omega_0 t \quad (2)$$

where  $A(t)$  represents an amplitude that varies slowly with time. The assumption that the time variation of the amplitude is small will be valid if the middle term of equation (1) is itself small and the equation is thereby constrained to be nearly linear. A restriction which insures near linearity of the differential equation is important in the analysis for it limits the study to systems which produce harmonic oscillations. The required restriction is, evidently

$$\epsilon \ll 1. \quad (3)$$

The analysis continues by differentiation of equation (2) and substitution of the first and second derivatives of the variable into equation (1). Details of the individual steps thenceforth, which are quite lengthy, appear in van der Pol's original paper<sup>(1)</sup> and are summarized by Edson<sup>(2)</sup>. The solution involves an assumption that the anode current of the vacuum tube may be approximately expressed in a cubic relationship to the voltage. This relationship is expressed in the equation

$$i = F(v) = -av + bv^3. \quad (4)$$

In this case the approximate solution of equation (1) may be expressed in terms of the coefficients a and b and in terms of the resistance

shunted across the tuned circuit. The expression for the final peak amplitude of voltage across the circuit is given as

$$V = \sqrt{\frac{a - \frac{1}{R}}{\frac{3}{4}b}} \quad (5)$$

and the final angular frequency of oscillation is given, to a first approximation, as

$$\omega_o = \sqrt{\frac{1}{LC}}. \quad (6)$$

These are the solutions obtained by the method of variation of parameters. The method of equivalent linearization leads to identical solutions. The basic method in the idea concerns the substitution, under certain prescribed conditions, of a linear resistance for a nonlinear resistance. Many oscillators may be considered as circuits containing at least one negative resistance. From this point of view Figure 3 may be replaced by the circuit of Figure 4. In the latter figure the negative resistance characteristics of the oscillator are contained with the element  $R_n$ .

The current which flows in the nonlinear resistance is subjected to a sinusoidal voltage and may be resolved into a fundamental component and its harmonics. The fundamental component of current is in phase with the voltage and has a magnitude which depends upon the voltage. In terms of the fundamental frequency, the nonlinear resistance may be replaced by a linear resistance if the magnitude is properly chosen.

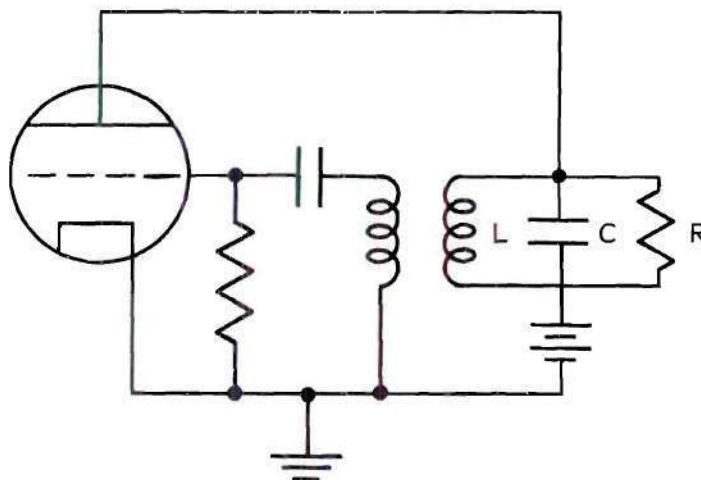


FIGURE 3. DIAGRAM OF A FEEDBACK OSCILLATOR.

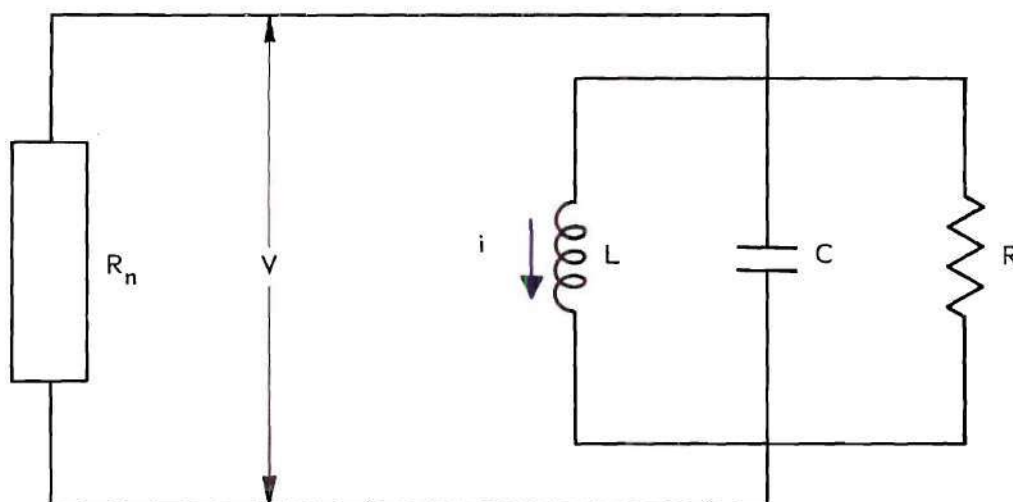


FIGURE 4. NEGATIVE RESISTANCE OSCILLATOR.

The method is illustrated by assuming that the final voltage across the tuned circuit is given by

$$v = V \sin \omega t. \quad (7)$$

If the quantity  $V \sin \omega t$  is substituted in each term on the right side of equation (4) and if the fundamental terms only are retained, the current is given as

$$i = aV + 3/4bV^3 = V(-a + 3/4bV^2). \quad (8)$$

Evidently the current is equivalent to that which would exist if the voltage  $V$  were applied to an equivalent resistance  $R_n$  whose magnitude is expressed in the equation

$$\frac{1}{R_n} = -a + 3/4bV^2. \quad (9)$$

The conditions for steady state oscillations in the circuit of Figure 4 require that the total susceptance between the terminals of the network shall be zero and that the circuit shall be lossless. These requirements are satisfied if

$$\frac{1}{R_n} + \frac{1}{R} = 0, \text{ and } \frac{1}{j\omega L} + j\omega C = 0. \quad (10)$$

When these equations are solved for the frequency and amplitude of free oscillations, with the aid of equation (9), there results

$$\omega = \sqrt{\frac{1}{LC}} \quad (11)$$

and

$$V = \sqrt{\frac{a - \frac{1}{R}}{3/4 b}}, \quad (12)$$

solutions which are identical to those obtained by the method of variation of parameters.

The two methods described provide solutions which are only approximate since certain simplifying solutions were required in order to reduce the original differential equation to a form permitting direct solution. It is possible to more closely approximate an exact solution by graphical means if the exact form of the voltage-current characteristics of the vacuum tube are known. In recent years considerable attention has been devoted to several methods of graphical solution of various nonlinear differential equations. These graphical methods have the merit of presenting a pictorial representation of the solution to the equation under study but are often tedious and exacting if accurate detail is desired. A graphical method of solution of van der Pol's equation was originated by Liénard<sup>(3)</sup>. His method is described in lucid form by le Corbeiller<sup>(4)</sup>. The basic method is briefly outlined here.

A second-order differential equation may be converted into a first-order equation by a change of variable. For example, consider Figure 4. Equations describing the currents and voltages in the circuit may be written as

$$i + \frac{V}{R} + C \frac{dV}{dt} + F(V) = 0, \quad (13)$$

and

$$V = L \cdot \frac{di}{dt} \quad (14)$$



where  $F(V)$  represents the current through the equivalent resistance  $R_n$ .

If the substitution

$$f(V) = \frac{V}{R} + F(V) \quad (15)$$

is made and the time variable is eliminated by the relationship

$$\frac{dV}{dt} = \frac{dV}{di} \cdot \frac{di}{dt} = \frac{V}{L} \cdot \frac{dV}{di} \quad (16)$$

one may write

$$i + f(V) + \frac{C}{L} V \cdot \frac{dV}{di} = 0, \quad (17)$$

whence

$$\frac{di}{dV} = - \frac{C}{L} \cdot \frac{V}{i + f(V)} \quad (18)$$

In equation (18) the slope of the curve relating  $i$  and  $V$  is stated in terms of those same variables. By calculating the slope at succeeding points it is possible to sketch the solution curve with considerable accuracy. This process is often called the method of isoclines.

A number of other graphical methods of solution appear in the literature. A unique and powerful, but tedious, method is described by Hsia<sup>(5)</sup>. The process in this case involves a combination of summations and of finite differences to replace a combination of integrals and derivatives. If the second-order nonlinear equation

$$\frac{d^2x}{dt^2} + f(x) \cdot \frac{dx}{dt} + g(x) = h(t) \quad (19)$$

is integrated once there is obtained

$$\frac{dx}{dt} + F(x) + \int_0^t g(x) dt = H(t) + K, \quad (20)$$

where

$$F(x) = \int_0^x f(x) dx, \quad H(t) = \int_0^t h(t) dt.$$

Letting  $\Delta x$  be the increment of  $x(t)$  for a small time interval  $\Delta t$  and with  $x_n$  the value of  $x$  at  $t = n\Delta t$  one may write for the instant  $n\Delta t$

$$\frac{dx}{dt} = \frac{x_n - x_{n-1}}{\Delta t} = \frac{\Delta x_n}{\Delta t} \quad (21)$$

and

$$\int_0^t g(x) dt - K = S_n(t). \quad (22)$$

The use of equations (21) and (22) and the substitution

$$\alpha = \tan^{-1} \frac{1}{\Delta t} \quad (23)$$

permits one to write equation (20) for a particular small increment of time, as

$$\Delta x_n \tan \alpha + F(x_n) + S_n(t) = H(n\Delta T) \quad (24)$$

a form which can be conveniently displayed piecemeal by graphical processes. A solution of van der Pol's equation can be readily determined

but if considerable accuracy is desired a large number of small increments must be utilized and thereby contribute to the tedious detail.

The remaining references to be cited, and these without description, refer to a graphical method of solution of nonlinear equations designated as the phase-plane process. The basically similar methods have been lucidly described by Boland<sup>(6)</sup> and by Ku<sup>(7)</sup>. Each entails the conversion of the second-order nonlinear differential equation into a first-order equation relating velocity and displacement, given as

$$\frac{dV}{dx} = \frac{F(t) + G(v, x)}{v}, \quad (25)$$

and relating the solution to the slope of the curve involved.

This brief outline of various methods of treating van der Pol's equation indicates the difficulty involved in obtaining a solution. It has, therefore, been usually considered appropriate by many authors to discuss the behavior of the oscillator from a physical standpoint without primarily laying stress on mathematical rigor. In this way it is possible to make certain simplifying assumptions which permit more of a direct solution to the basic equation describing the oscillatory condition. A justification of the assumptions made may then be obtained by experimental means. The next two sections of this paper include several simplified theories which apply to an oscillator which is subjected to a forcing function and which as a result may achieve a steady-state frequency and amplitude different from that of its natural or free-running condition. Under prescribed conditions the frequency of the oscillator may become equal to that of the forcing function. This condition, usually

designated as that of synchronization, is of primary interest in this paper and will serve as the basis of the following discussion.

### Simplified Theories of Synchronization of Oscillators by C-W Signals

If to the feedback oscillator of Figure 3 there is added a voltage  $E = P_0 \sin \omega_1 t$  in the grid circuit the differential equation of the circuit is essentially identical to equation (1) except that the new voltage appears as an added term. Van der Pol offered a method of solution of this equation which is quite similar to that of the method of variation of parameters employed with the free-running case.

The essential step in van der Pol's procedure consists in taking for the voltage  $v(t)$  a solution of the form

$$v(t) = b_1(t) \sin \omega_1 t + b_2(t) \cos \omega_1 t \quad (26)$$

in which the functions  $b_1(t)$  are assumed to be "slowly" varying functions of time, or, in other words, that the motion is essentially an oscillation with the frequency  $\omega_1$  of excitation but with slowly varying amplitude and phase. The latter assumption is to be interpreted that the first and second-order derivatives of  $b_1(t)$  and  $b_2(t)$  are themselves very small.

If equation (26) is differentiated twice there result two equations, the first containing  $b_1, b_2$ , and their first derivatives, the second containing their second derivatives in addition. In actual solutions the second-order derivatives are neglected but the presence of the basic quantities and their first derivatives permits the separation of the original second-order differential equation into two first-order equations.



These two equations form the basis of extended discussions of the amplitude and stability of the oscillations. The details are too numerous to describe here but a very complete discussion can be found in Stoker's text on nonlinear vibrations<sup>(8)</sup>. The significant results are displayed in the form of a family of response curves which are plotted against the "detuning", the frequency difference between that of the forcing function and of the free-running oscillator, and which employ the amplitude of the forcing function as a parameter. The resulting amplitude of oscillation and the regions of stable and unstable oscillations are illustrated in a series of figures presented by Stoker.

The results of purely analytical studies of basic nonlinear equations are less simple to apply than are the conclusions reached by other authors who have employed a more physical line of reasoning. As an example one may consider a very important paper which is ascribed to Adler<sup>(9)</sup>. He has studied the voltages and currents in an oscillator which is subjected to a synchronizing voltage and by a method of direct reasoning has obtained a fundamental differential equation which relates the relative phase of anode voltage, grid voltage, and externally injected voltage. His results have been widely utilized as a basis for more extended analysis. His method may be most easily understood by reference to Figure 5.

Figure 5 illustrates a tuned-plate oscillator, although the analysis is equally applicable to other varieties of harmonic oscillators. In the vector triangle shown the grid voltage is evidently the sum of the injected voltage  $V_1$  and the feedback voltage  $V_R$ . The phase angle  $\phi$

between  $V_R$  and  $V_g$  is a function of the resonant frequency and figure of merit of the tuned circuit and of the frequency of the forcing signal. It is known that in a simple tuned circuit, for small deviations of frequency,

$$\phi \doteq \frac{2Q}{\omega_0} (\omega - \omega_0). \quad (27)$$

It is also evident from Figure 5B that, for small  $\phi$

$$\phi \doteq \tan^{-1} \frac{V_1 \sin \theta}{V_g} \doteq \frac{V_1 \sin \theta}{V_g}, \quad (28)$$

and if equations (27) and (28) are combined, there is obtained

$$\omega - \omega_0 = \frac{\omega_0}{2Q} \cdot \frac{V_1}{V_g} \sin \theta. \quad (29)$$

It is further evident from the same figure that if  $\frac{d\theta}{dt}$  is non-zero a frequency transient exists. In this case the frequency  $\omega$  differs from the injected frequency  $\omega_1$  by the relationship

$$\omega_1 - \omega = \frac{d\theta}{dt}, \quad (30)$$

which may be rewritten as

$$(\omega_1 - \omega_0) - (\omega - \omega_0) = \frac{d\theta}{dt}. \quad (31)$$

Now if the expression for  $(\omega - \omega_0)$  from equation (29) is substituted into equation (31) there is obtained the very important non-linear differential equation

$$\frac{d\theta}{dt} = (\omega_1 - \omega_o) - \frac{\omega_o V_1}{2Q V_g} \sin \theta. \quad (32)$$

It is convenient to write this as

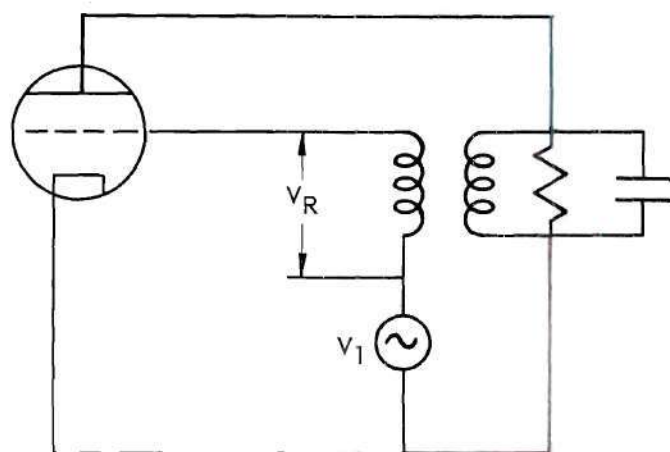
$$\frac{d\theta}{dt} = \omega_s - \omega_c \sin \theta, \quad (33)$$

where evidently,  $\omega_s = \omega_1 - \omega_o$  and represents the difference between the injected and free-running angular frequencies, and  $\omega_c = \frac{\omega_o V_1}{2Q V_g}$ , which will be shown to be equal to one-half the band of synchronization.

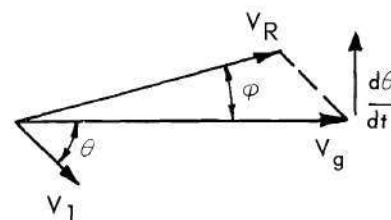
The symbols  $\omega_s$  and  $\omega_c$  will be widely used throughout this paper. They may be represented as regions of a frequency spectrum in Figure 6. Their significance is illustrated.

The injected angular frequency  $\omega_1$  falls at point (B) of Figure 6 and differs from the free-running frequency by the quantity  $\omega_s$ . Point B might equally well fall between points A and D without changing the physical conditions. Solutions of Adler's equation (32), to be discussed in some detail in later paragraphs, show that the angle  $\theta$  progresses monotonically to some final and constant value  $\theta_o$  when the input is a c-w signal and  $\omega_1$  falls within the limits C to D.

An introduction to the concept of the synchronizing phenomenon can hardly be completed without the mention of two more important papers which seek to explain the action. The first is by Huntoon and Weiss<sup>(10)</sup> and the second by van Slooten<sup>(11)</sup>. Their papers approach the problem from widely divergent standpoints but arrive at the same conclusion as was attained by Adler. The analysis due to Huntoon and Weiss makes use of



(A)



(B)

FIGURE 5. VOLTAGE RELATIONSHIPS IN A DISTURBED OSCILLATOR.

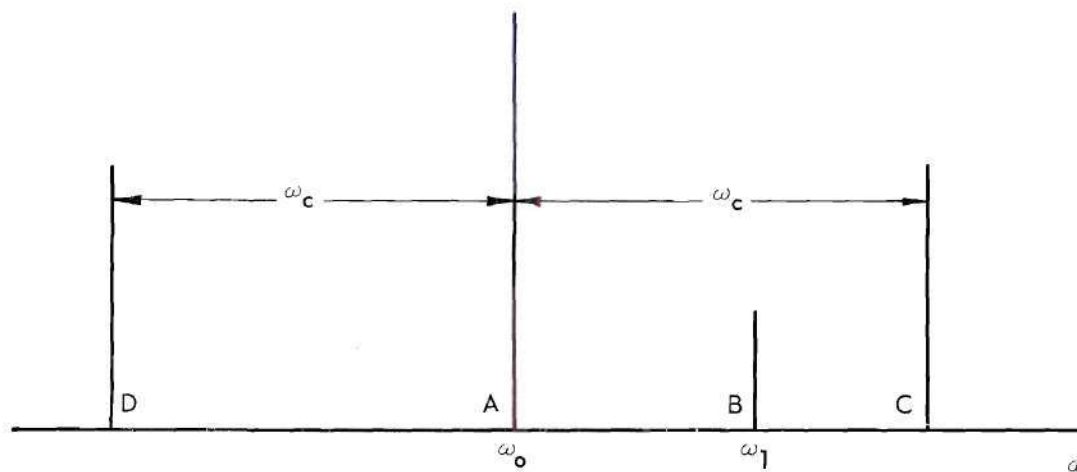


FIGURE 6. SYNCHRONIZATION FREQUENCY BANDS.



a fictitious series impedance in the feedback circuit of the oscillator with the injected synchronizing signal then expressed as equivalent to an  $I_Z$  drop in the fictitious impedance. By defining a complex set of compliance coefficients the authors obtain a differential equation which is very similar to that of Adler and the solution of which defines the transient change of phase of  $\theta$  in precisely the same form, if certain simplifying assumptions are made.

Van Slooten describes the mechanism of synchronization in terms of periodic pulses of current which are injected into the tuned circuit of an LC oscillator. He determines the phase and amplitude variation resulting as incremental variations, and with these establishes a differential equation relating frequency (a function of the phase shift), voltage, and period of the injected current pulses. This equation again closely resembles that due to Adler, if appropriate analogies are made between currents in the tuned circuit and voltages in the grid circuit. The final important result, however, is that the solution of the equation describes a transient rate of change of phase in a manner essentially identical to that of the solution of Adler's equation and to that of Huntoon and Weiss.

The preceding references have been briefly mentioned to show that the solution of a nonlinear differential equation equivalent to that in equation (32) represents the conclusions common to many authors. This solution will now be described in some detail.

#### Solutions of the Nonlinear Differential Equation of Synchronization.

The nonlinear differential equation was given in most compact

form as

$$\frac{d\theta}{dt} = \omega_s - \omega_c \sin \theta. \quad (32)$$

The condition of synchronization is evidently attained when  $d\theta/dt$  equals zero, at which time

$$\omega_s = \omega_c \sin \theta. \quad (34)$$

The maximum value of  $\omega_s$  occurs when  $\sin \theta = \pm 1$ , at which time  $\theta = \pm 90^\circ$ .

Two important conclusions may be deduced:

(a) The maximum phase angle which can exist between the input voltage  $V_1$  and the oscillator voltage  $V_g$  is  $90^\circ$ , and this condition applied when the frequency of the input signal lies at that point of the band of synchronization most remote from  $\omega_o$ ,

(b) The half-width of the band of synchronization is equal to  $\omega_c$ , which was defined in equation (29) as

$$\omega_c = \frac{\omega_o V_1}{2Q V_g}. \quad (35)$$

The nonlinear equation (32) can be solved by direct integration, using formula 436.00 of Dwight's Table of Integrals<sup>(12)</sup>, with the results expressed in closed form. Jones<sup>(13)</sup> has developed the results in the form

$$\theta = 2 \tan^{-1} \frac{1}{\omega_s} \left[ \omega_c - \sqrt{\omega_c^2 - \omega_s^2} \tanh \frac{1}{2} \sqrt{\omega_c^2 - \omega_s^2} (t + t_o) \right], \quad (36)$$

if  $\omega_s < \omega_c$ . Also, if  $K = \omega_s/\omega_c$ , this can be rewritten as

$$\theta = 2 \tan^{-1} \left[ \frac{1}{K} - \frac{\sqrt{1-K^2}}{K} \tanh \omega_c \frac{\sqrt{1-K^2}}{2} (t + t_0) \right]. \quad (36a)$$

Also, if  $\omega_s > \omega_c$ , the solutions are

$$\theta = 2 \tan^{-1} \frac{1}{\omega_s} \left[ \omega_c + \sqrt{\omega_s^2 - \omega_c^2} \tan \frac{1}{2} \sqrt{\omega_s^2 - \omega_c^2} (t + t_0) \right], \quad (37)$$

or

$$\theta = 2 \tan^{-1} \left[ \frac{1}{K} + \frac{\sqrt{K^2-1}}{K} \tan \frac{1}{2} \omega_c \frac{\sqrt{K^2-1}}{2} (t + t_0) \right]. \quad (37a)$$

These two equations illustrate the important difference between the synchronizing action of a signal which lies inside the band of synchronization ( $\omega_s < \omega_c$ ) and one which lies outside the band, ( $\omega_s > \omega_c$ ). In the first equation, (36), which is applicable to a signal within the band, the phase angle  $\theta$  is seen to be a function of the hyperbolic tangent of  $(t + t_0)$ . Since the quantity  $\tanh (t + t_0)$  is known to approach unity in an asymptotic manner as  $t$  increases without limit, the angle  $\theta$  will approach a final value of  $\theta_0$ , where  $\theta_0$  becomes

$$\theta_0 = 2 \tan^{-1} \frac{\omega_c - \sqrt{\omega_c^2 - \omega_s^2}}{\omega_s} \quad (38)$$

by virtue of equation (36) and the limiting value of  $\tanh (t + t_0)$ .

If the signal lies outside the band the effect upon the phase angle  $\theta$  is described by equation (37). As  $t$  increases the quantity

$\frac{1}{2} \sqrt{\omega_s^2 - \omega_c^2} (t + t_0)$  will pass through  $\frac{\pi}{2}$ ,  $-\frac{3\pi}{2}$ ,  $-\frac{5\pi}{2}$ , etc., and

the tangent of the angle will pass through  $+\infty$ ,  $-\infty$ , etc. At these instants  $\theta/2$  must be  $\frac{\pi}{2}$ , ---  $\frac{3\pi}{2}$ , --- etc. It is evident that within the band of synchronization the phasing action is well-behaved and orderly but that outside the band it can become violent and erratic. Experimenters have found that the frequency spectrum in the latter case may, at its least stable point, be so violent in fluctuation as to defy photography on presently available panoramic display systems.

It is to be emphasized that the preceding analysis has been concerned with the action resulting from a c-w synchronizing signal (or its equivalent in terms of current). It will be demonstrated in succeeding pages that the phasing actions, both the orderly one within the band of synchronization and the fluctuating one outside, may be put to use in a synchronizing action when the input signal is a periodically interrupted c-w wave.



## CHAPTER III

### TRANSIENTS IN PERIODIC MODULATION AND RELATED TOPICS

#### Experimental Observations as Related to the Problem

A large number of problems in applied mathematics and physics have found their origin in the observations of experimenters. If a phenomenon is observed, can be repeated, and is subject to controlled observation then it may be presumed that a relationship between its variables and parameters may be found and expressed in analytical form. Simplifying assumptions must often be made before a working solution can be obtained, and discrepancies between analytical and experimental results arise if the factors neglected in the analysis process are significant. However, it is very often possible to arrive at certain equations or formulas which within certain specified limits of error completely describe the physical process from which the problem originated.

Experimental observations have been utilized extensively in the present study and have provided definite clues to the manner in which the analysis should proceed. It was mentioned in the introduction that the preliminary experiment demonstrated conclusively that a form of synchronization was actually effected, because the average frequency of the oscillator was found to be identically equal to that of the synchronizing signal, if testing and measurement was restricted to a limited region centered at the free-running frequency of the oscillator. It was also mentioned that there was evidence of phase-modulation in the output of



the synchronized oscillator. This last-named effect provided the most important single clue as to the mechanism of synchronization. The manner in which a study of the changing phase angle of the oscillator contributed to a solution of the problem is best understood by a detailed description of a controlled experiment which supplemented that mentioned in the introduction.

In this experiment the response of the oscillator to a c-w synchronizing signal was first obtained. The circuit arrangement of the tuned-plate oscillator shown in Figure 5A was utilized and the phase angle between the input and output voltage was studied by means of Lissajou patterns. In the first portion of the experiment the angular frequency,  $\omega_1$ , of the injected signal was varied slowly and the angle  $\theta$  (as illustrated in Figure 5B) was studied. Synchronization was obtained by adjusting the input frequency until it was very nearly equal to that of the free-running oscillator. In succeeding steps the angular difference between injected and free-running frequencies,  $\omega_s = \omega_1 - \omega_0$ , was increased. The Lissajou pattern which illustrated the magnitude of the phase angle  $\theta$  was of simple form for all frequencies of input which produced synchronization, consisting of a straight line when  $\omega_1$  was equal to  $\omega_0$  and appearing as an ellipse for all other frequencies.

If the response of the tuned circuit of the oscillator is symmetrical about the free-running frequency then it is invariably observed that an open circle ( $\theta = 90^\circ$ ) represents the limiting point of synchronization and that any attempt to increase further the angular frequency difference  $\omega_s$  results in a "break" in the pattern and the appearance of

a rather violent beat-frequency effect in the envelope of output voltage. If, however, the circuit response is not symmetrical the phase may advance to an angle of greater than  $90^\circ$  on one side of  $\omega_0$  and of less than  $90^\circ$  on the other side. The region within which synchronization persists, the "band of synchronization" is thus seen to be unsymmetrical about the center frequency in some oscillators. In the experiment being discussed efforts were made to insure near-symmetry in order better to interpret the effects of the next portion of the experiment.

An equipment arrangement which was considerably more complete than that described in the introduction was prepared. This arrangement is shown in Figure 7 and permits both the generation of an interrupted wave train and a fairly complete analysis of the output of the oscillator. It is evident that the frequency of the output, the spectrum of the output, and the variations of the phase angle between input and output can be simultaneously studied by means of this arrangement.

In this portion of the experiment procedures identical to those with a c-w synchronizing signal were employed, except that the synchronizing signal was interrupted (gated) with a modulating frequency  $f_m$ . The resulting synchronizing signal is illustrated in Figure 8.

It was now observed, upon introduction of the voltage of Figure 8 as a synchronizing source, that the synchronizing action could still be effected. It was found that there existed a band of frequencies, centered at  $f_0$ , within which the frequency of the oscillator, as recorded by a frequency counter, was exactly equal to frequency of the input. This band could therefore be termed a "band of synchronization", but it was

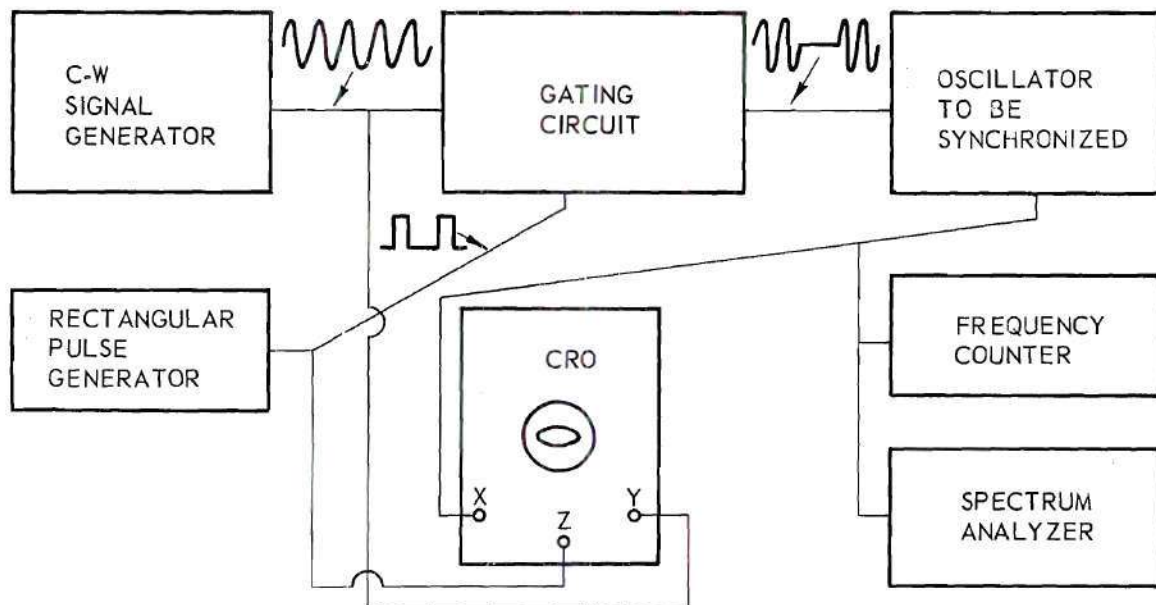


FIGURE 7. BLOCK DIAGRAM OF ARRANGEMENT FOR SYNCHRONIZATION BY INTERRUPTED WAVE TRAINS.

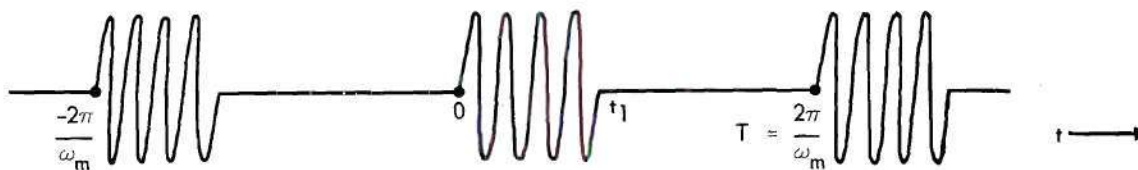


FIGURE 8. INTERRUPTED WAVE-TRAIN AS SYNCHRONIZING SOURCE.



observed to be much narrower than the similar band produced by a c-w synchronizing signal of the same amplitude.

The type of Lissajou pattern formed by the introduction of the original frequency upon the X-axis and the oscillator output upon the Y-axis of the oscilloscope provided significant information. In a preliminary test it was observed that when the modulating frequency was relatively high with respect to the angular frequency difference, (i.e.,  $\omega_m < \omega_1 - \omega_0$ ), the Lissajou pattern behaved almost exactly as it did when a c-w synchronizing signal was applied, opening to a full circle ( $\theta = 90^\circ$ ) at the extreme limit of the synchronization band. But if the modulating frequency was decreased, all other parameters remaining unchanged, the pattern became quite different.

In order to study the changing patterns, it was necessary to provide a form of synchroscope action. This was achieved by injecting the rectangular gating pulse into the Z-axis. With this arrangement it was possible to observe separately the pattern during the "on" time (presence of synchronizing signal) and during the "off" time (absence of synchronizing signal). Further careful study of the patterns revealed that the phase angle,  $\theta$ , behaved in a manner which was determined in part by the position of the synchronizing signal within the synchronizing band. The behavior of  $\theta$  was also affected by the ratio of the modulating frequency to the frequency difference between that of the input and the natural free-running frequency  $f_0$ . Inasmuch as the greatest phase excursions were observed at the edge of the band of synchronization primary consideration was given to the action in that region. The effect

upon the phase angle is best described by reference to a series of photographs which apply to different conditions and varied parameters. These are shown in Figure 9 and illustrate three separate conditions.

Each part of the figure represents a condition wherein the synchronizing signal lies at or very near the edge of the band of synchronization. In the upper figure, part (A), the modulating frequency is relatively high and the phase angle is seen to be nearly equal to  $90^{\circ}$  at all times. However, as the modulating frequency is decreased it is evident that the phase angle undergoes a greater excursion. Finally, with low modulation frequency the excursions become very large.

Careful study of the photographs of part (C) reveals four significant features. First, the excursions of the phase angle are much greater than was the case when the modulation period was short. Second, the magnitude of the total excursion during the "on" time exactly balances that during the "off" time. Third, the rate at which the phase progresses (i.e., the spacing between lines) is uniform during the "off" time but is non-uniform during the "on" time. Finally, when the modulation period is long the phase angle reaches and maintains, for a portion of the interval, a constant value (heavy ellipse of section (C)). This constant value corresponds to the constant angle maintained during synchronization by a c-w signal. As a final and separate observation, it will be noted that the phase angle varies, in section (C), between limits which roughly appear to be of the order of  $45^{\circ}$  -  $135^{\circ}$ .

These observations provide very helpful clues in development of analytical relationships. It will be found that all of these observations



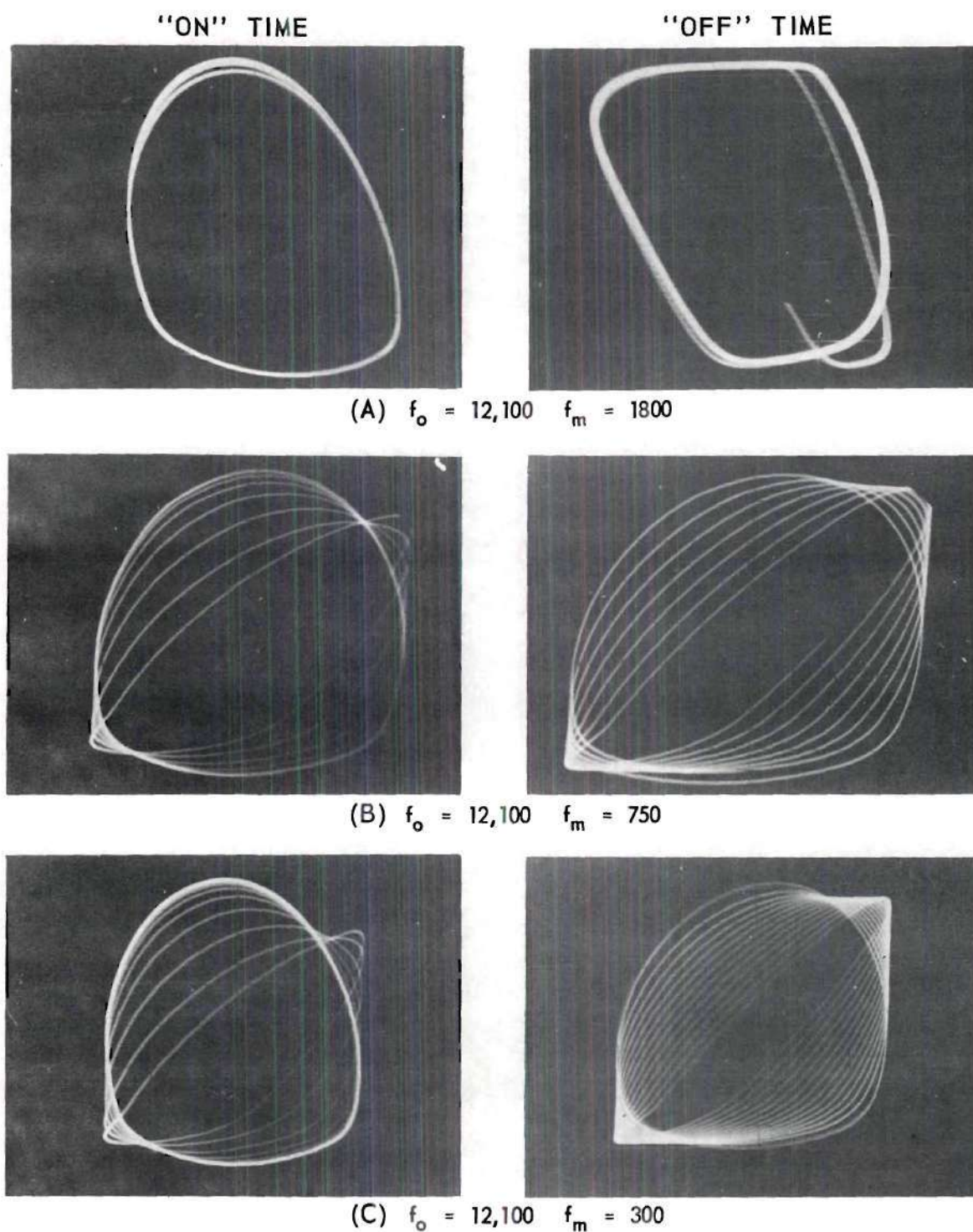
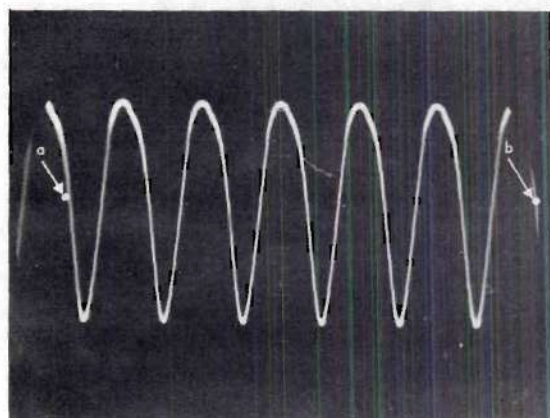


FIGURE 9. LISSAJOU PATTERNS ILLUSTRATING PHASE MODULATION IN OSCILLATOR.

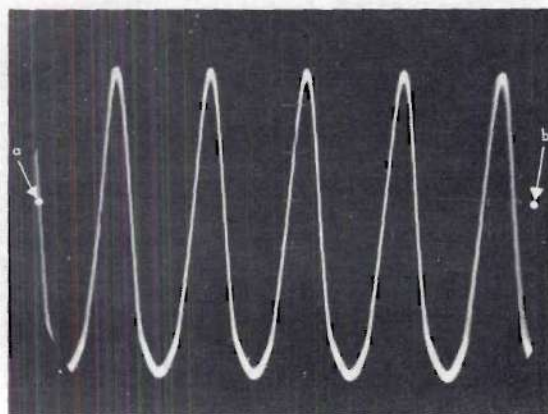
can be explained in the light of established theory and that the transient conditions of phase can be predicted in terms of circuit parameters. The necessary analytical relationships are developed in succeeding sections. However, consideration of one additional experiment will prove helpful in establishing the validity of assumptions which must be made.

A further insight into the behavior of the phase angle  $\theta$  may be gained if the synchronizing bandwidth of the oscillator is increased to a value considerably in excess of normal or usual conditions. Such an increase can be effected by decreasing the  $Q$  of the tuned circuit, or by increasing the ratio of  $V_1/V_g$ . The increased bandwidth permits the establishment of  $\omega_s = \omega_1 - \omega_o$  as an appreciable percentage (10 per cent or greater) of  $\omega_o$ , the free-running angular frequency. In this case the individual cycles of voltage of angular frequency  $\omega_o$  and  $\omega_1$  will vary in period by at least ten per cent. They may be observed and compared on an oscilloscope with calibrated baseline.

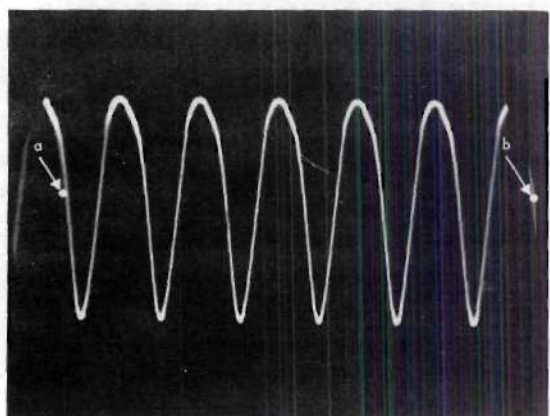
If the  $Q$  is decreased, or the ratio  $V_1/V_g$  increased so that the oscillator can be synchronized by a frequency markedly different from its free-running one, then a significant experiment can be conducted. The oscillator output is injected simultaneously into two oscilloscopes, synchronized Z-axis modulation is applied, and the waveforms occurring during "on" and "off" time are compared. For further reference, the waveforms occurring when the oscillator is allowed to free-run, and the waveform occurring when the oscillator is synchronized by a c-w signal of same frequency as used in the interrupted wave-train portion of the experiment, are observed and recorded. The various waveforms are illustrated in Figure 10.



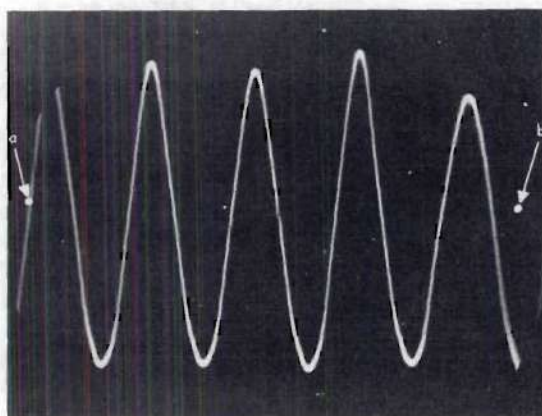
(A) WAVEFORM OF FREE-RUNNING OSCILLATOR,  $\omega = \omega_0$



(B) WAVEFORM OF OSCILLATOR SYNCHRONIZED BY C-W SIGNAL OF ANGULAR FREQUENCY  $= 85\% \omega_0$



(C) WAVEFORM OF OSCILLATOR DURING "OFF" TIME



(D) WAVEFORM OF OSCILLATOR DURING "ON" TIME OF INTERRUPTED WAVE TRAIN

FIGURE 10. VARIATION OF INDIVIDUAL CYCLES OF OSCILLATOR.



The experiment illustrated by this figure involves the following steps. The oscillator, of natural (free-running) frequency  $\omega_0$ , is coupled to the X-axis of an oscilloscope. The baseline upon which a portion of the signal appears is varied until an integral number of cycles appear between two reference points. These points are represented by a and b in each section of Figure 10. This baseline calibration remains fixed during the remainder of the experiment. In the next step a c-w synchronizing voltage whose angular frequency is about 15 per cent less than  $\omega_0$  is applied to the oscillator. This frequency is chosen as one which lies within the band of synchronization, consequently the oscillator is "locked" to the input and the oscillator now runs at the frequency of the c-w signal. About five and one-quarter cycles of oscillator voltage appear between the calibration points a and b, whereas six cycles previously appeared in the absence of synchronizing signal. (Compare Figure 10A and 10B).

The next and final steps involve the use of an interrupted signal as a synchronizing source. The signal is obtained by "gating" the c-w signal just described as a synchronizing source, hence the output of the gating circuit is of the form of Figure 8. In order to study the action of the oscillator during the time the signal is applied (the "on" time) and during the time it is absent (the "off" time), Z-axis modulation is furnished to the oscillator by the pulse generator which simultaneously gates the signal input. Synchroscope action is thus obtained and the waveforms existing during either of the referenced times can be independently studied and compared.

Figure 10C shows the situation during the "off" time. The oscillator voltage is observed to be identical to that occurring during the free-running condition, both in amplitude and in frequency. The same number of cycles occur within the time base a-b as were present when the oscillator was free-running. The significance of this observation is better understood by comparing this waveform to that which is present during the "on" time, illustrated in Figure 10D. This section (D) shows that the waveform in the presence of the synchronizing signal corresponds to none of the others, there being fewer cycles, (approximately four and one-half) within the period of comparison than were found in either the free-running or the c-w synchronized cases.

The conclusions reached from experimental results may be summarized in the following statements.

(a) During the "on" time, during the presence of synchronizing signal, a phase transient occurs which results in the frequency being different from both  $\omega_1$  and  $\omega_0$ , where  $\omega_1$  and  $\omega_0$  are, respectively, the angular frequencies of the injected synchronizing signal and of the free-running oscillator.

(b) During the "off" time, when no synchronizing signal is present, the oscillator frequency is equal to  $\omega_0$ .

(c) Inasmuch as the average frequency during a modulation period is exactly equal to  $\omega_1$ , the average frequency during the "on" time must be  $\omega_1 + \Delta\omega$ . If the interrupting gate is of the square-wave type, so that the "on" and "off" times are equal in duration, then  $\Delta\omega$  must be the negative of the corresponding  $\Delta\omega$  occurring during the "off" time. This has



already been shown to be  $\omega_s = \omega_1 - \omega_0$ . If the interrupting gate has the form of rectangular pulses, for which the on and off times are of unequal duration, then it may be shown in the same way that

$$\Delta\omega = - \frac{\frac{2\pi}{\omega_m} - t_1}{t_1} \omega_s, \quad (39)$$

where the time intervals are illustrated in Figure 8.

The action may be interpreted on a basis of phase deviations in the following manner. If the frequency is exactly equal to  $\omega_1$  it is evident that

$$\int_{\gamma=0}^{\gamma=2\pi/\omega_m=T} \frac{d\theta}{dt} \cdot d\gamma = 0 \quad (40)$$

which can be more precisely expressed as

$$\int_{\gamma=0}^{\gamma=t_1} \frac{d\theta}{dt} d\gamma + \int_{\gamma=t_1}^{\gamma=2\pi/\omega_m} \frac{d\theta}{dt} d\gamma = 0. \quad (41)$$

In the light of the conclusions reached from experimental data, and from Adler's differential equation, equation (41) can be expressed as

$$\int_0^{t_1} (\omega_s - \omega_c \sin \theta) dt + \int_{t_1}^{2\pi/\omega_m} \omega_s dt = 0. \quad (42)$$

This equation will be used as a basis for determining several of the requirements for synchronization.

Another important aspect of the phenomenon concerns the frequency spectrum of the oscillator voltage. Inasmuch as phase modulation is seen to occur during each portion of the modulation (gating) period the spectrum may be predicted to be of the form resulting from phase modulation and may be analyzed accordingly.

One final important experimental result must be recorded. To obtain the data upon which conclusions are based, the input angular frequency  $\omega_1$ , modulated (gated) with an angular frequency  $\omega_m$ , is injected as in the previous experiments and is then manually varied in the manner to be described. The input angular frequency is first made identical to  $\omega_0$  and is then decreased monotonically toward zero frequency. The procedure is then repeated, but in the reverse direction, the angular frequency being reset to  $\omega_0$  and then increased monotonically toward infinite frequency. During this procedure the inputs and output of the oscillator are monitored with a frequency counter. Upon completion of the test the frequency,  $f$ , as recorded by counter, is plotted. Figure 11 illustrates the results. The input frequency,  $f_1$ , is utilized as the independent variable and is shown on the abscissa, while the actual frequency is the dependent variable and is shown as the ordinate.

Two separate and important conclusions may be gained from this figure. First, it is seen that synchronization ( $f = f_1$ ) occurs over a band of frequencies centered around  $f_0$ . This region may be defined as a band of synchronization for the special case that this experiment considers. The process might be termed "synchronization by the fundamental component of input signal". This terminology is made more significant

by next observing that similar regions appear at frequencies which are centered around the frequencies  $f_0 \pm nf_m$ . Since these center frequencies correspond to the frequencies of the sidebands of the modulated input the situation illustrates a form of "side-band synchronization" and the first regions adjacent to  $f_0$  might be termed, "bands of synchronization by first sideband of  $f_1$ ", etc.

The experimental results just stated are repeatable and controllable. They serve as a basis for an analysis of the synchronization phenomenon in accordance with principles stated in the first paragraph of this section. They incorporate the effect of several parameters whence it is evident that the analysis of the process may be expected to be more elaborate than in the case of synchronization by c-w signals. For example, such parameters as interruption frequency,  $f_m$ , and the ratio of duration of "on" time and "off" time are evidently important. In addition, the frequency spectrum of both input and output are pertinent to a discussion of the phenomenon and, although they are not truly parameters, are items necessary to complete the discussion of any specific synchronizing situation.

Any analysis of the synchronizing process must include calculations of the deviations of the phase angle  $\theta$ . This must be related to the condition that the sum of the phase deviations must be zero if synchronization is to exist. An analysis should, in addition, establish the frequency spectrum which is found in the input signal and in the final oscillator voltage. These may be established by the usual methods of Fourier analysis, but with special emphasis upon the expected forms

of periodic structures peculiar to the problem under discussion. These are somewhat specialized, consequently the next several sections of this paper summarize aspects of Fourier analysis which will be required in later sections.

### General Forms of Fourier Series

It is well known that any complex periodic waveform whose period is  $T = 2\pi/\omega_m$  and which is presumed to exist throughout all time can be represented by the trigonometric Fourier series

$$f(\omega t) = a_0/2 + \sum_{n=1}^{\infty} (a_n \cos n\omega t + b_n \sin n\omega t) \quad (43)$$

where

$$a_n = \frac{1}{\pi} \int_{-\pi}^{\pi} f(\omega t) \cos n\omega t \, d(\omega t), \quad (44)$$

and

$$b_n = \frac{1}{\pi} \int_{-\pi}^{\pi} f(\omega t) \sin n\omega t \, d(\omega t). \quad (45)$$

It is perhaps less well known that the same wave form may be equally well represented in a complex Fourier series as follows,

$$f(\omega t) = \sum_{n=-\infty}^{\infty} C_n e^{jn\omega_m t} \quad (46)$$



where

$$C_n = \frac{1}{2\pi} \int_{-\pi}^{\pi} f(\omega t) e^{-jn\omega_m t} d(\omega t). \quad (47)$$

The forms represented in equations (43) and (46) are identical, a statement that can be proved by expanding equation (47) separately for  $n > 0$ ,  $n = 0$ , and  $n < 0$ , and then substituting the results into equation (46). Cuccia<sup>(14)</sup> described this relationship in detail. By combining forms and utilizing the identities relating exponential and trigonometric forms the exact equivalence may be seen.

The complex form may be derived in the following manner:

Case I.  $n > 0$

When  $n$  is greater than zero

$$e^{-j(+n)\omega_m t} = \cos n\omega_m t - j \sin n\omega_m t, \quad (48)$$

whence

$$C_n = \frac{1}{2\pi} \int_{-\pi}^{\pi} f(\omega t) \cos n\omega_m t d(\omega t) - j \int_{-\pi}^{\pi} f(\omega t) \sin n\omega_m t d(\omega t), \quad (49)$$

which may be written, comparing equation (44) and (45), as

$$C_{+n} = a_n/2 - j b_n/2. \quad (50)$$

Case II.  $n < 0$

When  $n$  is less than zero

$$e^{-j(-n)\omega_m t} = \cos n\omega_m t + j \sin n\omega_m t \quad (51)$$



whence

$$C_{-n} = \frac{1}{2\pi} \int_{-\pi}^{\pi} f(\omega t) \cos n\omega_m t d(\omega t) + j \int_{-\pi}^{\pi} f(\omega t) \sin n\omega_m t d(\omega t). \quad (52)$$

which can be written as

$$C_{-n} = a_n/2 + j b_n/2. \quad (53)$$

Finally, it is evident that

$$|C_n| = \sqrt{(a_n/2)^2 + (b_n/2)^2}. \quad (54)$$

The significance of the forms of  $C_n$  is, of course, that if the periodic function is even, only the real part will result and if odd only the imaginary part will result. If neither even nor odd it is often desirable to denote the value by use of equation (54). This is illustrated in later paragraphs.

#### The Complex Fourier Series in Phase Modulation

In general, any wave of constant amplitude which is represented by a single rotating vector may be expressed as

$$i = I e^{j\theta_t} \quad (55)$$

where  $\theta_t$  represents the instantaneous phase angle of the rotating vector. The instantaneous phase is related to the angular velocity of the rotating vector by the equation

$$\theta_t = \int \omega_t dt, \quad \omega_t = d\theta_t/dt \quad (56)$$

where  $\omega_t$  is the instantaneous angular velocity.

The usual form of sinusoidal phase modulation illustrates the process. In this form

$$\theta_t = \theta_o + \Delta\theta \sin \omega_m t \quad (57)$$

where

$$\theta_o = \omega_1 t. \quad (58)$$

By substituting into equation (55) one obtains

$$i = I e^{j(\omega_1 t + \Delta\theta \sin \omega_m t)} \quad (59)$$

which may be written in the form

$$i = I (e^{j\Delta\theta \sin \omega_m t}) (e^{j\omega_1 t}) \quad (60)$$

The complex Fourier series may be written as

$$i = I \left( \sum_{n=-\infty}^{\infty} C_n e^{jn\omega_m t} \right) e^{j\omega_1 t}, \quad (61)$$

where

$$C_n = \frac{\omega_1}{2\pi} \int_{-\pi/\omega_m}^{\pi/\omega_m} (e^{j\Delta\theta \sin \omega_m t}) e^{-jn\omega_m t} dt. \quad (62)$$

The combined exponential has been evaluated in many standard texts to yield Bessel functions of the first kind, whence equation (55) may be written as

$$i = I \sum_{n=-\infty}^{\infty} J_n(\Delta\theta) e^{j(\omega_1 + n\omega_m)t}. \quad (63)$$

There will now be given an example of the Fourier analysis of a phase-modulated signal which will later be seen to be almost directly applicable to the determination of the spectrum of an oscillator which is synchronized by an interrupted wave-train. The example is referred to as "Fourier Analysis of Square-Wave Frequency Modulation" and applies to a problem first solved by van der Pol<sup>(15)</sup> but it is analyzed from the standpoint of phase modulation.

Consider the Fourier analysis of the square-wave FM signal pictured in Figure 12A. Inasmuch as phase is the integral of frequency, as given in equation (56), the phase deviation may be obtained and is shown in part (B) of the same figure.

The instantaneous phase may be described as

$$\begin{aligned}\theta_t &= \omega_1 t + m(\pi + \omega_m t) & -\frac{\pi}{\omega_m} \leq t \leq 0 \\ &= \omega_1 t + m(\pi - \omega_m t) & 0 \leq t \leq \frac{\pi}{\omega_m}\end{aligned}\quad (64)$$

where

$$m = \Delta\omega/\omega_m = \text{modulation index.}$$

The complex Fourier coefficients may now be evaluated. Letting  $\phi = \omega_m t$ , one obtains

$$C_n = \frac{1}{\pi} \int_{-\pi}^0 e^{j(n\pi + m\phi - n\phi)} d\phi + \int_0^{\pi} e^{j(n\pi - m\phi - n\phi)} d\phi. \quad (65)$$

Performing the integration, and noting that  $e^{-jn\pi} = (-1)^n$ , one

obtains

$$\begin{aligned} C_n &= \frac{2m}{\pi(m^2 - n^2)} \left[ e^{jm\pi} - (-1)^n \right] \\ &= \frac{2m}{\pi(m^2 - n^2)} \left[ \cos m\pi - (-1)^n + j \sin m\pi \right], \end{aligned} \quad (66)$$

whence

$$|C_n| = \frac{2m}{\pi(m^2 - n^2)} \sqrt{\sin^2 m\pi + \left[ (-1)^n - \cos m\pi \right]^2}, \quad (67)$$

which may be written as

$$\begin{aligned} C_n &= \sum_{n=-\infty}^{\infty} \frac{2m}{\pi(m^2 - n^2)} \sin \frac{m\pi}{2}, \quad n \text{ even} \\ &= \sum_{n=-\infty}^{\infty} \frac{2m}{\pi(m^2 - n^2)} \cos \frac{m\pi}{2}, \quad n \text{ odd} \\ &= \sum_{n=-\infty}^{\infty} \frac{2m}{\pi(m^2 - n^2)} \sin (m-n) \frac{\pi}{2}, \quad \text{all } n \end{aligned} \quad (68)$$

Finally, the expression for the wave can be written as

$$\begin{aligned} i &= I \sum_{n=1}^{\infty} \frac{2m}{\pi(m^2 - n^2)} \sin (m-n) \frac{\pi}{2} \left[ e^{j(\omega_1 - n\omega_m)t} \right. \\ &\quad \left. + (-1)^n e^{j(\omega_1 + n\omega_m)t} \right] + \frac{2I}{m\pi} \sin \frac{m\pi}{2} e^{j\omega_1 t}. \end{aligned} \quad (69)$$

The general aspects of this series are illustrated in Figure 13, where  $\Delta\omega$  is kept constant and  $\omega_m$  is varied.



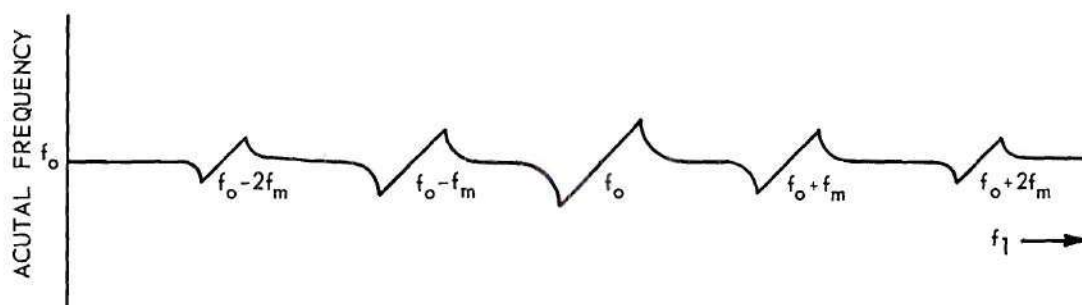


FIGURE 11. SYNCHRONIZING PATTERN OF INTERRUPTED WAVE TRAIN.

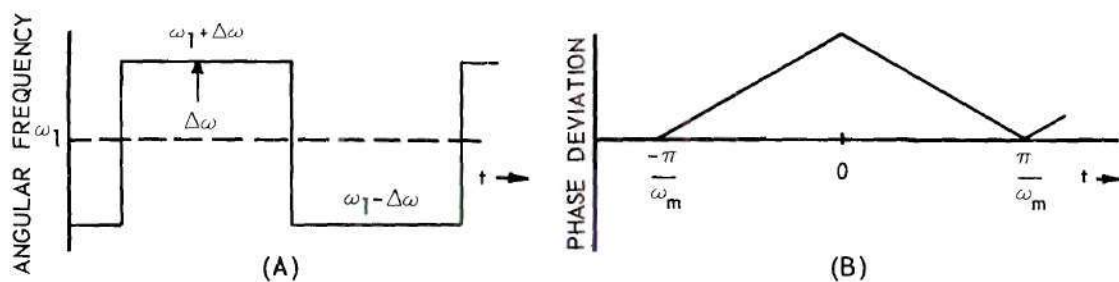


FIGURE 12. PHASE AND FREQUENCY DEVIATIONS IN SQUARE-WAVE FM.

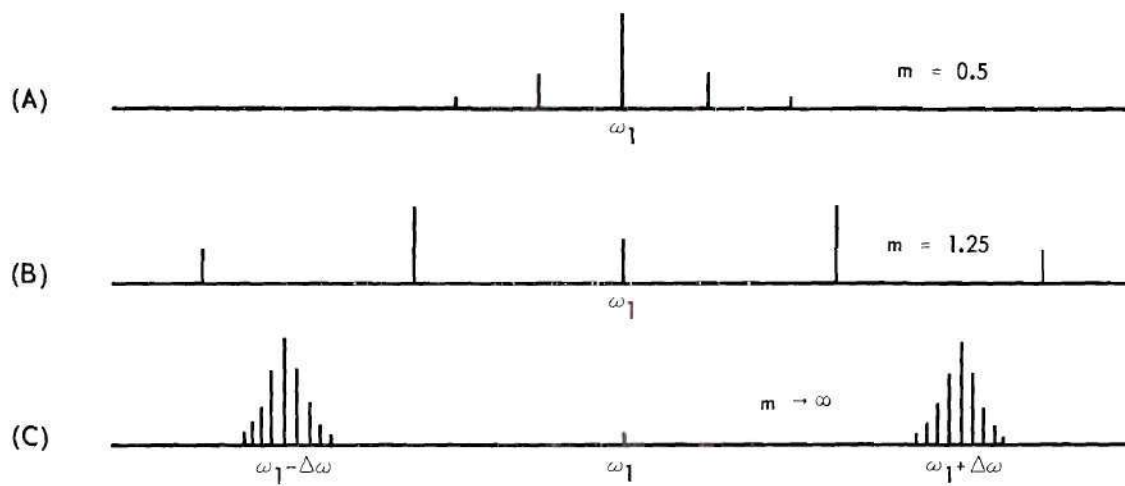


FIGURE 13. SPECTRUM BEHAVIOR OF SQUARE-WAVE FM.

For small values of  $m$ , corresponding to a value of  $\omega_m$  which exceeds  $\Delta\omega$  in magnitude, the energy is distributed among the carrier and the first pair of sidebands. As  $m$  is increased toward 2.5 the energy is spread out and quite well distributed among a large number of frequencies, but as  $m$  increases above 2.5 the largest spectral amplitudes occur in the vicinity of  $\omega_1 + \Delta\omega_1$  and  $\omega_1 - \Delta\omega_1$ . Finally, as  $\omega_m$  approaches zero all the energy concentrates in those two spectral lines.

It may be recognized that the upper figure of Figure (13) must correspond closely to the observed experimental synchronizing action described in the first section of this chapter and illustrated in Figure (9). The phase deviation during one portion of the period is actually linear and that during the other portion of the period is nearly linear, hence the spectrum of the oscillator voltage may be expected to reasonably approximate that of the upper figure of Figure (13). However, more precise formulas are developed in the succeeding sections.

#### Trigonometric Fourier Series in Phase Modulation

A generalized expression for a phase-modulated wave, due to Corrington<sup>(16)</sup> is developed as follows.

If the phase deviation term is expressed as  $\theta(t)$ , it is evident that an expression for the phase-modulated signal is given by

$$\begin{aligned} i &= I \sin [\omega t + \theta(t)] \\ &= I \sin \omega t \cos \theta(t) + I \cos \omega t \sin \theta(t). \end{aligned} \quad (70)$$

Now

$$\cos \theta(t) = \sum_{n=0}^{\infty} \left[ a_n \sin n\theta + b_n \cos n\theta \right], \quad (71)$$

and

$$\sin \theta (t) = \sum_{n=0}^{\infty} [c_n \sin n\theta + d_n \cos n\theta] , \quad (72)$$

where

$$\theta = 2\pi f_m t = \omega_m t.$$

Then

$$\begin{aligned} i = I \sin \omega t \sum (a_n \sin n\theta + b_n \cos n\theta) \\ + I \cos \omega t \sum (c_n \sin n\theta + d_n \cos n\theta) \end{aligned} \quad (73)$$

By multiplying through by  $\sin \omega t$  and  $\cos \omega t$ , and expanding the terms, the equation becomes

$$\begin{aligned} i = I \sum \left[ \frac{1}{2} (a_n + d_n) \cos (\omega - \omega_m)t \right. \\ - \frac{1}{2} (a_n - d_n) \cos (\omega + \omega_m)t \\ + \frac{1}{2} (b_n - c_n) \sin (\omega - \omega_m)t \\ \left. + \frac{1}{2} (b_n + c_n) \sin (\omega + \omega_m)t \right] . \end{aligned} \quad (74)$$

#### Spectrum of Wave Train Modulated with Rectangular Pulse

The interrupted wave train of Figure 8 is obtained by modulation (gating) a c-w signal by a rectangular pulse, of the form illustrated in Figure 14A. The frequency spectrum of a rectangular pulse is shown in part (B) of the same figure being computed according to the following analysis.

The coefficients of the Fourier series may be found, using the complex form

$$C_n = \frac{\omega_m}{2\pi} \int_{-\pi/\omega}^{\pi/\omega} e^{-jn\omega_m t} dt, \quad (75)$$

or

$$C_n = \frac{\omega_m}{-j2\pi n\omega_m} \left[ e^{-j(n\omega_m \frac{\pi}{\omega})} - e^{+j(n\omega_m \frac{\pi}{\omega})} \right], \quad (76)$$

$$= \frac{1}{n\pi k} \sin nk\pi, \quad (77)$$

where

$$k = \frac{\omega_m}{\omega} = \frac{T}{T_m} = \text{duty cycle.} \quad (78)$$

Since  $\sin nk\pi$  is zero for all integral values of the product  $nk$ , the harmonic component whose number  $n$  is equal to  $1/k$  or multiples thereof will also be zero. For example, if the pulse is a square wave it will be found that all even numbered components have zero amplitude since for a square wave  $k$  is equal to one-half. Otherwise stated, the spectrum of a square pulse contains only odd harmonics of the pulse repetition frequency,  $f_m$ .

If Figure 14 represents the spectrum of a rectangular pulse, then the spectrum of a sine wave which is amplitude modulated by the rectangular pulse can be immediately inferred from the well-known principle that the spectrum of an amplitude-modulated wave finds the spectrum of the modulating function centered about the carrier. The spectrum, to the



first zero of a sine wave of frequency  $f_1$  which has been modulated by a rectangular pulse, of frequency  $f_m$  and of duty cycle equal to one-third is illustrated in Figure 15.

This concludes the summary of those elements of Fourier analysis which will be required in the succeeding analysis. The next chapter takes up the fundamental problem of the method by which synchronization may be obtained when the synchronizing signal is an interrupted wave train.

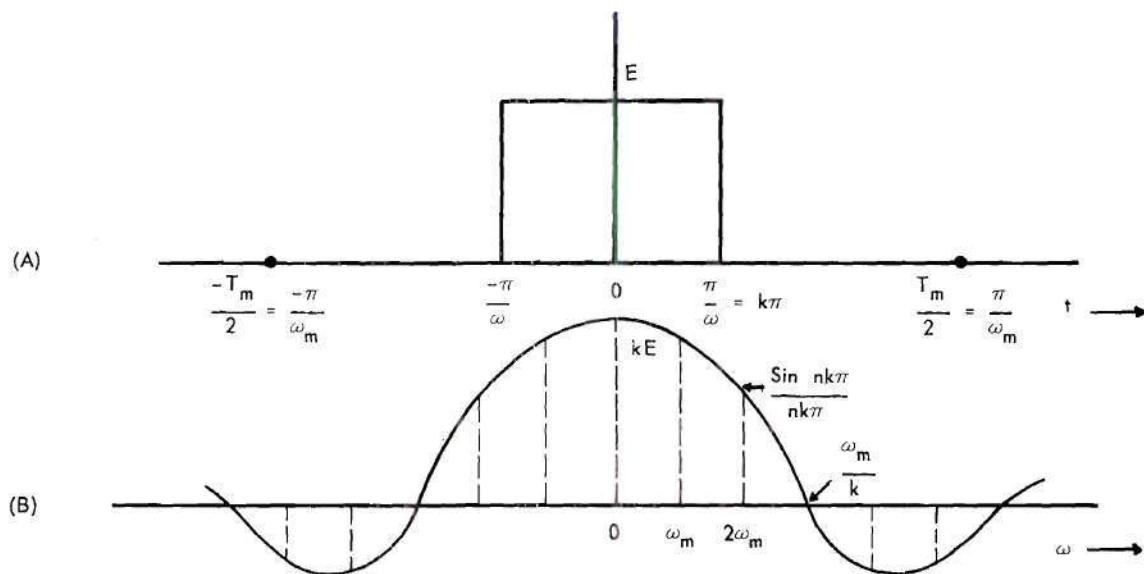


FIGURE 14. SPECTRUM OF A RECTANGULAR PULSE.

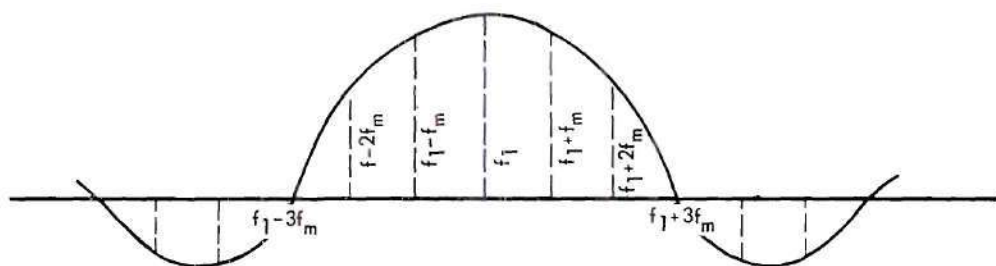


FIGURE 15. SPECTRUM OF SINE WAVE MODULATED BY RECTANGULAR PULSE.

## CHAPTER IV

### MECHANISM OF SYNCHRONIZATION WITH INTERRUPTED WAVE TRAINS

#### Phase Requirements in Synchronization

In the case of synchronization by a c-w signal it has been shown that the vector voltages may be represented in the form shown in Figure 16 and that

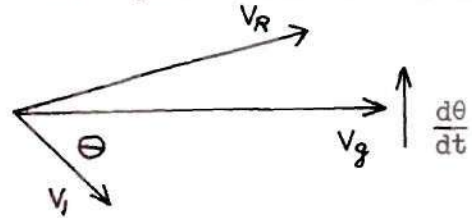


Figure 16. VECTOR TRIANGLE OF VOLTAGES

$d\theta/dt = \omega_s - \omega_c \sin \theta$ , where  $\omega_s = \omega_1 - \omega_0$  and  $\omega_c =$  one-half of the bandwidth of synchronization =  $\frac{\omega_0 V_1}{2Q V_g}$ . This quantity, it will be noted, is a constant for any given set of parameters,  $\omega_0$ ,  $V_1$ ,  $Q$  and  $V_g$ .

It is evident that synchronization occurs when (in the c-w case)

$$\frac{d\theta}{dt} = \omega_s - \omega_c \sin \theta = 0, \quad (79)$$

in which case,

$$\theta = \sin^{-1} \omega_s / \omega_c \quad (80)$$

and in the extreme limit of synchronization, when  $\omega_s = \omega_c$ ,

$$\theta = \sin^{-1} 1 = 90^\circ. \quad (81)$$

Obviously the conditions for synchronization are quite different when the synchronizing signal is periodically interrupted. An understanding

of the mechanism of synchronization in this case is facilitated by considering a special case of the nonlinear equation  $d\theta/dt = \omega_s - \omega_c \sin \theta$ . Using  $K = \omega_s/\omega_c$ , this equation can be rewritten as

$$\frac{d\theta}{dt} = \omega_c (K - \sin \theta) \quad (82)$$

and, since  $\omega_c$  is a constant, the change of phase angle is described by the quantity  $K - \sin \theta$ , with  $\omega_c$  playing the role of a simple scaling factor.

If the synchronizing signal is modulated (interrupted) by a rectangular pulse, the basic criterion for synchronization was shown in equation (42) to be

$$\int_0^{t_1} (\omega_s - \omega_c \sin \theta) dt + \int_{t_1}^{2\pi/\omega_m} \omega_s dt = 0$$

or

$$\omega_c \int_0^{t_1} (K - \sin \theta) dt + \omega_c \int_{t_1}^{2\pi/\omega_m} K dt = 0. \quad (83)$$

In the case of square-wave modulation, when  $t_1 = T/2$ , the equation can be expressed as

$$\int_0^{T/2} (K - \sin \theta) dt = - \int_{T/2}^T K dt. \quad (84)$$

The special case to be now considered occurs when the modulating frequency  $f_m$  is relatively large and the oscillator is synchronized at



one extreme limit of the band of synchronization. In Figure 9A photograph of the change of phase angle in the case of high modulating frequency and edge of synchronizing band showed that the angle  $\theta$  remained very nearly equal to  $90^\circ$  throughout the modulation cycle.

If  $\theta$  is assumed to remain constant, then the function  $\sin \theta$  may also be evidently assumed to be constant. In that case, equation (84) can be evaluated with ease, becoming

$$\frac{T}{2} (K - \sin \theta) = -\frac{KT}{2} \quad (85)$$

whence

$$K = \frac{\sin \theta}{2} . \quad (86)$$

If  $\theta$  reaches a maximum value of  $90^\circ$  it is evident that the maximum possible value that  $K$  may attain during square-wave modulation is one-half. In other words, the widest possible band of synchronization during square-wave modulation is one-half as wide as the band of synchronization which would result from a c-w signal of equivalent amplitude. The width of the band is maximum when the modulation frequency is high but is less when the modulation frequency decreases since in the latter case the angle  $\theta$  cannot remain at  $90^\circ$  and the average value of  $\sin \theta$  during a modulation cycle is less than unity.

If the mechanism of synchronization is to be completely described it is evident that more generalized relationship must be obtained. A quantity yet to be determined is the maximum value of the angular

frequency difference  $\omega_s$  which can be utilized when the signal is interrupted at a specified modulation frequency. The maximum value of the ratio  $K = \omega_s/\omega_c$  conveniently represents this maximum value and will be referred to as  $K_{\max}$ . It has been shown that in the case of square-wave modulation that the largest possible value of  $K_{\max}$  is one-half and that this value is attained only when the modulation frequency is high. Further consideration of equation (84) shows that for lower values of modulating frequency the values of  $K_{\max}$  are smaller. It may be concluded that for every value of modulating frequency there exists a maximum frequency deviation  $K_{\max}$ . In other words the bandwidth of synchronization is uniquely determined by the modulating frequency.

To digress briefly from the analytical development of the solution, it seems desirable to comment briefly upon the physical aspects of the mechanism of synchronization since the equations to be derived achieve greater significance when seen as mathematical representations of apparent phenomena. The Lissajou patterns of Figure 9 and the equation (83) both indicate that the phase angle  $\theta$  is an oscillating angle when the oscillator is synchronized by an interrupted wave train. During the absence of synchronizing signal the angle rotates in one direction at the angular velocity of  $\omega_1 - \omega_0$ , during the presence of synchronizing signal the relative gain, or loss, is made up and the angle rotates in the opposite direction at the angular velocity  $\omega_s - \omega_c \sin \theta$ . With high modulating frequencies the modulation period is very short and the angle can change but little, during low modulation frequencies the period is long and the angle can rotate a significant amount. If the

magnitude of rotation during the absence of synchronizing signal becomes too great to be regained during the presence of that signal then synchronization is lost.

A mathematical development of an equation which defines the relationship of the variables and parameters involved in the synchronization process begins by consideration of the basic criterion for synchronization.

$$\int_{\gamma=0}^{\gamma=2\pi/\omega_m} \frac{d\theta}{dt} d\gamma = 0 \quad (40)$$

and by combining the experimentally gained conclusions shown in Figure 9C that the phase angle may include values of  $\theta$  which are greater than  $90^\circ$  with the basic equation for  $\theta$

$$\theta = 2 \tan^{-1} \left[ \frac{1}{K} - \frac{\sqrt{1-K^2}}{K} \tanh \omega_c \frac{\sqrt{1-K^2}}{2} (t + t_0) \right]. \quad (36a)$$

The requirement that the net phase must be zero when measured over a complete modulation cycle is now considered by restating equation (83) in the more explicit form, after the constant  $\omega_c$  has been divided out, as

$$\int_0^{t_1} (K - \sin \theta) dt + \int_{t_1}^{2\pi/\omega_m} K dt = 0. \quad (87)$$

The quantity  $\int_0^{t_1} \sin \theta dt$  is evaluated in the following manner. Using

the general equation for  $\theta$ , one can write

$$\int \sin \theta \, dt = \int \sin 2 \tan^{-1} \left[ \frac{1}{K} - \frac{\sqrt{1-K^2}}{K} \tanh \omega_c \frac{\sqrt{1-K^2}}{2} (t + t_0) \right] dt. \quad (88)$$

This integral may be evaluated. If the substitutions,

$$\tanh \beta = \sqrt{1-K^2}, \quad \cosh \beta = 1/K \quad (89)$$

are made, one can further write

$$\begin{aligned} \theta &= 2 \tan^{-1} (\cosh \beta - \sinh \beta \tanh \phi) \\ &= 2 \tan^{-1} \left( \frac{\cosh \phi \cosh \beta - \sinh \phi \sinh \beta}{\cosh \phi} \right) \\ &= 2 \tan^{-1} \left( \frac{\cosh (\phi - \beta/2)}{\cosh \phi} \right). \end{aligned} \quad (90)$$

$\sin \theta$  can now be expressed as

$$\sin \theta = \frac{2 \cosh (\phi - \beta) \cosh^2 \phi}{\cosh^2 (\phi - \beta) + \cosh^2 \phi} \quad (91)$$

and the integral becomes

$$\int \sin \theta \, dt = \frac{2}{\omega_c \sinh \beta} \int_{\phi_1}^{\phi} \frac{2 \cosh (\phi - \beta) \cosh^2 \phi}{\cosh^2 \phi + \cosh^2 (\phi - \beta)} d\phi. \quad (92)$$

The use of identities reduces this to

$$\frac{2}{\omega_c \sinh \beta} \int_{\phi_1}^{\phi} d\phi + \frac{2}{\omega_c} \int_{\phi_1}^{\phi} \frac{\sinh \beta}{\cosh^2 \phi + \cosh^2 (\phi - \beta)} d\phi \quad (93)$$

$$= \frac{2(\phi - \phi_1)}{\omega_c \sinh \beta} + \frac{2}{\omega_c} \int_{\phi_1}^{\phi} \frac{\operatorname{sech}^2 (\phi - \beta/2) \tanh \beta/2}{1 - \tanh^2 (\phi - \beta/2) \tanh^2 \beta/2} d\phi \quad (94)$$



which is an elementary integral. One then obtains

$$\frac{2(\phi - \phi_1)}{\omega_c \sinh \beta} + \frac{2}{\omega_c} \left[ \tan^{-1} \tanh(\phi - \beta/2) \tanh \beta/2 - \tan^{-1} \tanh(\phi_1 - \beta/2) \tanh \beta/2 \right] \quad (95)$$

where, as previously defined

$$\phi = \omega_c \sqrt{\frac{1 - K^2}{2}} (t + t_0), \text{ and } \beta = \tanh^{-1} \sqrt{1 - K^2}. \quad (96)$$

Now consider the complete integral  $\int_0^{t_1} (K - \sin \theta) dt$ . The evaluation of the constant, that is, of  $\int_0^{t_1} K dt$ , is direct and gives as a result the quantity  $Kt_1$ . The evaluation of  $\sin \theta$  in its integral is given in the preceding equations and leads to the final form of equation (95). Now if the first expression of that equation, namely,

$$\frac{2(\phi - \phi_1)}{\omega_c \sinh \beta}$$

is reduced by replacing  $\phi$  and  $\beta$  by their equivalent expressions from equation (96) it is found that the final result is also the quantity  $Kt_1$ .

The two equal quantities,  $Kt_1$ , vanish by virtue of the negative sign preceding  $\sin \theta$ . Accordingly, the integral  $\int_0^{t_1} (K - \sin \theta) dt$  reduces to the negative of the term in brackets in equation (95).

Relationships involving the parameter  $K$  and the bandwidth of synchronization can now be determined. The first step is to replace the terms in equation (87) by their evaluated equivalents. If this is done,

and the quantities  $\phi$  and  $\beta$  are again replaced by their equivalents in terms of  $t$  and  $K$ , the result is

$$2 \tan^{-1} \left\{ \frac{1-K}{\sqrt{1-K^2}} \tanh \left[ \omega_c \frac{\sqrt{1-K^2}}{2} (t_1 + t_0) - \tanh^{-1} \frac{1-K}{\sqrt{1-K^2}} \right] \right\} \\ - 2 \tan^{-1} \left\{ \frac{1-K}{\sqrt{1-K^2}} \tanh \left[ \omega_c \frac{\sqrt{1-K^2}}{2} t_0 - \tanh^{-1} \frac{1-K}{\sqrt{1-K^2}} \right] \right\} = \omega_c K (2\pi/\omega_c - t_1). \quad (97)$$

This equation, (97) is probably the single most important equation appearing in this paper. It will henceforth be called the EQUATION OF SYNCHRONIZATION. It is an equation which must be satisfied for every condition of synchronization. The left side shows the change of phase angle that occurs during the presence of the synchronizing signal while the right side shows the change of phase angle that occurs during the absence of synchronizing signal. These changes must be balanced if the average frequency of the output, as measured over one complete modulating cycle, is to be identically equal to frequency of the input.

Unfortunately, equation (97), the equation of synchronization, does not in itself uniquely define either of the quantities  $t_1$  and  $t_0$  for any specific value of  $K$ . Approximate methods which do provide a unique relationship between the maximum permissible frequency difference, defined as  $K_{\max}$ , and the minimum permissible value of  $t_1$  can be employed by taking into account the simplifying assumptions which were employed in the case of high modulating frequencies. It will be recalled that, when the modulating period is very short and operation is within but near the limits of the band of synchronization, the phase angle  $\theta$  must remain very close to  $90^\circ$  throughout the modulating cycle. This relationship is utilized

in the present analysis by assuming that, for high modulating frequencies, the angle  $\theta$  is equal to  $90^\circ$  when  $t = 0$ .

Equation (36a) is referred to. This equation was given as the direct solution of the basic nonlinear differential equation  $d\theta/dt = \omega_s - \omega_c \sin \theta$ . The solution, substituting  $K = \omega_s/\omega_c$  was given as

$$\theta = 2 \tan^{-1} \left[ \frac{1}{K} - \frac{\sqrt{1-K^2}}{K} \tanh \omega_c \sqrt{\frac{1-K^2}{2}} (t + t_0) \right]. \quad (36a)$$

If now the additional substitutions,  $\theta = 90^\circ$  when  $t = 0$  are made, there is obtained

$$\omega_c t_0 = \frac{2}{\sqrt{1-K^2}} \tanh^{-1} \frac{1-K}{\sqrt{1-K^2}} \quad (98)$$

for all  $\omega_c$ .

For this condition it may now be shown that the quantity  $(\phi - \beta/2)$  vanishes, a result of the definition already given,

$$\tanh \beta = \sqrt{1-K^2}, \quad \cosh \beta = 1/K, \quad (89)$$

from which simple identities give

$$\beta/2 = \tanh^{-1} \frac{1-K}{\sqrt{1-K^2}} = \phi_1. \quad (99)$$

With this identity the second term within the bracket of equation (95) also vanishes. Also, using  $\phi_1 = \beta/2$ , the bracketed expression becomes

$$\begin{aligned} & \tan^{-1} \left[ \tanh (\phi - \phi_1) \tanh \phi_1 \right] \\ &= \tan^{-1} \left[ \frac{1-K}{\sqrt{1-K^2}} \tanh \omega_c \sqrt{\frac{1-K^2}{2}} t_1 \right]. \end{aligned} \quad (100)$$

This result is extremely important in relating transient and steady-state theory, as may be shown in the following manner.

It will be recalled that the general criterion for synchronization is

$$\int_0^{t_1} (K - \sin \theta) dt + \int_{t_1}^{2\pi/\omega_m} K dt = 0 \quad (87)$$

a general solution to which is expressed by equation (97). For the present modified case ( $\theta = 90^\circ$ ,  $t = 0$ ) the solution is relatively simple, becoming

$$2 \tan^{-1} \left[ \frac{1-K}{\sqrt{1-K^2}} \tanh \omega_c \frac{\sqrt{1-K^2}}{2} t_1 \right] = \omega_c K \left( \frac{2\pi}{\omega_m} - t_1 \right) \quad (101)$$

and in the case of square-wave modulation, when  $t_1 = T/2$ , is simply

$$\frac{1-K}{\sqrt{1-K^2}} \tanh \left( \frac{\omega_c \sqrt{1-K^2}}{4} T \right) = \tan \frac{\omega_c K T}{4} \quad (102)$$

Inasmuch as this equation is based upon the assumption that the period,  $T$ , is very short, a solution may be obtained by use of the first terms of the series:

$$\tanh x = x - x^3/3 \dots\dots, \quad \tan x = x + x^3/3 \dots\dots \quad (102)$$

Utilization of the series for both the hyperbolic and the trigonometric tangents in equation (102) finally yields the relationship

$$\omega_c T = \sqrt{\frac{48(1-2K)}{2K^3 - K^2 - K + 1}} \quad (103)$$

which shows that  $T \rightarrow 0$  as  $K \rightarrow 1/2$ . That is to say,  $f_m \rightarrow \infty$  as  $K \rightarrow 1/2$ .



This result shows, as was predicted by physical reasoning, that during square-wave modulation the maximum value of  $K$  is equal to one-half. Further, since  $K$  is defined as the ratio  $\omega_s/\omega_c$ , the results also show that the maximum possible value of  $\omega_s$ , consistent with synchronization, is one-half of  $\omega_c$ .

The same procedure used in arriving at equation (103) may be applied for the relationships involved in other duty cycles. Restating the definition

$$k = t_1/T = \text{duty cycle} \quad (104)$$

where

$$T = 2\pi/\omega_m,$$

a final relationship is developed as follows

$$\omega_c T = \sqrt{\frac{12 (K-k)}{k^3 (K^2 + K - 1 - K^3) - (1-k)^3 K^3}} \quad (105)$$

from which it is evident that

$$T \rightarrow 0 \quad \text{when } K \rightarrow k. \quad (106)$$

The relationships expressed in equation (103) and (106) are significant when transient and steady-state theory are compared. For example, it was shown in the derivation of the Fourier components of pulse-amplitude modulated waves that the amplitude of the fundamental component of the wave of duty cycle  $k$  was equal to the product of the amplitude of the unmodulated wave and of  $k$ , the duty cycle. Here, in equation (106)

it is shown that, for modulation frequencies which are large compared to the band of synchronization, the synchronizing action of an interrupted wave-train of duty cycle  $k$  is less than that of the unmodulated wave in the ratio of  $k:1$ . In other words, the band of synchronization due to an interrupted wave-train which is interrupted at such a rate that  $\omega_m/\omega_c \gg 1$  may be calculated as though the oscillator were receiving a c-w synchronizing signal whose amplitude was equal to the fundamental component of the interrupted wave train. Thus steady-state theory may be used to predict, in part, the expected response of the disturbed oscillations.

It has thus been shown that the bandwidth of synchronization may be computed if  $\omega_m/\omega_c \gg 1$ . However, a generalized expression by which to determine the band of synchronization for any value of the ratio  $\omega_m/\omega_c$  is required. The desired expression may be obtained through a method of maximization related to the deviation of the phase angle when the oscillator is synchronized by the interrupted wave-train. The conditions which describe the phasing action within the band of synchronization are described in the following paragraphs.

Equation (97), the equation of synchronization, specifies that the total change of the phase,  $\Delta\theta$ , occurring during the presence of synchronizing signal (the left side of equation (97) is exactly balanced by the change occurring during the absence of signal (the right side of the same equation). A graphical representation of the action is shown in Figure 17. The various portions of each curve of that figure are explained as follows.

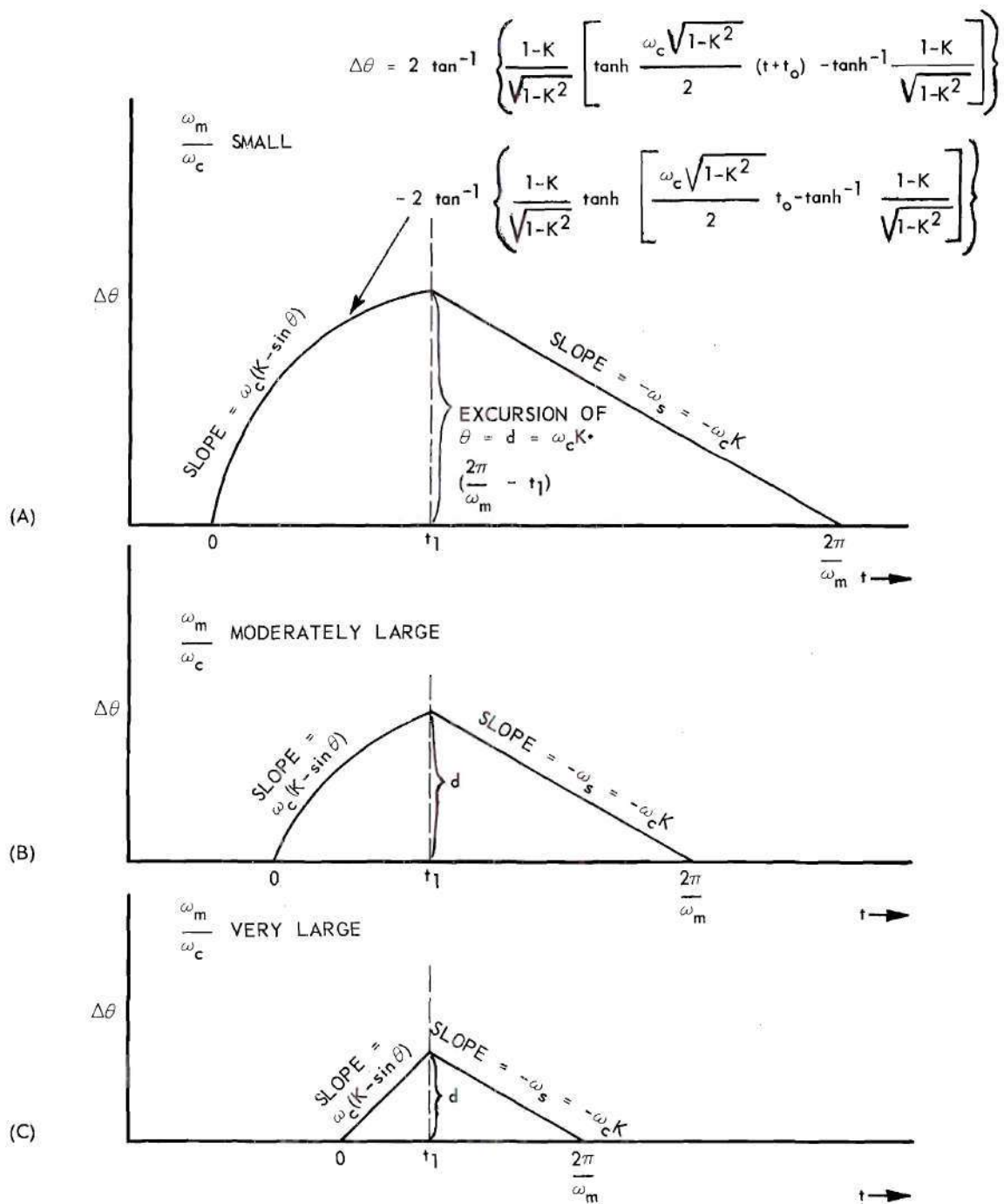


FIGURE 17. PHASE DEVIATIONS IN THE SYNCHRONIZED OSCILLATOR.

In the absence of signal ( $t_1 \leq t \leq 2\pi/\omega_m$ ) the rate of change of angle is given by  $d\theta/dt = \omega_1 - \omega_0 = \omega_s =$  a constant, hence the slope of each curve in that portion of the period is equal to a constant value. This condition is illustrated in each of the three curves which represent different ratios of  $\omega_m/\omega_c$ .

The phase deviations during the presence of synchronizing signal ( $0 \leq t \leq t_1$ ) is determined by the left side of equation (97) and is a nonlinear function of the time variable. Now if  $\omega_m$  is very large the modulating period is so short that the phase deviation must remain small. In addition, it has already been shown that under this condition the phase angle  $\theta$  remains very close to  $90^\circ$  throughout the cycle, hence the quantity  $\omega_c(K - \sin \theta)$  is also very nearly a constant, and the effect is to reduce the nonlinearity of the phase deviation curve to a minimum. This case is represented in part (C) of Figure 17. The other two curves represent cases of lower modulating periods wherein the period is sufficiently long to permit considerable nonlinearity to develop.

The particular item of interest in these figures which is significant in the discussion of the bandwidth of synchronization is the excursion of  $\theta$  during any modulation period. This is represented in each part of the figure by the quantity  $\underline{d}$ .

It is evident that for each value of modulating period,  $2\pi/\omega_m$ , there exists some maximum value of phase excursion  $\underline{d}$ . Now the excursion  $\underline{d}$  increases with increased slope of the straight portion of each curve, but this in turn becomes greater in direct proportion to the magnitude of the frequency difference,  $\omega_s = \omega_1 - \omega_0$ . Finally, the maximum possible



value of  $\omega_s$  determines the bandwidth of synchronization for any particular value of modulating frequency.

Analytically, this maximum excursion of  $\underline{d}$  may be determined by the method of undetermined coefficient, or Lagrange multipliers. The method includes the stated principle that if it is desired to maximize a function  $F(x,y)$ , subject to the condition that another function is identically zero, that is, that  $\phi(x,y) = 0$ , then the condition to satisfy the condition of a maximum may be determined by the three simultaneous equations:

$$\begin{aligned}\frac{\partial F}{\partial x} + \lambda \frac{\partial \phi}{\partial x} &= 0, \\ \frac{\partial F}{\partial y} + \lambda \frac{\partial \phi}{\partial y} &= 0, \\ \phi(x,y) &= 0.\end{aligned}\tag{107}$$

In the case under discussion the variables  $x$  and  $y$  are replaced by  $t_1$  and  $t_0$ . If  $t_1$  is set equal to  $kT$  the variables become  $T$  and  $t_0$ . These quantities appear in the basic equation (97) and inasmuch as that equation is used in the analysis here it is convenient to rewrite it in abbreviated form as

$$\begin{aligned}2 \tan^{-1} a \tanh \left[ c(t_1 + t_0) - b \right] - 2 \tan^{-1} a \tanh (ct_0 - b) \\ = \omega_c K (2\pi/\omega_m - t_1) = \omega_c K (T - kT) = \omega_c KT (1-k),\end{aligned}\tag{108}$$

or

$$2 \tan^{-1} (a \tanh A) - 2 \tan^{-1} (a \tanh B) = \omega_c KT (1-k),\tag{109}$$

where

$$a = \frac{1 - K}{\sqrt{1 - K^2}}, \quad b = \tan^{-1} a, \quad c = \omega_c \frac{\sqrt{1 - K^2}}{2},$$

$$A = c(t_1 + t_0) - b, \quad \text{and } B = ct_0 - b. \quad (110)$$

It is desired to maximize

$$F(T, t_0) = 2 \tan^{-1} (a \tanh A) - 2 \tan^{-1} (a \tanh B)$$

subject to

$$\phi(T, t_0) = 0 = 2 \tan^{-1} (a \tanh A) - 2 \tan^{-1} (a \tanh B) - \omega_c K T (1 - k).$$

If equation (107) is utilized, there is obtained, after differentiation and some simplification, the three following simultaneous equations  $T$ ,  $t_0$ , and  $\lambda$ .

$$\frac{ac (\lambda + 1)}{1 + (a^2 + 1) \sinh^2 A} - \frac{\omega_c K \lambda (1 - k)}{2} = 0,$$

$$(\lambda + 1) \left[ \frac{ac}{1 + (a^2 + 1) \sinh^2 A} - \frac{ac}{1 + (a^2 + 1) \sinh^2 B} \right] = 0, \quad (111)$$

$$\text{and } \phi(T_1, t_0) = 0.$$

The solution is direct in this example because of the simplicity of the second equation. It is evident that it is satisfied if

$$1 + (a^2 + 1) \sinh^2 A = 1 + (a^2 + 1) \sinh^2 B \quad (112)$$

which occurs if

$$A = \pm B. \quad (113)$$

The solution  $A = + B$  is trivial since in that case the excursion  $\underline{d}$  would be identically equal to zero for all values of  $t$ . Therefore the solution  $A = - B$  must satisfy the conditions. If it is utilized, equation (109) can be written as

$$-4 \tan^{-1} (a \tanh B) = \omega_c K T (1-k), \quad (114)$$

and, since

$$A = c(t_1 + t_0) - b = ct_1 + ct_0 - b = ct_1 + B, \quad (115)$$

and, with

$$A = - B, \text{ also, with } t_1 = kT$$

there is obtained

$$B = - ct_1/2 = - ckT/2$$

so equation (114) can finally be written as

$$-4 \tan^{-1} (a \tanh \frac{ckT}{2}) = \omega_c K T (1-k). \quad (117)$$

This equation is extremely important because it permits calculation of the band of synchronization for any value of duty cycle  $\underline{k}$ . It is best illustrated by an example. Let it be assumed that square-wave modulation is applied, in this case the duty cycle  $\underline{k}$  has a magnitude of one-half. For simplification the scaling factor,  $\omega_c$ , can either be set equal to unity or incorporated into the time function (i.e., let  $\omega_c T = T'$  as a new variable). Either method is valid, but in this example the value

of  $\omega_c$  will be taken as unity. Next, let the parameter  $K = 0.35$ .

(Note: equation (103) showed that  $\underline{K}$  cannot exceed a magnitude of  $1/2$  when  $\underline{k} = 1/2$ ). Now, with  $\underline{k} = 1/2$  and  $\underline{K} = 0.35$  equation (117) reduces to

$$-4 \tan^{-1} (0.694 \tanh 0.174T) = 0.175T. \quad (118)$$

This transcendental equation can be solved without great difficulty and in this case leads to an answer of approximately  $T = 13$ . Then  $\omega_m$ , which is  $2\pi/T$ , becomes equal to  $0.484$ . The given data and the results can be more generally stated as: given that the ratio of  $\omega_s/\omega_c$  is equal to  $0.35$  it is found that the minimum permissible modulating frequency ratio,  $\omega_m/\omega_c$ , is  $0.484$ .

Equation (117) combined with equations (103) and (105) permit calculation of the band of synchronization for any prescribed condition. Data for three values of duty cycle have been computed and plotted in Figure 18. Data for the case of square-wave modulation have been computed and plotted in Figure 19. This latter figure also illustrates the results of experiments whose purpose was to determine the relationships expressed in equation (117).

An example will illustrate the quantities described by Figures (18) and (19). Let it be presumed that an oscillator is subjected to an interrupted wave-train which has a modulating (interrupting) frequency  $f_m$ , a duty cycle  $\underline{k}$ , and a frequency  $f_1$ . The following data apply:

- $f_o$  = free-running frequency of oscillator = 20,000 cps
- $V_g$  = grid-voltage of free-running oscillator = 1.6 v. peak
- $Q$  = effective  $Q$  of oscillator tuned circuit = 5



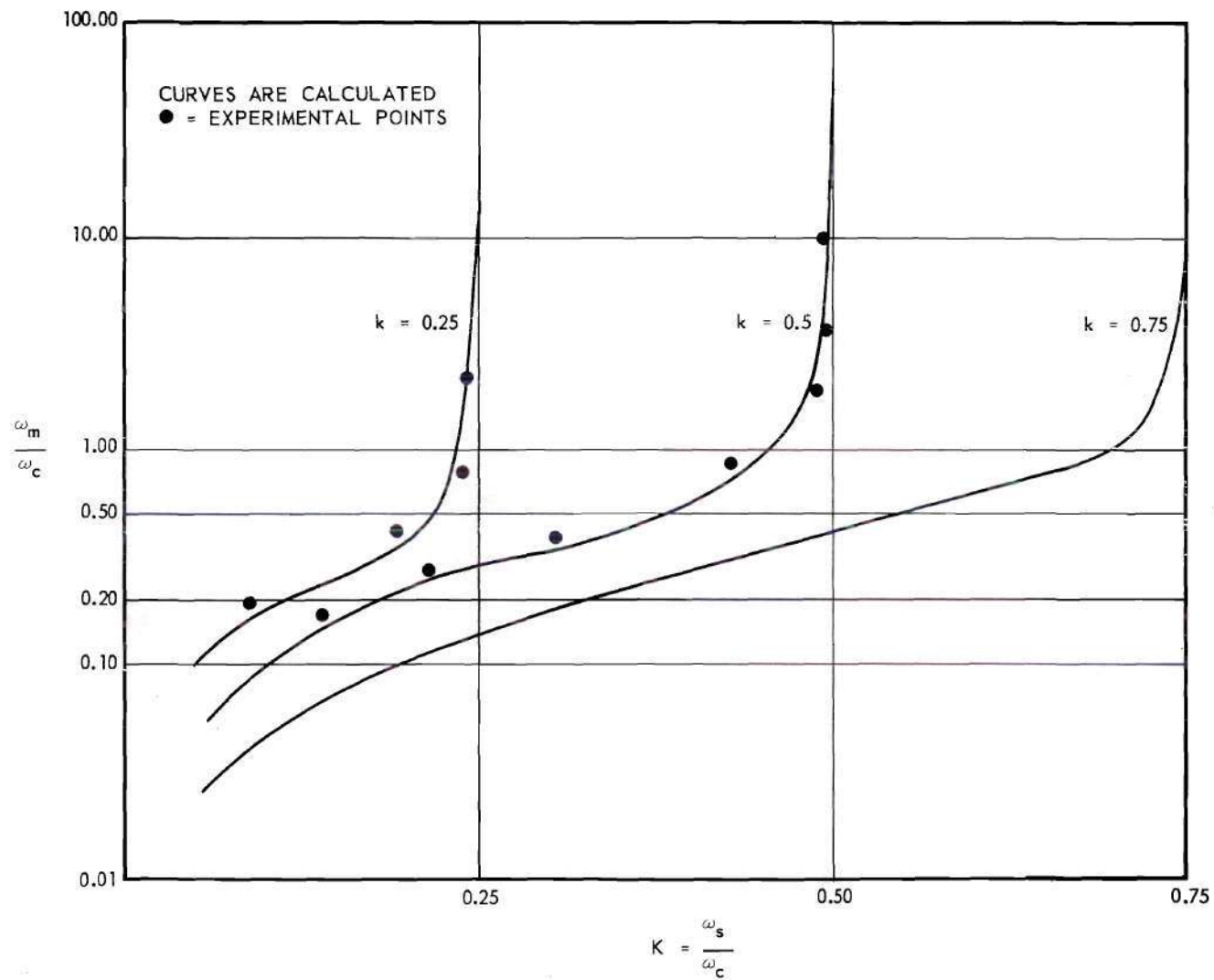


FIGURE 18. MODULATION FREQUENCIES REQUIRED FOR SYNCHRONIZATION.

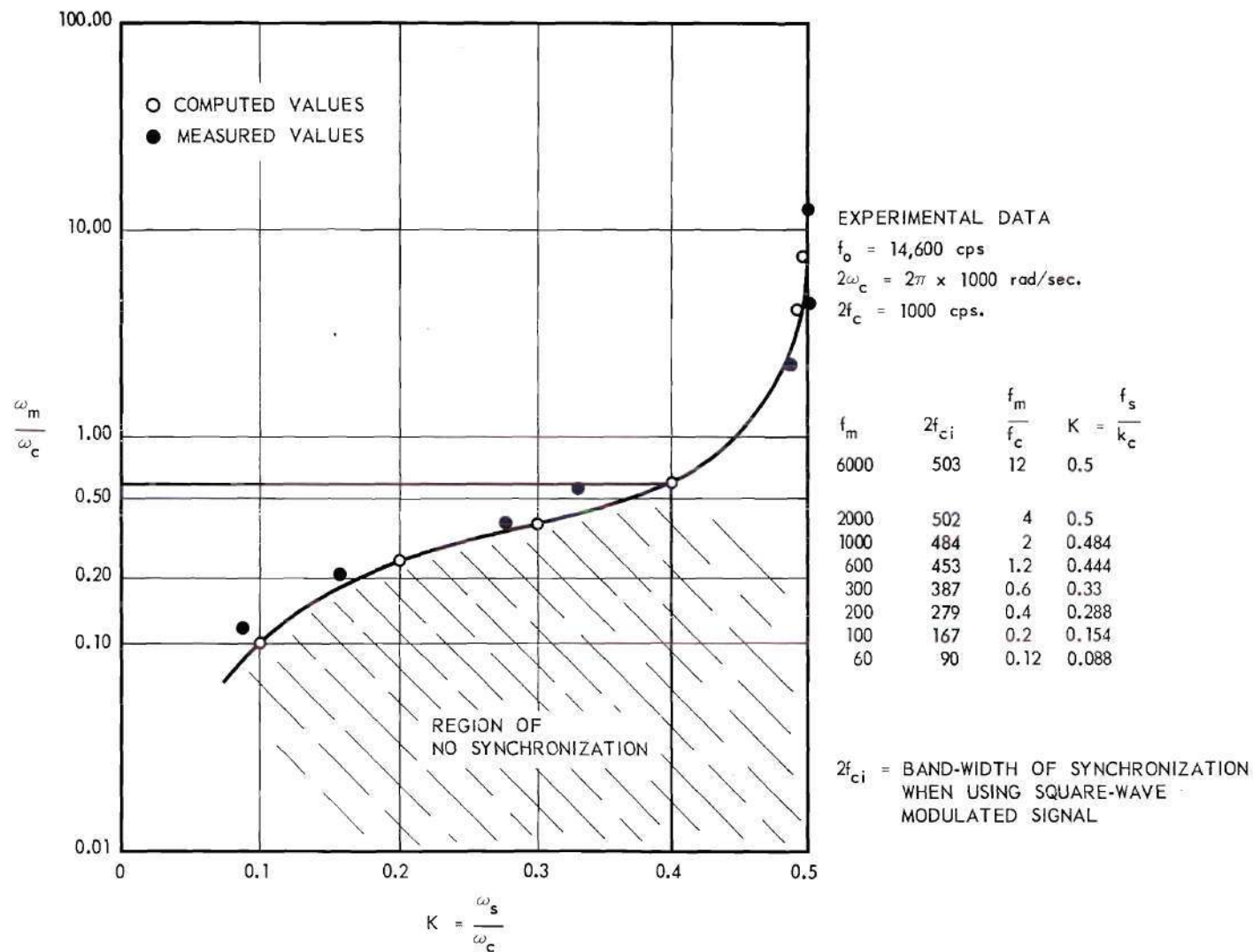


FIGURE 19. MODULATION FREQUENCIES AND BANDS OF SYNCHRONIZATION WHEN SIGNAL IS MODULATED WITH SQUARE WAVE.

$V_1$  = amplitude of synchronizing signal = 0.2 volts peak

$k$  = duty cycle of interrupted wave train =  $1/2$ .

Then,

$$\omega_c = \frac{\omega_o V_1}{2Q V_g} = 500\pi \text{ rad/sec, and } f_c = 250 \text{ cps.}$$

For this example, it has been assumed that the duty cycle,  $k$ , is equal to one-half. Then  $K_{\max}$ , for high modulating frequencies, is also one-half, which is to say that  $f_1$  must fall within the limits of  $20,000 \pm 125$  cps. Suppose that  $f_1$  is selected to be 20,100 cycles. For this case  $K = f_s/f_c = 100/250 = 0.4$ . Figure (19) is entered with this value of  $K$ , and the intersection of the vertical line  $K = 0.4$  and the curve  $k = 1/2$ , is located. It is then found that the ratio of  $\omega_m/\omega_c$  corresponding to this point is approximately 0.55, whence the minimum allowable value of  $\omega_m$  is  $275\pi$  radians/sec and  $f_m = 1375$  cps. Therefore it is concluded that if synchronization is to persist under the assumed conditions the rate of interruption of the input signal must be equal to or greater than 1375 times per second. Equivalent procedures follow for other values of duty cycle.

The curves of Figures 18 and 19 are seen to assume the status of "Go-No Go" divisions. For any particular duty cycle, the region above and to the left of its applicable curve represents the area of synchronization whereas that to the right and below represents the area of no synchronization. The curve itself of course represents the extreme limit of synchronization and is not presumed to represent a desirable condition of operation. It will be shown that the index of phase modulation becomes

large near the bounding curve but decreases as one moves to the left and up within the region of synchronization.

### Summary of Chapter

It has been shown that the phase angle,  $\theta$ , representing the instantaneous phase between synchronizing signal and oscillator voltage, oscillates during both presence and absence of synchronizing signal. When the oscillation is within prescribed bounds synchronization may be attained, the basic requirement being that the net phase during a modulation period shall be zero. If the oscillation exceeds the prescribed bounds synchronization is not possible. The maximum excursion of the oscillation increases with increase of modulation period, therefore it is evident that there is a minimum modulation frequency for which synchronization can persist.

It has been shown that the minimum modulation frequency and the maximum deviation of synchronizing frequency are uniquely related. It has been further shown that, for high modulating frequencies, the bandwidth of synchronization is equal to the product of  $\omega_c$  (the bandwidth with c-w synchronizing signal) and of  $k$ , the duty cycle. Since the amplitude of the fundamental component of the input is equal to the product of the unmodulated amplitude and of  $k$ , the duty cycle, it follows that:

The synchronizing action of an interrupted wave train whose interruption frequency is such that  $\omega_m/\omega_c \gg 1$  is the same as though the oscillator were receiving a c-w synchronizing signal whose amplitude was equal to the fundamental component of the interrupted wave train.



## CHAPTER V

### FREQUENCY SPECTRUM OF SYNCHRONIZED OSCILLATOR

#### Phase Deviations in Disturbed Oscillator

In the introduction it was pointed out that if an oscillator is synchronized by a c-w signal its frequency spectrum is very simple. Prior to the injection of the synchronizing signal the spectrum contains energy at the free-running frequency  $f_0$  and its harmonics. After injection of a "locking" signal of frequency  $f_1$  the spectrum contains energy at the new frequency and its harmonics, the energy at the original frequency having disappeared. If it is presumed that the synchronizing signal is a pure sinusoidal wave, containing the fundamental frequency  $f_1$  only, then any harmonics of  $f_1$  appearing in the output of the oscillator must be due to the nonlinear action of the self-limiting circuit.

When the synchronizing signal is an interrupted wave train the frequency spectrum of the output must be expected to be less simple. That some complexity must exist may be inferred from a consideration of steady-state theory and from transient theory. From the steady-state viewpoint one may consider the synchronizing signal as an interrupted wave train whose form and spectrum are shown in Figure 15. It is seen that the synchronizing signal contains not only the frequency  $f_1$  but also the frequencies  $f_1 \pm nf_m$ . The presence of these added frequencies in the input would result in their presence in the output also. The oscillator, acting as a regenerative amplifier, amplifies some frequencies and attenuates

others in amounts proportional to the selectivity of the amplifier (oscillator).

A much more definitive approach is found in transient analysis, and the information relative to phase variations assembled in the previous chapter can be directly utilized. For example, it was shown that the basic criterion for synchronization was

$$\omega_c \int_0^{t_1} (K - \sin \theta) dt + \omega_c \int_{t_1}^{2\pi/\omega_m} K dt = 0 \quad (83)$$

where

$$\theta = 2 \tan^{-1} \left[ \frac{1}{K} - \frac{\sqrt{1-K^2}}{K} \tanh \omega_c \frac{\sqrt{1-K^2}}{2} (t + t_0) \right]. \quad (36a)$$

and it was demonstrated that the minimum modulating (gating) frequency for which synchronization could persist was given by equation (102).

These minimum values were illustrated in Figures 18 and 19 by the curves which separate the regions of "synchronization" and those of "no synchronization".

It is convenient to begin an analysis by defining a modulation index of the form used in the discussion of square-wave frequency modulation. This was given in chapter 3 as

$$m = \Delta\omega/\omega_m. \quad (64)$$

An equivalent form applicable to the present analysis is

$$m = \omega_s/\omega_m, \quad (119)$$

which is conveniently expressed as

$$m = K \frac{\omega_c}{\omega_m} . \quad (120)$$

Significant information applicable to the magnitude of the modulation index can be obtained from the coordinate data of Figures 18 and 19. These figures contain curves which define the limiting conditions for synchronization, but in particular they represent plots of functions wherein  $\omega_s$  is the independent variable and  $\omega_m$  is the dependent variable. Therefore it is evident that every point of each figure represents a specific ratio of  $\omega_s$  to  $\omega_m$ , and hence represents the specific modulation index which is associated with that point.

Figure 19 is shown in part in Figure 20. The latter figure contains boundary curves copied from the original figure and also includes several decimal values which are interpolated between segments of the boundary curves and appear at several points within the region of synchronization. These numbers represent the modulation index (the ratio  $\omega_s/\omega_m$ ) which correspond to their respective positions in the figure. They show that, just as predicted in the previous chapter, the index corresponding to any selected value of  $K$  reaches its maximum value when  $\omega_m$  is the minimum for which synchronization is maintained, (that is, at the boundary curve) and decreases as  $\omega_m$  is increased. The increase is found, by definition of the modulation index, to be in inverse proportion to  $\omega_m$ .

A graphic illustration of the phase variations in each portion of a modulation cycle was shown in Figure 17 where it served as a guide in

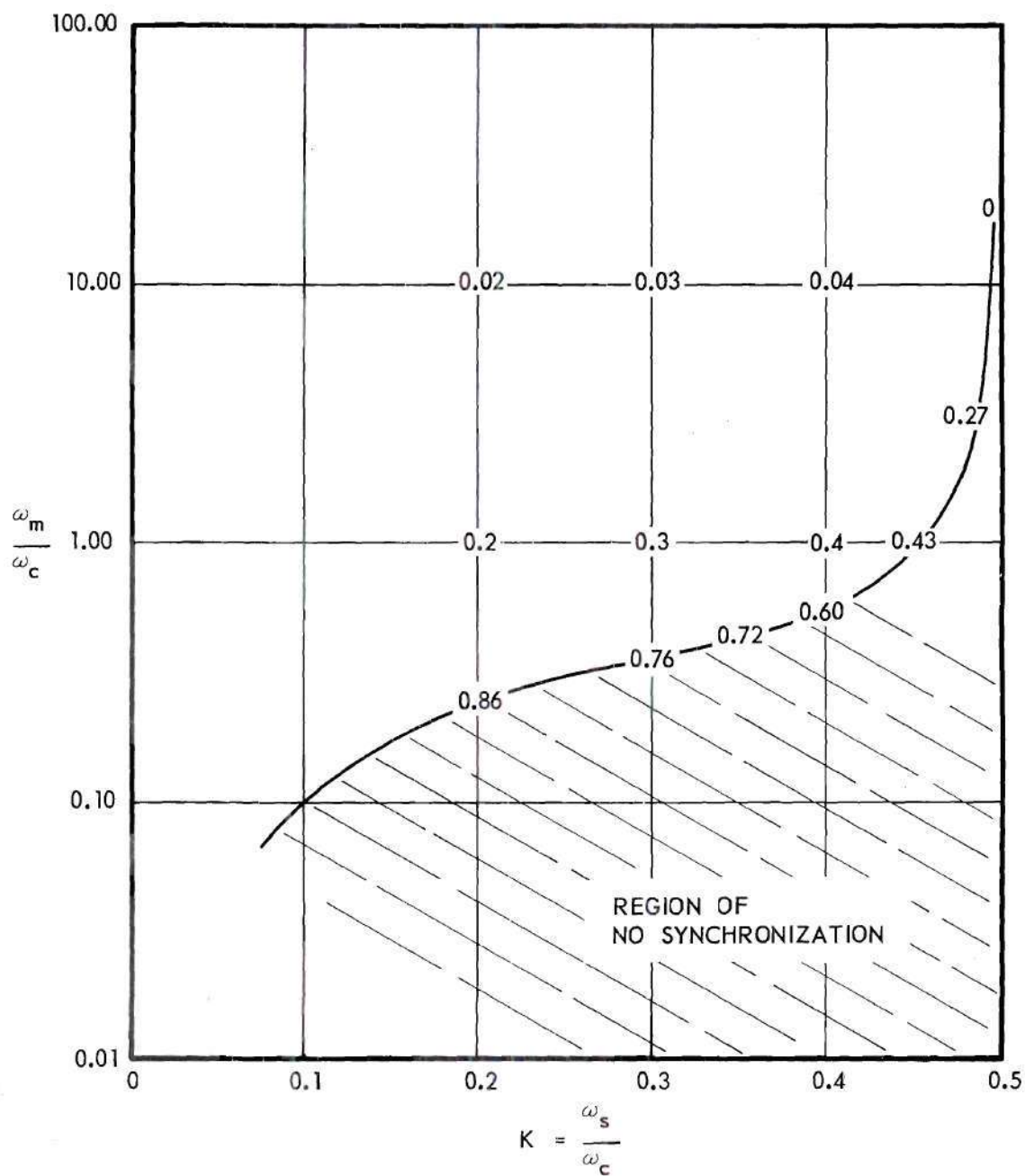


FIGURE 20. MODULATION INDICES OF PHASE-MODULATED OSCILLATOR VOLTAGE.



determining the limits of the band of synchronization appropriate to a selected value of the ratio  $K = \omega_s / \omega_m$ . The same figure is useful in the discussion of the frequency spectrum because the linearity (or non-linearity) of the variations in phase is illustrated therein. However, before attributing special significance to any part of that figure it is necessary to define the quantities considered and the parameters involved.

The synchronizing signal which is utilized was illustrated previously in Figure 8. It showed that the synchronizing voltage was applied between time zero and time  $t_1$  but was absent during the remainder of the modulation cycle. It is repeated for reference in Figure 21.

Inasmuch as the oscillator is to be synchronized to frequency  $f_1$ , the variation of the phase angle  $\theta$  is referred to the vector which rotates with angular frequency  $\omega_1$ . This method of reference is in accord with the definitions used in previous sections. Then

$$\begin{aligned} \frac{d\theta}{dt} &= \omega_s - \omega_c \sin \theta \\ &= \omega_c (K - \sin \theta), \end{aligned} \quad 0 \leq t \leq t_1 \quad (121a)$$

and

$$\frac{d\theta}{dt} = \omega_s = \omega_c K, \quad t_1 \leq t \leq 2\pi/\omega_m \quad (121b)$$

and if  $\omega_m$  is very large,  $\theta$  is approximately  $90^\circ$  (at the edge of the band of synchronization) whence  $\sin \theta$  is then unity. In this case

$$\frac{d\theta}{dt} = \omega_c (K - 1). \quad 0 \leq t \leq t_1 \quad (122)$$

Figure 17 graphically illustrated the variations of  $\theta$  for each of three values of the ratio  $\omega_s/\omega_m$ . In that figure, the time  $t_1$ , which represents the instant at which the synchronizing signal is interrupted (becomes zero) has been chosen to lie on the same vertical line in all three examples. This location is a matter of convenience only and has no significance in the analysis.

Consider part (C) of Figure 17. The curves shown illustrate the case given in equation (122) when  $\omega_m$  is very high and the rate of change of  $\theta$  is approximately a constant during the presence of the synchronizing signal. But the rate of change of angle during the absence of synchronizing signal ( $t_1 \leq t \leq 2\pi/\omega_m$ ) is always a constant and equal to  $\omega_c K$ . The straight lines in each of the parts (A), (B) and (C) have a slope given by  $\omega_c K$ . In part (C) the slope of the left portion is very nearly constant, hence two constant slopes produce the triangular shape.

Next consider the case when  $\omega_m$  is small, in part (A) of the figure. In this case the angle oscillates over a relatively wide range and the phase deviation follows the curve derived from the nonlinear equation for  $\Delta\theta$  in the region  $t = 0$  to  $t = t_1$ .

The form of the frequency spectrum associated with each of these figures may be inferred by comparison of Figures 17(C), 12 and 13. These latter figures showed that if the phase deviations were linear and the modulation frequency was high then the spectrum was very simple, consisting of a carrier,  $f_1$ , and small sidebands of frequencies  $f_1 \pm nf_m$ . Now the triangular form of Figure 17(C) is essentially identical to that of Figure 12, hence it may be expected to be associated with a frequency

spectrum 13(A). Non-symmetry will result in some changes in the spectrum, but these will be changes in form rather than in substance.

This somewhat special case of high modulating frequency is important because its frequency spectrum is simple and stable. It is therefore desirable to record generalized equations applicable to linear variations in phase which will permit calculation of the spectrum for any value of duty cycle. The analysis required has been performed and appears in the literature. The following discussion is due to Corrington<sup>(16)</sup>.

#### Spectrum of Rectangular Pulse F-M Wave

A wave, the frequency and phase of which are given in Figure 22, is subjected to analysis.

If the phase deviation,  $\Delta\theta$ , is expressed as  $S(t)$  the equation for the modulated wave can be written

$$\begin{aligned} e &= E \sin \left[ \omega_t + S(t) \right] \\ &= E \sin \omega_t \cos S(t) + E \cos \omega_t \sin S(t). \end{aligned} \quad (123)$$

Since  $\cos S(t)$  is symmetric about the origin it can be expanded in a cosine series. Similarly,  $\sin S(t)$  is skew symmetric about the origin and can be expanded in a sine series.

From Figure 22

$$\begin{aligned} \cos S(t) &= \cos m\theta & 0 \leq \theta \leq \pi x \\ &= \cos \frac{\pi x (\pi - \theta)}{1 - x} & \pi x \leq \theta \leq \pi \\ &= \sum_{n=0}^{\infty} b_n \cos 2n\pi x t, \end{aligned} \quad (124)$$

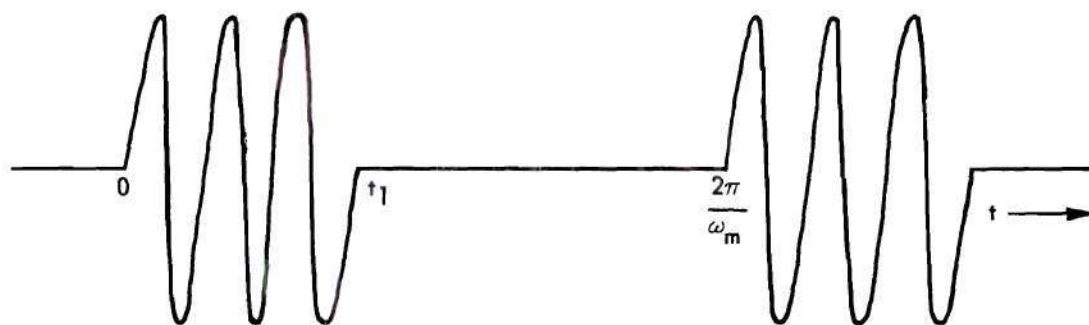


FIGURE 21. INTERRUPTED WAVE-TRAIN SYNCHRONIZING SIGNAL.

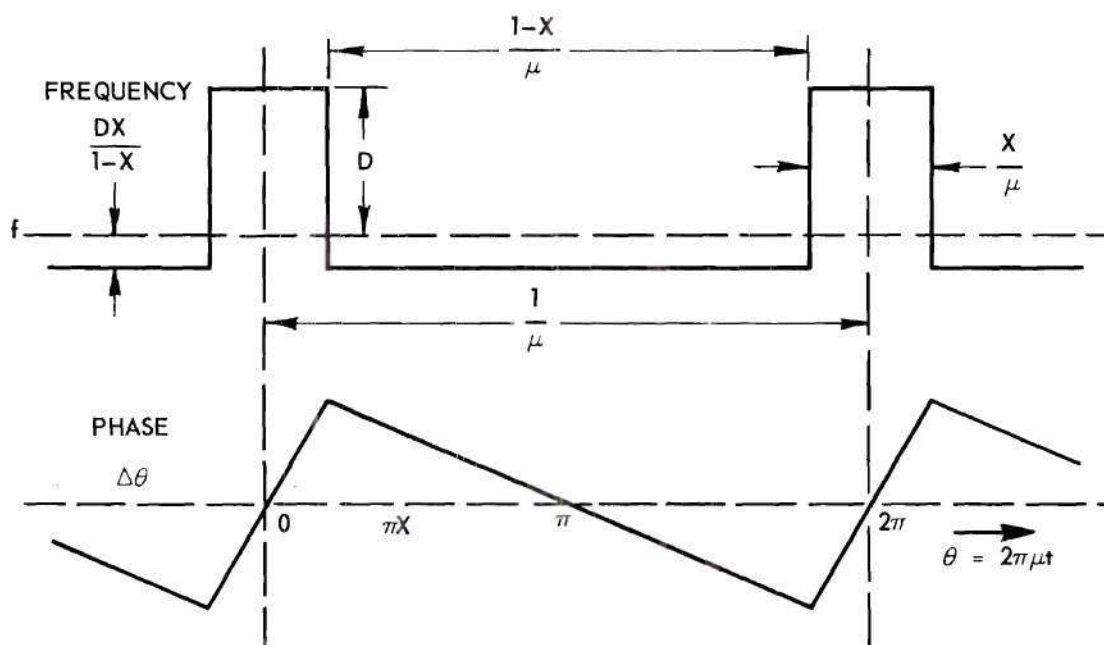


FIGURE 22. PHASE AND FREQUENCY OF RECTANGULAR-PULSE FM WAVE.



where

$$b_n = \frac{2}{\pi} \int_0^{\pi x} \cos m\theta \cos n\theta d\theta + \frac{2}{\pi} \int_{\pi x}^{\pi} \cos \frac{mx(\pi-\theta)}{1-x} \cos n\theta d\theta, \quad (125)$$

and

$$b_0 = \frac{1}{\pi mx} \sin \pi mx. \quad (126)$$

Similarly,

$$\begin{aligned} \sin S(t) &= \sin m\theta & 0 \leq \theta \leq \pi x \\ &= \sin \frac{mx(\pi - \theta)}{1-x} & \pi x \leq \theta \leq \pi \\ &= \sum_{n=0}^{\infty} c_n \sin 2n\pi t, \end{aligned} \quad (127)$$

where

$$c_n = \frac{2}{\pi} \int_{\theta}^{\pi x} \sin m\theta \sin n\theta d\theta + \frac{2}{\pi} \int_{\pi x}^{\pi} \sin \frac{mx(\pi - \theta)}{1-x} \sin n\theta d\theta. \quad (128)$$

The integrals are evaluated and the values of  $c_n$  and of  $b_n$  are substituted in the general equation (74) to give, finally

$$e = \frac{mE}{\pi (m-n) (mx - nx + n)} \sin \pi x (m-n) \sin (\omega + 2n\pi\mu) t. \quad (129)$$

The carrier and first pair of sidebands are given as

$$\text{Carrier} = E \frac{\sin \pi mx}{\pi mx} \sin \omega t, \quad (130)$$

$$\begin{aligned} \text{First upper s.b.} = \frac{mE}{\pi(m-1) (mx-x+1)} \sin \pi x (m-1) \\ \sin (\omega + 2n\pi\mu) t, \end{aligned} \quad (131)$$

$$\begin{aligned} \text{First lower s.b.} = \frac{mE}{\pi(m+1) (mx+x-1)} \sin \pi x (m+1) \\ \sin (\omega - 2n\pi\mu) t. \end{aligned} \quad (132)$$

The indeterminate cases must be evaluated separately:

$$\begin{aligned} \text{Case I. } m = n \quad \frac{1}{2} (b_n + c_n) &= x, \\ \text{Case II. } \frac{mx}{1-x} = -n \quad \frac{1}{2} (b_n + c_n) &= \frac{1}{\pi(m-n)} \\ &\sin \pi x(m-n) + (-1)^n(1-x), \end{aligned} \quad (133)$$

$$\begin{aligned} \text{Case III. } m = -n \quad \frac{1}{2} (b_n - c_n) &= -x, \\ \text{Case IV. } \frac{mx}{1-x} = n \quad \frac{1}{2} (b_n - c_n) &= \frac{1}{\pi(m+n)} \\ &\sin \pi x(m+n) + (-1)^n(1-x). \end{aligned}$$

If  $x = 1/2$ , Figure 22 illustrates square-wave frequency-modulation and equation (129) reduces to the same form as equation (68) and

equation which was developed directly from square-wave modulation using the complex Fourier analysis.

Some aspects of the spectra are illustrated in Figure 23 for a few values of modulation index  $\underline{m}$  and duty cycle  $\underline{k}$ . Modulation indices of 0.25, 0.50, 0.75, and 1.50 are illustrated, and each of the corresponding spectra is plotted for three separate values of duty cycle of 0.10, 0.25, and 0.50. The frequency of the modulating signal has been maintained constant in order that the various spectra may be easily compared.

It is seen for all values of  $\underline{m}$  less than unity that the sidebands are relatively small compared to the carrier, but for modulation indices of 1.50 or greater the sidebands may exceed the carrier in amplitude. When the modulation index is equal to 1.5 and the duty cycle is equal to 0.50 (a duty cycle of this value corresponds to that of square-wave modulation) both the first and second pairs of sidebands are of greater amplitude than the carrier. This condition is in accordance with the results obtained by van der Pol and described in chapter 3.

The modulation index of an oscillator synchronized by an interrupted wave train has been defined as the ratio of  $\omega_s$  to  $\omega_m$  and representative indices computed from this ratio appeared in Figure 20. In the analysis thus far given the effect of phase modulation has been calculated upon the basis of linear rates of change of phase. When the phase change can be represented by straight lines the Fourier analysis results in the formulas already given.

The actual rate of change of phase is nonlinear, although the deviation from linearity is in most cases insufficient to produce spectra

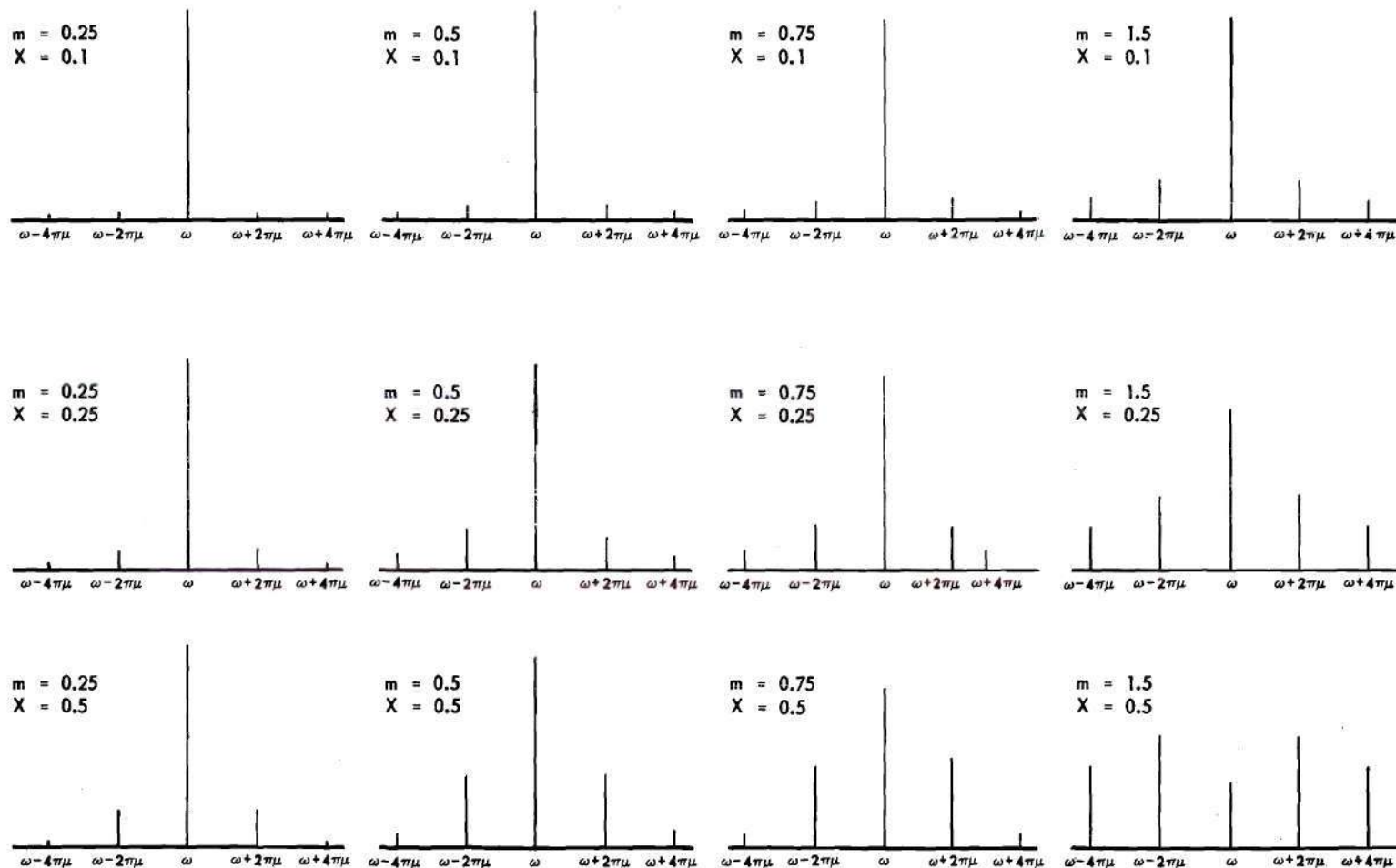


FIGURE 23. FREQUENCY SPECTRA OF RECTANGULAR-PULSE FM WAVE.



greatly different from those shown in Figure 23. An introduction to the actual form of the phase deviation was given in Figure 17 but numerical values were not included there.

Actual magnitudes of  $\Delta\theta$ , the phase deviation in an oscillator synchronized by an interrupted wave train, have been calculated for two selected values of the ratio  $K = \omega_s/\omega_m$  chosen from data supplied in Figure 20. The values selected are representative of those existing when the modulation frequency is the minimum possible. That is, they represent indices lying along the curve which separates the region of synchronization from that of no synchronization. It was previously stated, and it may be seen from Figure 20 that the largest indices are found at the bounding curve which also corresponds to the condition of greatest phase nonlinearity.

The values of  $K$  which have been selected for illustration are 0.2 and 0.4. For each of these values of  $K$  the corresponding value of the ratio  $\omega_m/\omega_c$  has been determined from Figure 20. The phase deviation  $\Delta\theta$  has then been calculated and plotted for each value of  $K$  and by using  $\omega_c t$  as the total abscissa. The results are shown in Figure 24 where an arbitrary reference on the abscissa and positive and negative time intervals have been employed in order to present both curves on a comparative basis.

The curves are best understood by considering the oscillator action corresponding to a selected value of  $K$ . For example, when  $K = 0.4$ , the modulation index found at the boundary curve in Figure 20 is given as 0.6. Hence  $K = \omega_s/\omega_c = 0.4$  and  $m = \omega_s/\omega_m = 0.6$  from which it follows that  $\omega_c T \approx 10$ . Inasmuch as square-wave modulation is involved, the time element

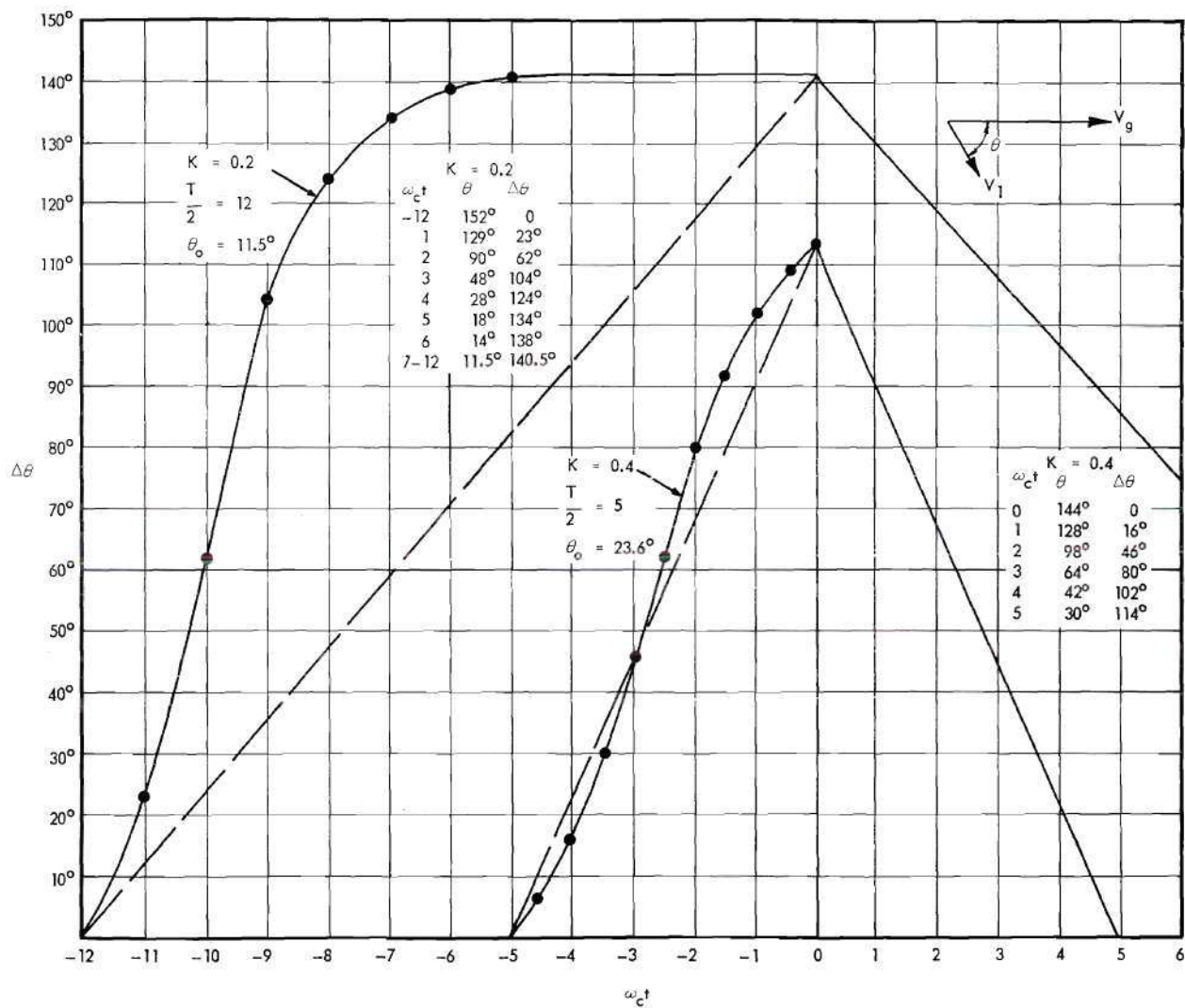


FIGURE 24. PHASE DEVIATIONS OF AN OSCILLATOR SYNCHRONIZED BY SQUARE-WAVE MODULATED WAVE TRAIN.

must be equally divided between presence and absence of synchronizing signal. This division may be observed in the figure. The succeeding steps in developing the curves includes determination, using equations (110) and (116), of the value of the quantity  $\omega_c t_0$ . It will be recalled that this quantity represented the constant of integration in the equation

$$\theta = 2 \tan^{-1} \left[ \frac{1}{K} - \frac{\sqrt{1-K^2}}{K} \tanh \omega_c \frac{\sqrt{1-K^2}}{2} (t + t_0) \right]. \quad (36a)$$

After determination of the value of the constant, discrete values of the angle  $\theta$  are calculated, employing values of  $\omega_c t$  between zero and  $\pm 5$ , ( $\omega_c T = 10$ ). The calculated values of  $\theta$  appear in the tables inserted in Figure 24. The left portion of each curve of that figure represents the action of the phase angle during the presence of synchronizing signal, the right portion represents the action during the absence of synchronizing signal.

The deviation from linearity of the left portion of the curve corresponding to  $K = 0.4$  is relatively small but is very much greater when  $K = 0.2$ . In the latter case the value of  $\omega_c T$  is calculated and shown to be approximately twenty-four ( $-12 \leq \omega_c t \leq 12$ ). The considerably greater time during which the phase angle may change results in the larger phase deviation calculated and illustrated. Time element is sufficiently great, in fact, to permit  $\theta$  to reach and maintain its terminal value  $\theta_0$ , where  $\theta_0 = 2 \tan^{-1} (1 - \sqrt{1-K^2})/K$ .

The usual methods of Fourier analysis may be employed to compute the spectra resulting from each of these curves but numerical integration

must be used in order to calculate the desired components. In Figure 25 the spectrum for each of the two curves of Figure 24 are shown. The spectrum which would have resulted from the straight lines of Figure 24 (dotted plus solid) are also shown for purposes of comparison.

The method of numerical analysis used to compute the components follows that described by Scarborough<sup>(17)</sup> in his text on numerical mathematical analysis. A harmonic analysis of the curves employed the method in which 24 equi-spaced ordinates are used and which results in approximate evaluation of the first eleven harmonics.

The considerable nonlinearity of the reference curves leads to a difference between the resultant spectrum and the spectrum which would exist if the phase deviations were linear. Fortunately, operation of the synchronized oscillator may usually be expected to occur at frequencies other than those at the "edge of the band of synchronization". In this case the modulation index is much smaller and more nearly linear phase deviations result. Hence the spectra of Figure 23 may be utilized with small error in most cases.

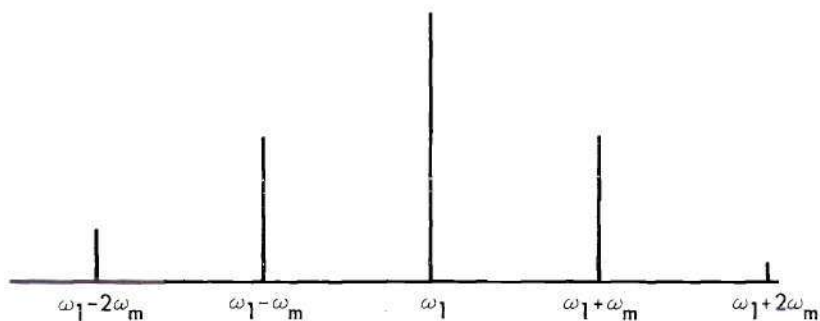
Experimentally determined spectra are shown in Figure 26. It is seen that these correspond in general form quite closely to those spectra computed and plotted in Figure 23, but that effects of nonlinearity appear in the form of nonsymmetry of the sidebands. Actually, a complete prediction of the effect upon the sidebands must include one additional factor. This factor is the amplitude modulation which is present in an oscillator which is synchronized by an interrupted wave train. Such amplitude variation is not great, if the synchronizing signal is considerably



$$K = 0.2 \quad m = 0.76$$

CALCULATED FOR STRAIGHT LINE

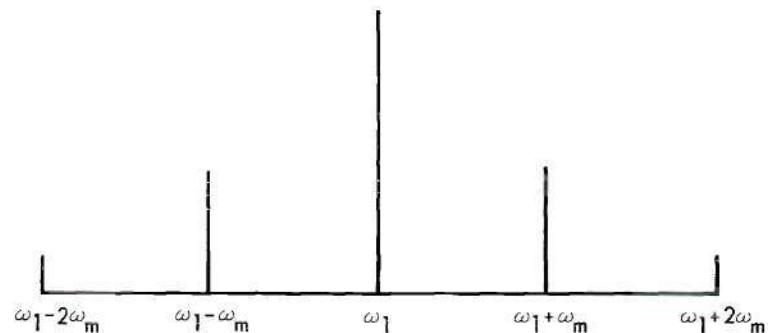
$$0.78 \sin \omega_1 t + 0.42 \sin (\omega_1 + \omega_m) t + 0.413 \sin (\omega_1 - \omega_m) t \\ + 0.05 \sin (\omega_1 + 2\omega_m) t + 0.127 \sin (\omega_1 - 2\omega_m) t$$



$$K = 0.4 \quad m = 0.64$$

CALCULATED FOR STRAIGHT LINES

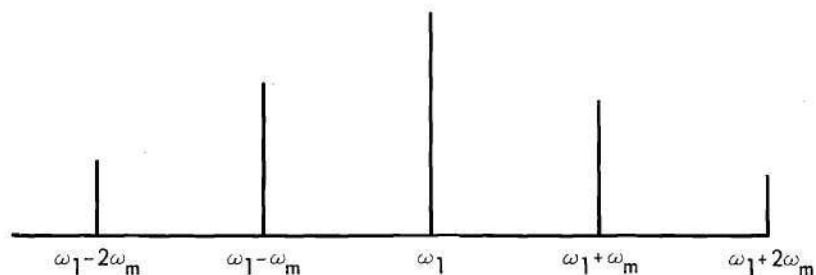
$$0.84 \sin \omega_1 t + 0.369 \sin (\omega_1 + \omega_m) t \\ + 0.1 \sin (\omega_1 + 2\omega_m) t$$



$$K = 0.2$$

CALCULATED FROM CURVES

$$0.686 \sin \omega_1 t + 0.384 \sin (\omega_1 + \omega_m) t + 0.475 \sin (\omega_1 - \omega_m) t \\ + 0.178 \sin (\omega_1 + 2\omega_m) t + 0.212 \sin (\omega_1 - 2\omega_m) t \\ + 0.132 \sin (\omega_1 + 3\omega_m) t + 0.111 \sin (\omega_1 - 3\omega_m) t$$



$$K = 0.4$$

CALCULATED FROM CURVES

$$0.819 \sin \omega_1 t + 0.414 \sin (\omega_1 + \omega_m) t \\ + 0.402 \sin (\omega_1 - \omega_m) t + 0.14 \sin (\omega_1 + 2\omega_m) t$$

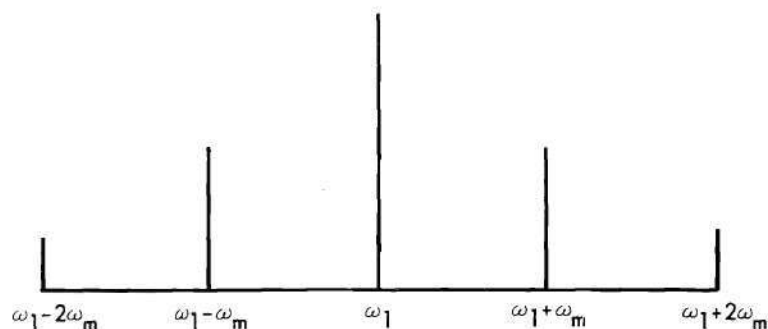


FIGURE 25. SPECTRA OF OSCILLATOR WITH PHASE DEVIATION OF FIGURE 24.

ALL SPECTRA TAKEN WITH  
OSCILLATOR SYNCHRONIZED  
AND WITH FREQUENCY AT  
EDGE OF BAND OF SYNC.

EXPERIMENTAL DATA TUNED  
PLATE OSCILLATOR BANDWIDTH  
C-W SYNC =  $2f_c = 1000$  cps.  
 $V_1 = 1/6 V_{go}$ . SQUARE-WAVE  
MODULATED SYNC SIGNAL  
 $f_o = 14,610$  cps.

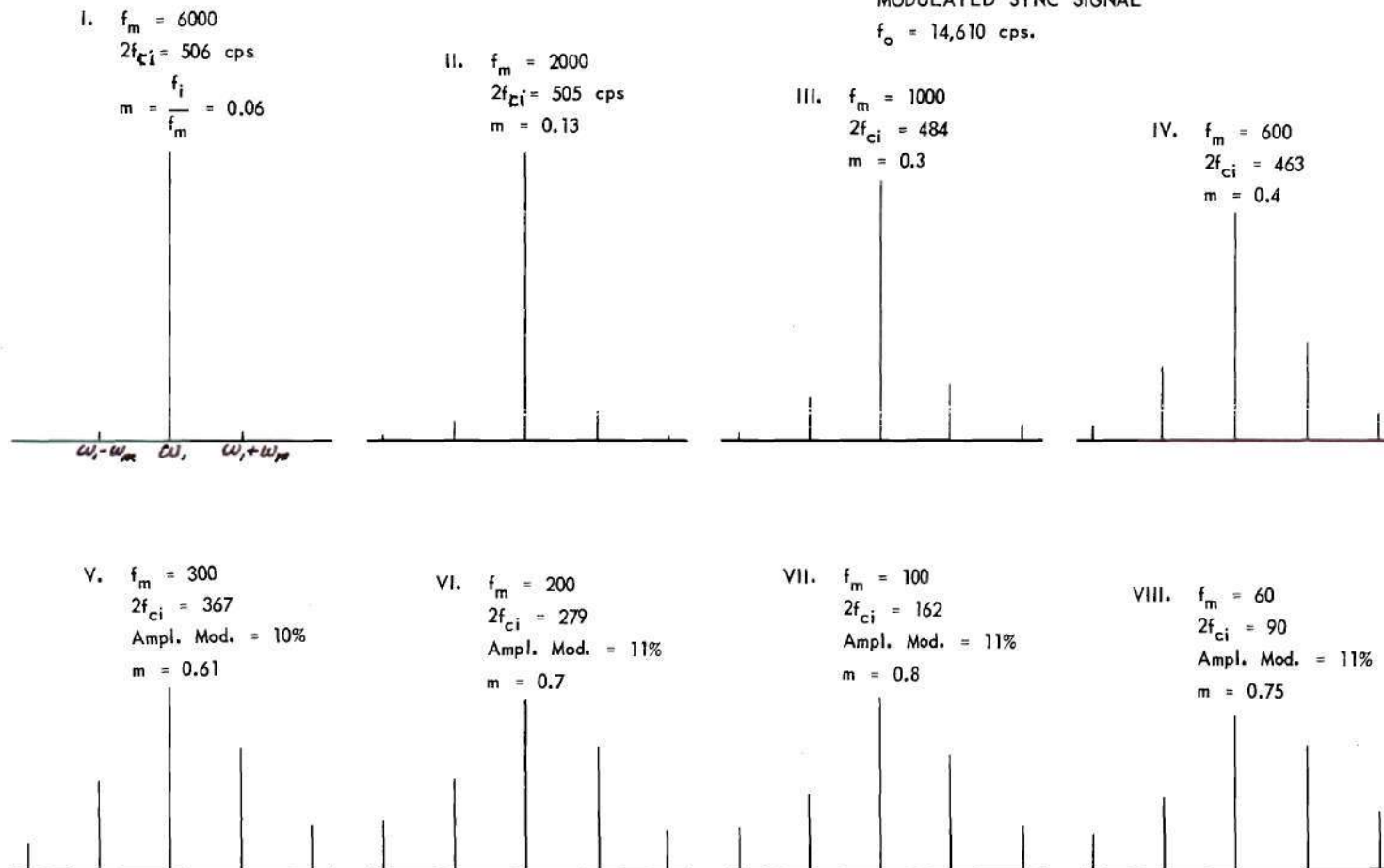


FIGURE 26. FREQUENCY SPECTRA OF OSCILLATORS SYNCHRONIZED BY SQUARE-WAVE INTERRUPTED SYNCHRONIZED SIGNAL.

smaller than the normal oscillator voltage, but its effect must be taken into consideration. The next section of this chapter described the expected magnitude of amplitude modulation and its effect upon the spectrum of the synchronized oscillator.

### Simultaneous Phase and Amplitude Modulation

The amplitudes of the frequency components of a signal which is subjected to linear phase-modulation were computed in a previous section of this chapter. A general solution was given in equation (129) which is repeated here for reference,

$$e = \frac{mE}{(m-n)(mx - nx + n)\pi} \sin \pi x (m-n) \sin (\omega + 2n\pi\mu) t \quad (129)$$

which can be written as  $e = F(n) \sin (\omega + 2n\pi\mu)t$ , where  $F(n)$  represents the amplitude of the  $n$ th sideband.

The analysis of the modulated signal considered the effect of a varying phase angle but did not consider the effect of amplitude modulation. If amplitude modulation is present it will produce a change in the spectrum previously computed.

It was shown previously that if the phase deviation,  $\Delta\theta$ , is expressed as  $S(t)$ , then the equation for the phase-modulated wave can be written as

$$e = E \sin [\omega t + S(t)] \quad (123)$$

The presence of simultaneous amplitude modulation is expressed by including a quantity  $M_A(\theta)$  as a multiplying factor. If  $\theta$  again represents the time factor  $2\pi\mu t$ , the added multiplying factor is periodic with

the same period as the phase-modulating factor. In this case the change in the frequency spectrum resulting from the presence of amplitude modulation can be computed in a relatively simple manner.

The multiplying factor  $M_A(\theta)$  is expressed as in a Fourier series, as follows:

$$M_A(\theta) = A_0 + \sum_{n=1}^{\infty} (A_n \sin n\theta + B_n \cos n\theta), \quad (134)$$

whence the wave is expressed as

$$e = \left[ A_0 + \sum_{n=1}^{\infty} (A_n \sin 2n\pi\mu t + B_n \cos 2n\pi\mu t) \right] \cdot F(n) \sin (\omega + 2n\pi\mu t) . \quad (135)$$

The general solution of equation (135) involves many terms and the numerical calculation required may be very tedious if all significant terms are considered. Fortunately, the spectrum of the synchronized oscillator being investigated does not include a large number of sidebands of large amplitude. The sidebands resulting from phase-modulation were shown in the previous section to be, in most cases, considerably smaller than the carrier. The additional energy due to simultaneous amplitude modulation will now be shown to be quite small when the amplitude of the synchronizing signal is considerably less than that of the free-running oscillator voltage.

The amplitude modulation which is generated is directly due to the varying phase angle  $\theta$ . It was shown previously that the phase angle  $\theta$  oscillates about some mean value and with a total excursion which is



subject to calculation. It was also shown that if the synchronizing signal was placed at either extreme edge of "the band of synchronization" then the mean value of  $\theta$  was  $90^\circ$ . The oscillation of  $\theta$  about this mean value was small for large values of the angular modulating frequency  $\omega_m$  but increased with decreasing modulating frequencies.

The action is visualized with the aid of vector triangles of voltage which are similar to those given in the early discussion of the phenomenon of synchronization. Figure 27 illustrates the oscillating phase angle and the effect upon the amplitude of the oscillator voltage.

The oscillator grid voltage is equal to the sum of the vector  $V_L$ , which represents the injected synchronizing signal, and of  $V_R$ , which represents the voltage returned from the tuned circuit of the oscillator. The magnitude of  $V_g$  is given to a close approximation by

$$V_g = V_R + V_L \cos \theta. \quad (136)$$

In Figure 27  $V_{La}$  represents the condition when  $\theta$  is minimum and  $V_{Lb}$  the condition when  $\theta$  is maximum. If  $\theta_{max}$  is very nearly equal to  $180^\circ - \theta_{min}$ , it follows directly that the maximum and minimum values of  $V_g$  (i.e.,  $V_{ga}$  and  $V_{gb}$ ) are symmetrically displaced about a mean value of  $V_{go}$  and that the relative change is given by  $V_L \cos \theta_{min} / V_g$ .

The form of the envelope of oscillator voltage is predicted by these vector triangles. Actual observed forms of these envelopes are illustrated in the sketches of Figure 28. The left figure represents a case when the modulating frequency is relatively low. In this case the effects of the time constant of the grid circuit are negligible and

the envelope follows very closely the changes which would be predicted from the vector triangle. Note that during that portion of the modulating cycle when the synchronizing signal is absent the amplitude is constant and equal to that of the undisturbed oscillator. The envelope shown in the right hand figure illustrates one observed when the modulating frequency was considerably higher. Here the time constant of the grid circuit does not permit the rapid return of amplitude to that of the undisturbed oscillator and a more nearly triangular form of envelope results. The effect of the time constant is also to reduce the magnitude of the change in amplitude.

The analysis of the effects of amplitude-modulation which follows is based upon the figure at the left because the relative amount of modulation is greater. The upper half of the envelope representing one modulation period is shown in Figure 29, but with the curved portion replaced by a straight line. This substitution simplified the analysis without significantly affecting the computed values of those frequency components which constitute the spectrum of this envelope.

The Fourier series representing this envelope is now computed, using the terminology illustrated and subject to the following condition

$$\begin{aligned} f(\theta) &= E \left( 1 + \frac{C\theta}{\chi\pi} \right), & 0 \leq \theta \leq 2\chi\pi, \\ &= E & 2\chi\pi \leq \theta \leq 2\pi. \end{aligned} \quad (137)$$

In the usual manner

$$f(\theta) = E \left[ a_0 + \sum_{n=1}^{\infty} (a_n \sin n\theta + b_n \cos n\theta) \right],$$

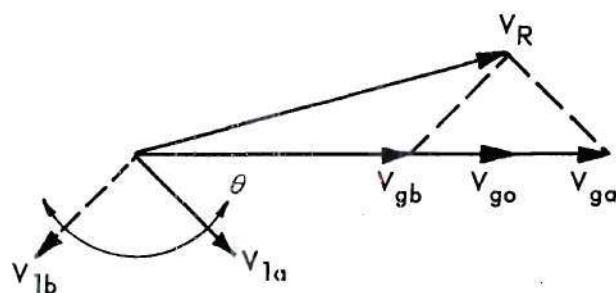


FIGURE 27. VECTOR TRIANGLES OF OSCILLATOR VOLTAGE ILLUSTRATING AMPLITUDE MODULATION.

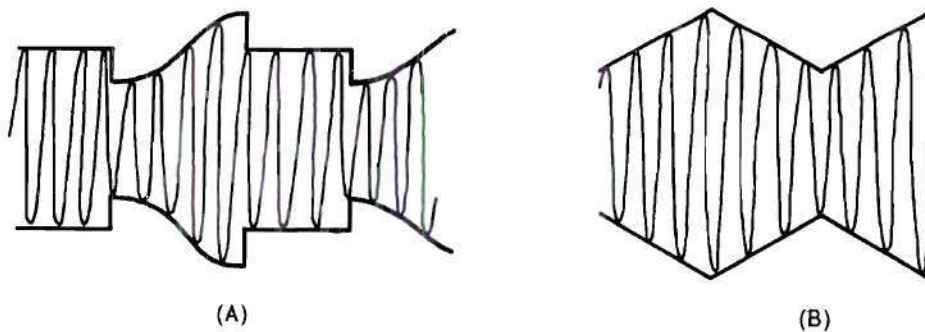


FIGURE 28. FORMS OF OSCILLATOR VOLTAGE ILLUSTRATING AMPLITUDE MODULATIONS.

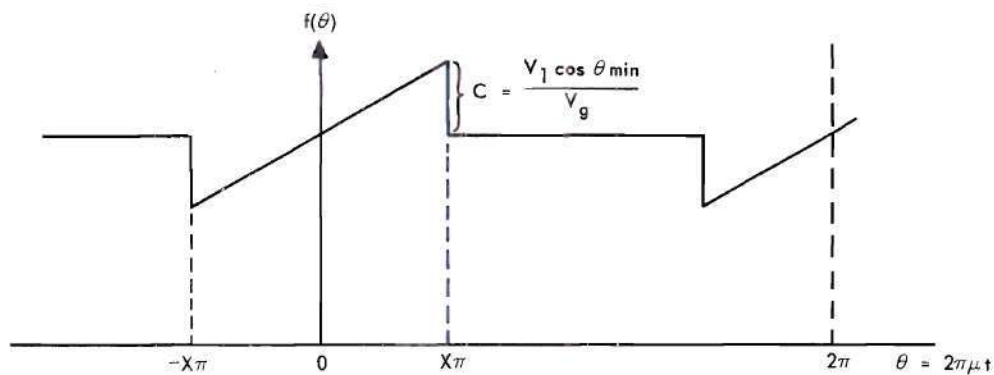


FIGURE 29. UPPER HALF OF ENVELOPE OF VOLTAGE OF SYNCHRONIZED OSCILLATOR.

where

$$a_n = \frac{1}{\pi} \int_0^{2\pi} f(\theta) \sin n\theta$$

and

$$b_n = \frac{1}{\pi} \int_0^{2\pi} f(\theta) \cos n\theta.$$

The substitution of the values for  $f(\theta)$  leads to the following results:

$$a_n = -\frac{2C}{n\pi} \cos n\pi, \quad b_n = 0, \quad \text{and} \quad a_0 = 1. \quad (138)$$

The application of the series to a specific case illustrates the effect upon the spectrum of the amplitude modulation which is due to a varying phase angle. The case selected is that spectrum appearing in the bottom row of Figure 23 for which the modulation index was given to be 0.75 and the duty cycle was given as 0.5. The spectrum there illustrated was originally calculated by the use of equation (129), an equation which considered phase modulation only. When the values of  $m = 0.75$  and of  $x = 0.5$  were substituted in equation (129) the first five terms of the phase-modulated wave were found to be expressible as

$$e = E \left[ 0.783 \sin \omega_1 t + 0.416 \sin (\omega_1 + \omega_m) t + 0.416 \sin (\omega_1 - \omega_m) t \right. \\ \left. + 0.13 \sin (\omega_1 + 2\omega_m) t + 0.13 \sin (\omega_1 - 2\omega_m) t \right]. \quad (139)$$

The amplitude modulating factor is now taken into account by the use of the series whose coefficients are calculated by use of equation



(138). For this illustration the amplitude excursion  $C$ , illustrated in Figure 29, is selected to have the value  $1/6$ . This numerical value is obtained by assuming a ratio of  $V_1/V_g$  of  $1/6$  and then calculating  $C$  (which is equal to  $V_1 \cos \theta_{\min}/V_g$ ) as though  $\cos \theta_{\min}$  were equal to unity. This is a realistic assumption for in the previous chapters it was shown that when the modulation index was large (i.e., greater than 0.5) the excursion of the phase angle  $\theta$  was such as to make the angle approach  $180^\circ$  at its maximum and  $0^\circ$  at its minimum.

If now the value of  $x = 0.5$  is placed in equation (138) the coefficients of the series for amplitude modulation becomes, simply

$$\begin{aligned} a_n &= -\frac{2C}{n\pi} (-1)^{n/2} & n \text{ even,} \\ &= 0 & n \text{ odd.} \end{aligned} \quad (140)$$

The evaluation of these coefficients for the given value of  $C$  of  $1/6$  permits writing the first few terms of the amplitude modulation series as

$$e = E \left[ 1 + 0.053 \sin 2\omega_m t - 0.027 \sin 4\omega_m t + 0.014 \sin 6\omega_m t \dots \right] \quad (141)$$

Referring to equation (135) it is seen that the total spectrum which includes the effects of phase modulation and of amplitude appears as an infinite series of products of terms. Since the sidebands due to phase modulation and those due to amplitude modulation diminish rapidly, sufficient information regarding the spectrum can be gained by employing only a few of the possible number of terms. The effect of amplitude

modulation will be small unless the amplitude of the synchronizing signal is unusually large. Practical values of the ratio  $V_1/V_g$  may be considered to be of the order of 1/10 or less, the ratio of 1/6 adopted here for illustration was chosen because some of the experimental work employed that ratio and comparison of calculated and experimental results is facilitated thereby.

If the product of equations (139) and (140) is taken and the necessary trigonometric simplifications carried through, the first several terms of the product are given closely as

$$e = E \left[ 0.784 \sin \omega_1 t + 0.418 \sin (\omega_1 + \omega_m) t + 0.418 \sin (\omega - \omega_m) t \right. \\ \left. + 0.114 \sin (\omega + 2\omega_m) + 0.114 \sin (\omega - 2\omega_m) t \right] . \quad (142)$$

If this equation is compared to equation (139) it is seen that the effect of amplitude modulation is small. Similar analyses may be applied to any specific condition but it has been concluded from experimental observations and analyses of the form recorded here that the effect of amplitude modulation upon the spectrum may be usually neglected in comparison to the effect of phase modulation unless the synchronizing signal is of large amplitude.

## CHAPTER VI

### SYNCHRONIZATION BY SIDEBANDS OF INTERRUPTED WAVE TRAINS

#### Physical Viewpoint of Sideband Synchronization

In chapter 3 an experiment was described in which the frequency of the synchronizing signal was varied over wide limits. In this experiment it was demonstrated that the frequency of the oscillator was "locked" to that of the input not only in the region centered around  $f_o$ , the free-running undisturbed frequency of the oscillator, but also in regions centered about the frequencies  $f_o \pm nf_m$ , where  $f_m$  is the frequency of the modulation (gating) and  $n$  is an integer. Inasmuch as frequencies of  $f_o \pm nf_m$  correspond to sidebands of the modulated input it may be said that the oscillator is subjected to synchronization by these sidebands.

The action occurring in this phenomenon can be explained in a manner similar to that employed in chapter 4. In that chapter it was shown that synchronization was effected if the net phase, when measured over a modulation period, was equal to zero. Analytically this requirement was expressed as

$$\int_{\tau=0}^{\tau=2\pi/\omega_m} \frac{d\theta}{dt} d\tau = 0. \quad (40)$$

An equivalent expression can be stated for the condition of synchronization by sidebands. It is

$$\int_{\tau=0}^{\tau=2\pi/\omega_m} \frac{d\theta}{dt} d\tau = 2N\pi \quad (N = 1, 2, 3, \dots) \quad (143)$$

and states that a "locked" condition exists between the input and output if exactly  $N$  cycles are gained, or lost, per modulation cycle.

Relationships between frequencies involved, or used for reference, are shown for two particular cases in Figure 30. A condition of "synchronization by the first upper sideband" is illustrated. The angular frequency of the input signal is  $\omega_1$  and it is modulated with an angular frequency  $\omega_m$ . In part (A) of Figure 30 the first upper sideband,  $\omega_1 + \omega_m$ , falls near but slightly below the angular frequency  $\omega_0$ , whereas in part (B) the frequency  $\omega_1$  has been changed sufficiently to let the first upper sideband fall near to but slightly above  $\omega_0$ .

If an experiment is conducted for the purpose of illustrating these relationships, and if the input and output frequencies are monitored with counters, it is observed that there is a narrow band of frequencies (cross-hatched in the figure and designated with half-width as  $\omega_{lsb}$ ) within which the following action occurs.

(1) If an injected signal of frequency  $f_1$  and modulating frequency  $f_m$  is so positioned that the frequencies  $f_1 + f_m$  or  $f_1 - f_m$  lie within the band (cross-hatched) the oscillator is observed to shift its frequency from  $f_0$  to  $f_1 + f_m$  or  $f_1 - f_m$ , whichever is applicable.

(2) If the frequency of the input is then shifted exactly  $\underline{n}$  cycles the frequency of the oscillator also shifts exactly  $\underline{n}$  cycles so that the frequency difference between input and output remains exactly



equal to the modulating frequency  $f_m$ . This action persists until the edge of the band is reached when synchronizing action is lost.

(3) The synchronizing action persists over a band which is much narrower than is the band which exists when c-w signals are applied. That band has already been designated as  $2f_c$ , where  $f_c = \omega_c/2\pi$ . The synchronizing band is also narrower than is that region designated as "bandwidth of synchronization by fundamental component of input signal" which was defined in chapter 4.

(4) The band is distinctly defined if the modulating frequency is relatively high and moderately well-defined at all modulating frequencies.

From this experiment it is concluded that well-defined relationships exist between the parameters of the circuit and of the injected signal. The following paragraphs are devoted to an analysis of the factors involved and of the necessary conditions for synchronization.

A physical understanding of the action is facilitated by a study of the vector diagram of voltages. The basic triangle of voltages was first used in the explanation of synchronization by c-w signals and appeared as Figure 31. This figure can also be applied to the present problem.

In Figure 31 the injected voltage is represented by the vector  $V_1$ . This vector rotates at an angular velocity  $\omega_1$ . The grid voltage of the oscillator is represented by  $V_g$  and rotates at an angular velocity of  $\omega$ . The angle between them changes at the rate  $d\theta/dt$  unless the oscillator is synchronized by a c-w signal in which case  $d\theta/dt$

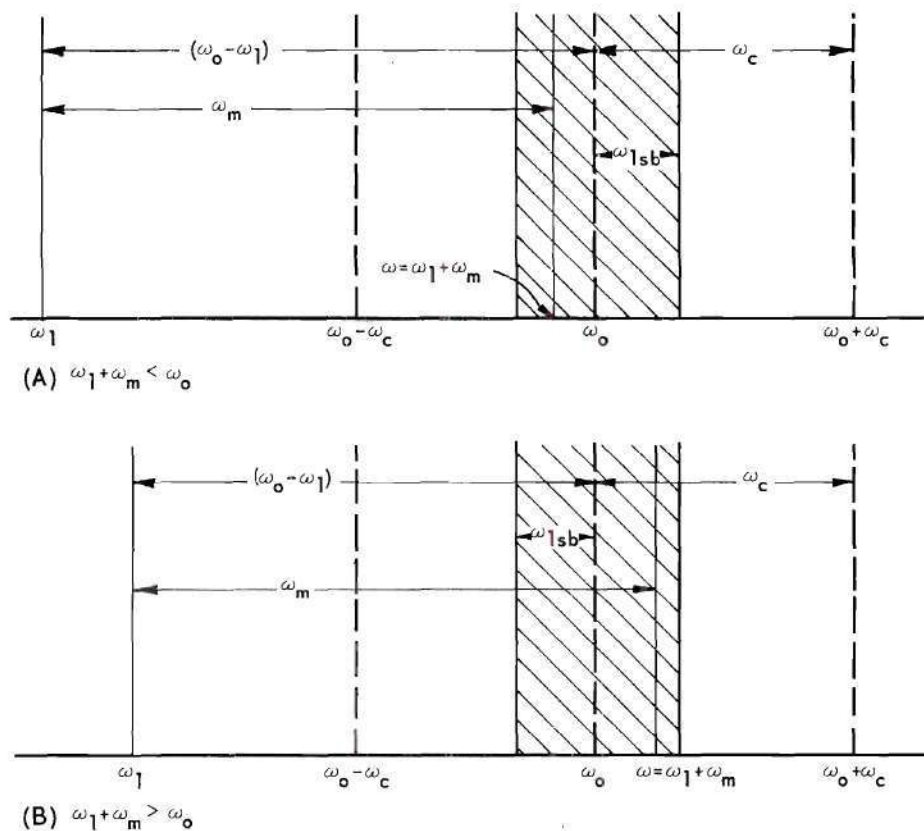


FIGURE 30. ANGULAR FREQUENCIES INVOLVED IN SYNCHRONIZATION BY FIRST UPPER SIDEBAND.

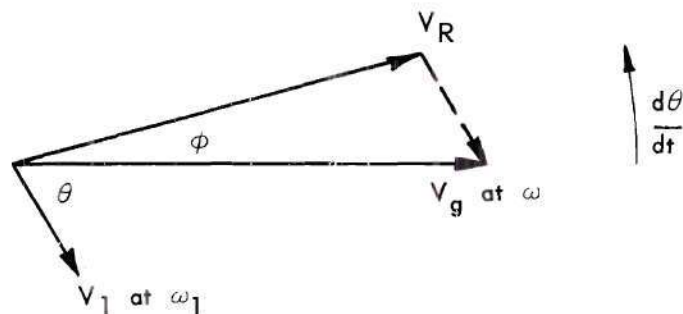


FIGURE 31. VECTOR DIAGRAM OF OSCILLATOR VOLTAGES.

becomes identically equal to zero. The vector  $V_R$  represents the voltage returned from the tuned circuit of the oscillator and is normally not in phase with  $V_g$ .

In the case of synchronization by c-w signals the angle  $\theta$  reaches and maintains a constant value  $\theta_0$ . In the case of synchronization by the fundamental component of an interrupted wave train the angle has been shown to oscillate continuously but is so constrained in its movements that its net deviation with respect to the vector  $V_1$  is identically equal to zero, if the measurement of phase includes a complete modulation cycle. In the case being considered in this chapter neither of these conditions apply. The phase requirements indicate that the action of the synchronizing signal must be to speed up or slow down the rate of phase deviation by just the right amount so that the net deviation, as measured over a modulation cycle, can be exactly  $2N\pi$  radians.

To illustrate the action, an experiment is considered in which a vector of voltage  $V_1$ , interrupted with a modulating frequency  $f_m$ , is to be compared to the vector  $V_g$  of the oscillator. It is first presumed that the vector  $V_1$ , rotating at angular frequency  $\omega_1$ , remains exterior to the oscillator. That is, the oscillator is not subjected to any disturbing force and hence is illustrated by a vector  $V_g$  which rotates at angular velocity  $\omega_0$ . If the frequencies correspond to those illustrated in part (B) of Figure 30 then the relative rate of angular velocity of the two vectors,  $\omega_0 - \omega_1$ , will be less than  $\omega_m$ .

In the next step in the experiment the vector  $V_1$  is injected into the grid of the oscillator so that the voltages may add as represented in Figure 31. Thereupon the vector  $V_g$  is found to rotate so

that its average velocity, measured over a modulation cycle, is  $\omega_1 + \omega_m$ . This can occur only if the vector  $V_g$  has been speeded up during the "on" time (presence of synchronizing signal) by just the right amount to make its average value identically  $\omega_1 + \omega_m$ .

An analytical explanation begins as before with the basic equation describing the deviation of the angle  $\theta$

$$\begin{aligned}\frac{d\theta}{dt} &= \omega_s - \omega_c \sin \theta \\ &= \omega_c (K - \sin \theta)\end{aligned}$$

where  $\omega_s$ ,  $\omega_c$ , and  $K$  have the same connotation as in the previous chapter.

The phase deviations of the angle  $\theta$  can be illustrated in much the same way as in chapter 5. The form of the synchronizing signal may be presumed to be the same as in Figure 21, and the phase deviations may be shown in a form similar to that of Figure 17. In that figure the net deviation was zero, in the present case (first sideband) the net deviation must be  $2\pi$ . Figure 32 illustrates the phasing conditions applicable to both parts of Figure 30.

In part (A) consider the lower (dotted) line the slope of which is  $\omega_c K = \omega_1 - \omega_o$ . This line represents the phase deviations of  $V_g$  with respect to  $V_1$  for an undisturbed oscillator when  $V_1$  remains exterior to the oscillator. During a modulation period,  $T$ , the angle  $\theta$  completes an excursion  $\Delta\theta_1$  which is less than  $2\pi$ . Next consider the effect when the synchronizing signal is injected during the time interval



$t = 0$  to  $t = t_1$ . If its effect during this time interval is to speed up the rate of change of  $\theta$  according to the value of the equation

$$\frac{d\theta}{dt} = \omega_c (K - \sin \theta)$$

then it is possible for the net phase to be equal to  $2\pi$  radians. Such a condition is illustrated in Figure 32 which shows that the speeded up or slowed down rate of phase deviation during the presence of synchronizing signal may be sufficient to meet the synchronizing requirements and that a net phase deviation of  $2\pi$  radians per modulation period may be obtained. In part (B) the reverse situation is illustrated wherein the effect of the synchronizing signal during the "on" time must be to slow down the rate of phase excursion of the angle  $\theta$ .

Analyses which are accurate within the limitations of the necessary simplifying assumptions can be applied to predict the relationships between the parameters involved. The procedure follows somewhat the same lines as in the previous chapters. It is first necessary to establish formulas for the phase angle  $\theta$  and the phase deviation  $\Delta\theta$ , then the excursions of the angle  $\theta$  must be anticipated and described. This information is assembled in the next section, and finally the synchronization equation (143) is applied.

#### Phase Deviations Occurring During Synchronization by Sidebands

In chapter 2 the equations for the phase angle  $\theta$  were shown to be direct solutions of the basic differential equation  $d\theta/dt = \omega_s - \omega_c \sin \theta$ . The solution for the case when  $\omega_s$  was less than  $\omega_c$  (that is,

the synchronizing signal lies within the band of synchronization) contained a hyperbolic tangent of the time function. The equation was utilized as a basis for determining the relationships between interrupting frequency and bandwidth of synchronization.

In the same section the equation was given for the case when  $\omega_s$  was greater than  $\omega_c$  and appeared as equations (37) and (37a). The latter will be utilized in the present analysis and is given here as equation (144),

$$\theta = 2 \tan^{-1} \left[ \frac{1}{K} + \frac{\sqrt{K^2-1}}{K} \tan \omega_c \frac{\sqrt{K^2-1}}{2} (t + t_o) \right]. \quad (144)$$

In this equation the variation of  $\theta$  is now dependent upon the tangent rather than the hyperbolic tangent of the time quantity and may be expected to vary rapidly for some values of the time quantity in accordance with the known properties of the tangent of an angle.

The analysis is begun by considering the criterion for synchronization for sidebands

$$\int_{\tau=0}^{\tau=2\pi/\omega_m} \frac{d\theta}{dt} d\tau = 2 N\pi, \quad (N = 1, 2, 3, \dots) \quad (143)$$

which can be more explicitly expressed as

$$\omega_c \int_0^{t_1} (K - \sin \theta) dt + \omega_c \int_{t_1}^{2\pi/\omega_m} K dt = 2 N\pi. \quad (145)$$

The integrand containing the quantity  $(K - \sin \theta)$  can be evaluated in a manner almost identical to that followed in equations (87) through (96)

and the equation finally yields

$$\begin{aligned}
 & 2 \tan^{-1} \left\{ \frac{K-1}{\sqrt{K^2-1}} \tan \left[ \omega_c \frac{\sqrt{K^2-1}}{2} (t_1 + t_0) - \tan^{-1} \frac{K-1}{\sqrt{K^2-1}} \right] \right\} \\
 & - 2 \tan^{-1} \left\{ \frac{K-1}{\sqrt{K^2-1}} \tan \left[ \omega_c \frac{\sqrt{K^2-1}}{2} t_0 - \tan^{-1} \frac{K-1}{\sqrt{K^2-1}} \right] \right\} \\
 & = 2 N\pi - \omega_c K(2\pi/\omega_m - t_1). \quad (146)
 \end{aligned}$$

It is convenient to use  $T = 2\pi/\omega_m$  and  $t_1 = kT$  as has been the practice heretofore. With this substitution the right hand side of equation (146) becomes

$$2 N\pi - \omega_c KT(1-k). \quad (167)$$

Equation (146) is similar in form to the equation defining synchronization by the fundamental component of the synchronizing signal. That equation appeared in chapter 4 as equation (97) and was discussed in considerable detail. It was shown that each value of the constant of integration,  $t_0$ , is associated with a specific value of the variable  $t$ , if the equation is to be satisfied. In particular, it was shown that there exists a certain  $t_0$  for which the variable  $t$  is equal to  $T_{\max}$  and, since  $\omega_m = 2\pi/T$ , this greatest possible value of  $T$  determines the minimum modulating frequency consistent with synchronization. The value of  $T$  could, in theory, vary between the limits of zero and infinity and it could, in practice, vary over wide limits. The situation was illustrated in Figures 18 and 19 which showed the variation of  $\omega_m = 2\pi/T$  and the limiting conditions for synchronization.



When synchronization is effected by sidebands of the injected signal the permissible variations of the modulation period  $T$  are relatively small. The limitations are imposed by the fact that each sideband is represented by an angular frequency of  $\omega_1 \pm n\omega_m$ , or what is the same thing,  $\omega_1 \pm n \frac{2\pi}{T}$ . Evidently  $\omega_1$  and  $T$  are uniquely related. Finally, the difference frequency  $\omega_1 - \omega_o = \omega_c K$  may be expected in most cases to be not greatly different in magnitude from  $\omega_1 - n\omega_m$ . This condition for the first sideband is illustrated in Figure 33. This figure is equivalent in form to Figure 30(B) but is normalized with respect to  $\omega_c$  by making that quantity equal to unity and replacing  $\omega_o - \omega_1$  by  $K$ .

The band within which synchronization by the first sideband occurs is represented by the cross-hatched area. The band of synchronization by a c-w signal of same amplitude is  $2x(\omega_c = 1) = 2$ . The injection angular frequency  $\omega_1$  lies outside the band of synchronization therefore  $K = \omega_o - \omega_1$  is greater than unity. If  $\omega_1$  now remains fixed but  $\omega_m$  is made variable, the frequency  $\omega = \omega_o + \omega_m$  may vary within very limited bounds if it is to remain within the cross-hatched area. When  $\omega = \omega_o + \omega_m$  is adjusted to become identically equal to  $\omega_o$  it is evident that

$$\omega_m = 2\pi/T = K, \quad \text{or} \quad T = 2\pi/K \quad (148)$$

whence it is further evident that the period  $T$  varies only about the center value of  $2\pi/K$  and then by amounts which are relatively small.

The extent of the cross-hatched area, or the "bandwidth of synchronization by the first sideband of the injected signal" may be



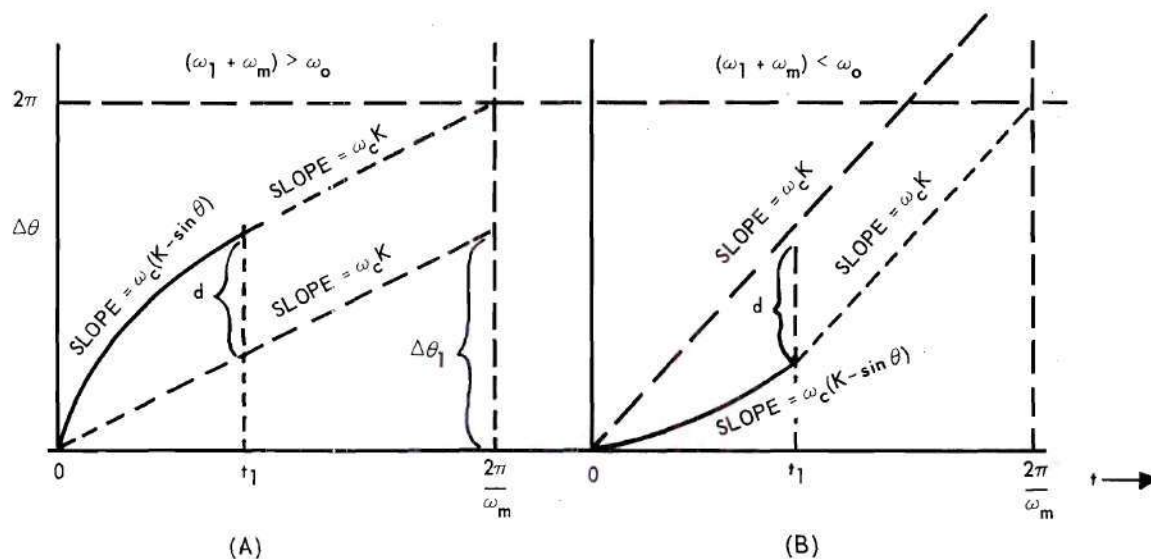


FIGURE 32. PHASE DEVIATIONS OF DISTURBED OSCILLATOR WITH RESPECT TO INPUT OF ANGULAR FREQUENCY  $\omega_1$ .

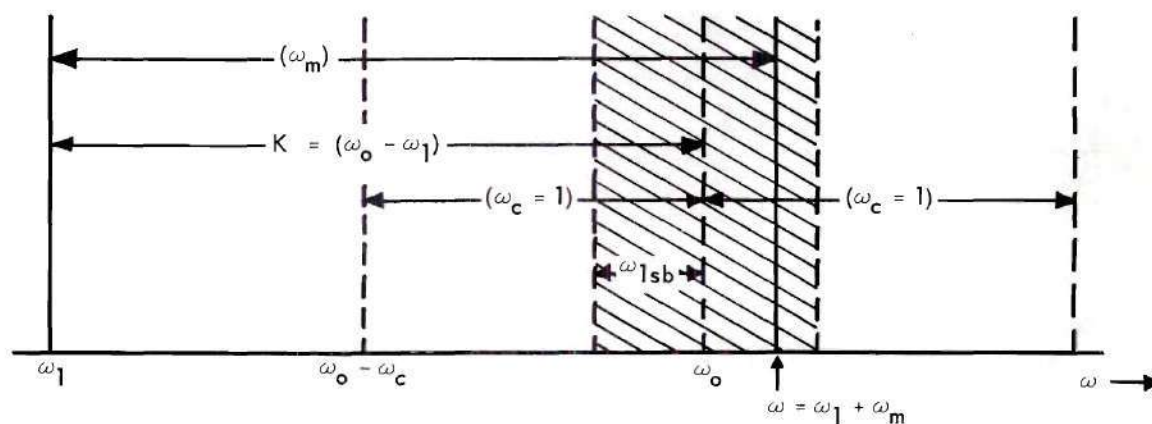


FIGURE 33. ANGULAR FREQUENCIES INVOLVED IN SYNCHRONIZATION BY FIRST SIDEBAND.

determined by a process of maximization similar to that used in the previous chapter. The quantities involved in the analysis are represented in Figure 32 where the effect of the nonlinear phasing action during the presence of synchronizing signal (the "on" time) is illustrated by the curved lines with slopes of  $\omega_c(K - \sin \theta)$ . In this figure it is seen that the difference in magnitude of the ordinate at the time  $t_1$  is represented by the quantity  $\underline{d}$ . This quantity is evidently a measure of the change in total excursion of the angle  $\theta$  that can be effected by the synchronizing signal. It follows, by comparison of Figures 33 and 32 that  $\underline{d}$  is zero when the angular frequency  $\omega_1 + \omega_m$  is equal to  $\omega_o$  and that  $\underline{d}$  increases as  $\omega_1 + \omega_m$  recedes from  $\omega_o$ , reaching its maximum value consistent with synchronization, when  $\omega_1 + \omega_m$  lies at either extreme of the cross-hatched area.

The conditions determining the permissible excursion of  $\underline{d}$  can be analyzed by finding the maximum value of

$$d = \omega_c \int_0^{t_1} (K - \sin \theta) dt - \omega_c K t_1 \quad (149)$$

subject to the condition that

$$\omega_c \int_0^{t_1} (K - \sin \theta) dt + \omega_c \int_{t_1}^{2\pi/\omega_m} K dt = 2\pi. \quad (150)$$

The integral of equation (150) is identical to that of equation (146), if  $N = 1$ . Also the integral of equation (149) is equal to the left side of equation (146) decreased by the quantity  $K t_1$ .

The method of maximization follows that of chapter 5 except that the hyperbolic tangent is replaced by the tangent of the angle  $\theta$ . The results are quite similar in form, and lead to the equation

$$\sin^2 A = \sin^2 B, \quad (151)$$

which is satisfied if

$$A = \pm B \quad (152)$$

and  $2\pi$  radians may be added to  $B$  if physical conditions so prescribe.

With the aid of equation (152) the synchronization equation may be expressed as a function of one unknown. For example,

$$A = ct_1 + ct_0 - b = \pm B, \quad (153)$$

and it was given that

$$ct_0 - b = B, \quad (110)$$

therefore

$$ct_1 = -B \pm B. \quad (154)$$

Evidently the positive sign in the parenthesis must be deleted or  $t_1$  would be a constant, a condition contrary to experimental conclusions. Therefore, using the negative sign and replacing  $t_1$  by  $kT$ , an equation for the modulating period may be written

$$T = \frac{-2B}{ck} \quad (155)$$

and the quantity  $KT(1-k)$  becomes

$$\frac{-2BK}{c} \left( \frac{1-k}{k} \right). \quad (156)$$

With these relationships between A, B, and T, the equation of synchronization becomes

$$-4 \tan^{-1} (a \tan B) = 2N\pi + \frac{2BK(1-k)}{ck}. \quad (157)$$

Finally, since  $B = -ct_1/2 = -ckT/2$ , as shown by equation (116), the equation may be expressed in terms of T. Values of T have been computed using equation (157) for the condition of square-wave modulation ( $k = 1/2$ ) and for various magnitudes of K. From these values of T the quantity  $\omega_m$ , ( $\omega_m = 2\pi/T$ ), corresponding to each value of T has been computed and finally a quantity denoted as  $\omega_{lsb}$  has been tabulated. The term  $\omega_{lsb}$  is analogous to the term  $\omega_c$  which was used in synchronization by a c-w signal.  $\omega_c$  represented one-half of the bandwidth of synchronization due to a c-w signal. In a similar manner the term  $\omega_{lsb}$ , which is illustrated in Figure 33 and which is numerically given by the equation

$$\omega_{lsb} = \omega_o - (\omega_l + \omega_m), \text{ and } = K - \omega_m \text{ when } \omega_c = 1 \quad (158)$$

represents one-half of the bandwidth of synchronization by the first sideband of the interrupted wave train.

The results of the calculation of  $\omega_{lsb}$  appear both in Table 1 and Figure 34. The table lists the computed values and Figure 34 illustrates the width of this "band of synchronization" by showing the ratio



TABLE 1  
WIDTH OF BAND OF SYNCHRONIZATION DUE TO  
FIRST SIDEBAND OF INTERRUPTED WAVE TRAIN

$K = \omega_1 - \omega_0$ (when $\omega_c = 1$ )	$T$	$\omega_m = 2\pi/T$	$\omega_{lsb} = K - \omega_m$
10	0.65	9.68	0.32
9	0.725	8.67	0.33
6	1.11	5.67	0.33
3	2.38	2.64	0.36
2	3.9	1.62	0.38
1.5	5.9	1.06	0.44
1.25	8.11	0.77	0.48
0.75	13.6	0.46	0.29
0.85	13.33	0.47	0.33
0.85	12.8	0.49	0.36
0.7	14.0	0.45	0.25

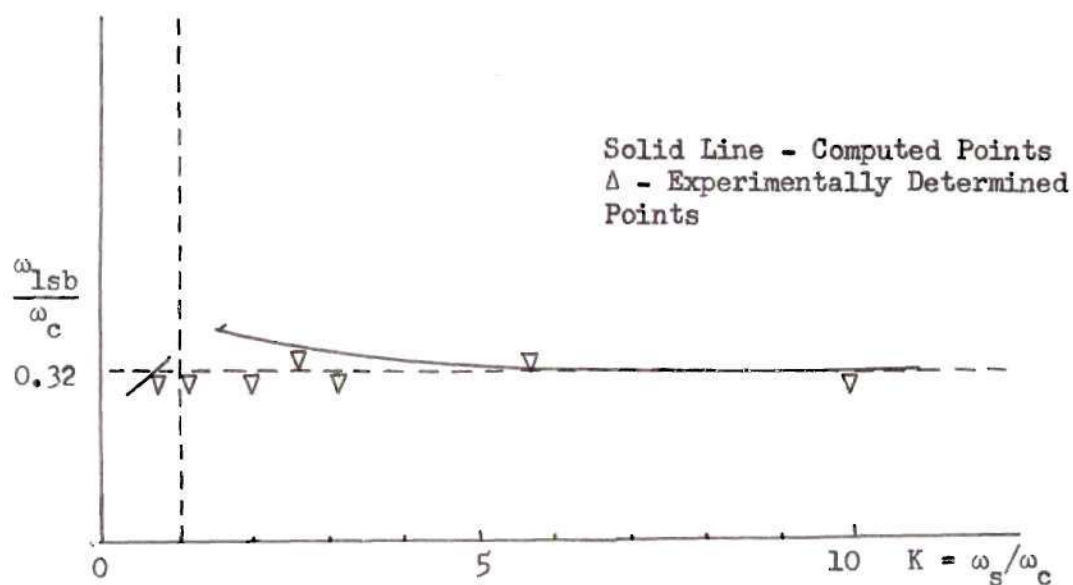


FIGURE 34. BANDWIDTH OF SYNCHRONIZATION BY FIRST SIDEBAND OF SQUARE-WAVE INTERRUPTED WAVE TRAIN

of  $\omega_{lsb}$  to  $\omega_c$  for each of several values of  $K$ . Values of  $\omega_{lsb}$  have not been computed for magnitudes of  $K$  equal or approximately equal to unity, since the synchronization equation is undefined in that region. This follows from the fact that the quantities  $\underline{a}$  and  $\underline{c}$  become identically equal to zero when  $K$  becomes equal to unity.

Table 1 and Figure 34 show that the relative width of the band of synchronization for a signal which is interrupted by a square-wave is equal to 0.32 when the modulating frequency is high. It has already been shown in chapter 4 that the bandwidth of synchronization by the fundamental component of signal is equal to 0.5. Reference is now made to Figure 15 and to equation (77). The figure cited shows that the spectrum of a c-w signal which is interrupted by a rectangular pulse has an envelope given by  $\frac{\sin nk\pi}{nk\pi}$ , where  $\underline{k}$  is the duty cycle of the interrupted wave, and also shows that the fundamental component of the spectrum has an amplitude which is equal to the product of the amplitude of the unmodulated signal and the duty cycle of the interrupting signal. In the case of square-wave modulation the fundamental component must then have an amplitude which is one-half that of the original (unmodulated) signal. The synchronizing action of this waveform has been shown to give a bandwidth of synchronization which, at its maximum, is also equal to one-half the bandwidth of synchronization due to a c-w signal of same amplitude.

The calculation of the other components of the spectrum shows that the amplitude of the first sideband is given by

$$\frac{\sin \pi}{\pi}$$

and that this is numerically equal to 0.32. But Table 1 and Figure 34 show that the average ratio  $\omega_{\text{lsb}}/\omega_c$  is also numerically equal or very nearly equal to the same value, i.e., 0.32. The two equal numerical values have been obtained, it will be noted, by completely different methods.

These results are significant, particularly in view of the uniformity of response as the frequency difference is varied. It may therefore be tentatively concluded, from this example of square-wave modulation of the synchronizing signal and in a manner quite similar to that of chapter 4, that:

"The synchronizing action of the 'first sideband' of the synchronizing signal may be computed by steady-state theory by calculating the bandwidth of synchronization of a c-w signal whose amplitude is equal in magnitude to the first sideband of the actual synchronizing signal".

It may also be shown that other duty cycles result in synchronizing actions which are comparable to that expected from a c-w signal having an amplitude equal to the strength of the sideband under consideration. In particular, it can be easily demonstrated that when the duty cycle is very short the synchronizing action of the first sideband approaches that of the fundamental.

Consider equation (157) in the case when  $k$  becomes very small, i.e.,  $k \ll 1$ . When  $k$  is small, the quantity  $\frac{1-k}{k}$  is very large and the quantity  $\frac{2Bk}{c} \left(\frac{1-k}{k}\right)$  can remain less than  $2\pi$  (as required to satisfy the equation when  $N$  is equal to unity) only if  $B$  approaches zero. But  $B$  was defined to be equal to the quantity  $ct_0 - b$ , whence  $ct_0 \rightarrow b$  as  $B \rightarrow 0$ .

This relationship is now utilized in the equation for the angle  $\theta$

$$\theta = 2 \tan^{-1} \left[ \frac{1}{K} + \frac{\sqrt{K^2-1}}{K} \tan (ct + ct_0) \right] \quad (159)$$

and at time  $t = 0$ , with  $ct_0 = -b = \tan^{-1} \frac{K-1}{\sqrt{K^2-1}}$ , there results

$$\begin{aligned} \theta &= 2 \tan^{-1} \left[ \frac{1}{K} + \frac{\sqrt{K^2-1}}{K} \tan \left( \tan^{-1} \frac{K-1}{\sqrt{K^2-1}} \right) \right] \\ &= 2 \tan^{-1} \left[ \frac{1}{K} + \frac{K-1}{K} \right] = 90^\circ. \end{aligned} \quad (160)$$

This equation states that when the duty cycle is very small the phase angle  $\theta$  is very nearly equal to  $90^\circ$  during the "on" time. Since the sine of  $90^\circ$  is unity the basic equation for synchronization by the first sideband ( $N = 1$ ) becomes

$$\int_0^{kT} (K - 1) dt + \int_{kT}^T K dt = 2\pi, \quad (161)$$

whence, after integration, there results

$$KT - kT = 2\pi$$

and

$$K - k = 2\pi/T = \omega_m, \quad \text{or} \quad K = \omega_m + k. \quad (162)$$

But, since  $\omega_{lsb} = K - \omega_m$ , there is obtained

$$\omega_{lsb} = (\omega_m + k) - \omega_m = k. \quad (163)$$



This equation states that for small values of duty cycle the half-width of the "band of synchronization by the first sideband" is equal numerically to  $k$ , the duty cycle. Now, again referring to the spectrum of a rectangular-pulse-modulated signal, it may be quickly computed that for small duty cycles the amplitude of the first sideband approaches that of the fundamental. But this amplitude was shown to be equal to  $kE$ , where  $E$  is the amplitude of the signal before modulation and is also the amplitude of signal during the "on" time.

The final conclusions to be gained from the foregoing analysis correspond in form to those reached in chapter 4 when synchronization by the fundamental component was evaluated. It has been shown, by a specific value in the case of square-wave modulated signals and in general for all cases of small duty cycle, that the theoretical magnitude of the "bandwidth of synchronization by the first sideband of the injected signal" is equal, or very nearly equal, to the bandwidth which would be obtained by a c-w signal of amplitude equal to that of the first sideband.

The same logic and procedure may be extended to other sidebands. In some cases a simplified approach may suffice to explain the action. For example, it is shown by Fourier analysis that the second sideband of a square-wave modulated signal should have zero amplitude. In this case the synchronizing action of the second sideband should be non-existent. An analytical expression leading to this conclusion can be obtained very simply from the equation of synchronization for the second sideband

$$\omega_c \int_0^{T/2} (K - \sin \theta) + \omega_c \int_{T/2}^T K dt = 4\pi. \quad (164)$$

If  $K$  is considerably greater than unity it is evident that the primary quantity in the first integral is  $K$  and that the nonlinearity produced by  $\sin \theta$  will be relatively small. In this case the angle  $\theta$  will have an excursion of very nearly  $2\pi$  during the time interval  $t = 0$  to  $t = T/2$ , and the integral of  $\sin \theta$  must be equal, or very nearly equal to zero, since the bounds of integration encompass one complete cycle. In this case it is quickly shown that  $\omega_m$  can have one value only, that of  $\omega_m = K/2$ , which is another way of saying that the bandwidth of synchronization is zero.

The final conclusions applicable to this section are simply that the synchronizing action of a particular sideband of an interrupted wave train may be predicted within small limits of error by utilizing steady state theory and computing the bandwidth of synchronization due to a signal with an amplitude equal to that of the sideband in question.

#### Frequency Spectrum of Oscillator Synchronized by Sidebands of Injected Signal

The frequency spectrum of an oscillator which has been synchronized by a sideband of an interrupted wave train can be computed in the same manner as was utilized for synchronization by the fundamental of the input. The phase modulation which occurs determines the basic form of the spectrum but there is normally less non-linearity with sideband synchronization than with synchronization by the fundamental. The validity of this statement can be inferred from an inspection of the integral which determines the deviation of phase during the "on" time. This integral has appeared many times, and is

$$\omega_c \int_0^{t_1} (K - \sin \theta) dt. \quad (165)$$

In the case of synchronization by the fundamental component of signal the quantity  $K$  was stated to be less than unity. In that case the quantity  $\sin \theta$  plays a prominent role in the total value of the expression  $(K - \sin \theta)$ . But in the present case, synchronization by sidebands,  $K$  is usually much greater than unity whence it is evident that  $\sin \theta$  can have relatively little influence upon the rate of change of the phase angle.

Figure 32 illustrated the type of phase deviation which exists and which will determine the frequency spectrum of the synchronized oscillator. If the curved portion is approximated by a straight line it is found that there is little error in computing the spectrum except for minimum values of the frequency difference  $\omega_c K$ . The following analysis utilizes straight lines, but methods of numerical analysis must be applied in some few cases.

The phase deviations in an oscillator which is synchronized by a sideband of the injected signal are presented in Figure 35. If the slope of that portion of the curve existing between  $\phi = 2k\pi$  and  $\phi = 2\pi$  is  $m_2$ , the slope of the first portion may be given as

$$\frac{N - m_2 (1 - k)}{k}.$$

With the aid of this expression the value of the phase deviation,  $\Delta\theta$ , is

$$\begin{aligned}
 \Delta\theta &= \frac{N - m_2(1-k)}{k} \phi & 0 \leq \phi \leq 2k\pi \\
 &= a + m_2\phi & 2k\pi \leq \phi \leq 2\pi
 \end{aligned} \tag{166}$$

where  $a = 2N\pi - 2m_2\pi = 2\pi(N - m_2)$ .

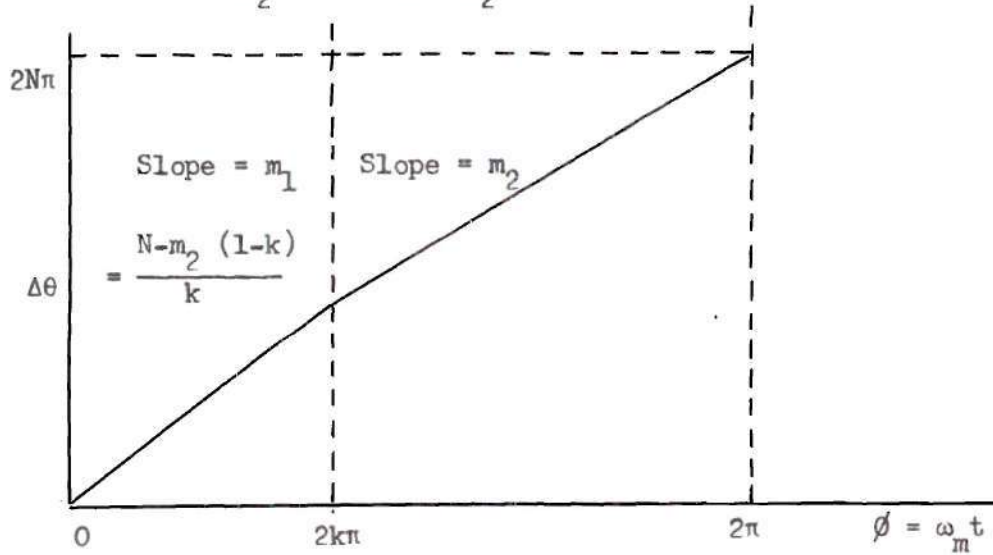


FIGURE 35. PHASE DEVIATIONS IN OSCILLATOR SYNCHRONIZED BY SIDEBANDS OF INJECTED SIGNAL.

Consider  $\cos \Delta\theta$ , to be expanded in a Fourier series.

$$a_n = \frac{1}{\pi} \int_0^{2k\pi} \cos m_1\phi \sin n\phi \, d\phi + \frac{1}{\pi} \int_{2k\pi}^{2\pi} \cos (a + m_2\phi) \sin n\phi \, d\phi,$$

and

$$b_n = \frac{1}{\pi} \int_0^{2k\pi} \cos m_1\phi \cos n\phi \, d\phi + \int_{2k\pi}^{2\pi} \cos (a + m_2\phi) \cos n\phi \, d\phi. \tag{167}$$



Also consider  $\sin \Delta\theta$ , to be expanded

$$c_n = \frac{1}{\pi} \int_0^{2k\pi} \sin m_1 \phi \sin n\phi \, d\phi + \frac{1}{\pi} \int_{2k\pi}^{2\pi} \sin(a+m_2\phi) \sin n\phi \, d\phi$$

and

$$d_n = \frac{1}{\pi} \int_0^{2k\pi} \sin m_1 \phi \cos n\phi \, d\phi + \frac{1}{\pi} \int_{2k\pi}^{2\pi} \sin(a+m_2\phi) \cos n\phi \, d\phi. \quad (168)$$

also

$$a_0 = \frac{1}{2\pi} \int_0^{2k\pi} \cos m_1 \phi \, d\phi + \frac{1}{2\pi} \int_{2k\pi}^{2\pi} \cos(a+m_2\phi) \, d\phi, \text{ and}$$

$$b_0 = \frac{1}{2\pi} \int_0^{2k\pi} \sin m_1 \phi \, d\phi + \frac{1}{2\pi} \int_{2k\pi}^{2\pi} \sin(a+m_2\phi) \, d\phi. \quad (169)$$

When the integrals are evaluated the amplitude of the various components of the spectrum is computed by use of the relationships derived in chapter 3. By this means, there is obtained

$$\begin{aligned} e = E \sum_{n=-\infty}^{\infty} & \left[ \frac{1}{2} (b_n + c_n) \cos(\omega - n\omega_m)t \right. \\ & - \frac{1}{2} (b_n - c_n) \cos(\omega + n\omega_m)t \\ & + \frac{1}{2} (a_n - d_n) \sin(\omega - n\omega_m)t \\ & \left. + \frac{1}{2} (a_n + d_n) \sin(\omega + n\omega_m)t \right]. \quad (170) \end{aligned}$$

The results of evaluating equations (167), (168), and (169) are summarized as follows:

$$\frac{1}{2} (b_n + c_n) = \frac{1}{2\pi} \left[ \frac{1}{m_1 - n} \sin 2(m_1 - n)k\pi \right. \\ \left. + \frac{1}{m_2 - n} \left\{ \sin [a + 2(m_2 - n)\pi] - \sin [a + 2k(m_2 - n)\pi] \right\} \right],$$

$$\frac{1}{2} (b_n - c_n) = \frac{1}{2\pi} \left[ \frac{1}{m_1 - n} \sin 2k(m_1 - n)\pi \right. \\ \left. - \frac{1}{m_2 - n} \left\{ \sin [a + 2(m_2 - n)\pi] - \sin [a + 2k(m_2 - n)\pi] \right\} \right],$$

$$\frac{1}{2} (a_n + d_n) = \frac{1}{2\pi} \left[ \frac{1}{m_1 + n} [1 - \cos 2k(m_1 + n)\pi] \right. \\ \left. - \frac{1}{m_2 + n} \left\{ \cos [a + 2(m_2 + n)\pi] - \cos [a + 2k(m_2 + n)\pi] \right\} \right],$$

$$\frac{1}{2} (a_n - d_n) = \frac{1}{2\pi} \left[ \frac{1}{m_1 - n} [1 - \cos 2k(m_1 - n)\pi] \right. \\ \left. + \frac{1}{m_2 - n} \left\{ \cos [a + 2(m_2 - n)\pi] - \cos [a + 2k(m_2 - n)\pi] \right\} \right],$$

$$a_0 = \frac{1}{2m_1\pi} \sin 2km_1\pi \\ + \frac{1}{2m_2\pi} [\sin (a + 2m_2\pi) - \sin (a + 2km_2\pi)],$$

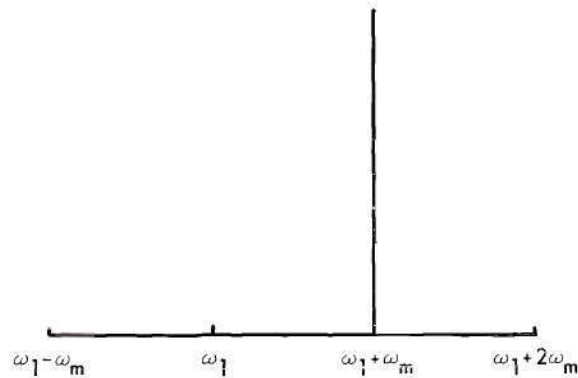
$$b_o = \frac{1}{2m_1\pi} [1 - \cos(2km_1\pi)] - \frac{1}{2m_2\pi} [\cos(a + 2m_2\pi) - \cos(a + 2km_2\pi)] \quad (174)$$

Equation (174) has been utilized for the calculation of the spectrum shown in Figure 36. Values of duty cycle,  $k$ , of  $1/3$  and  $1/2$  have been chosen for illustration in order that a convenient comparison with experimentally determined data may be made.

Experimental data have been employed in Figure 37. The left half of the figure illustrates the results of applying a synchronizing signal of duty cycle  $k = 1/3$  and one whose amplitude relative to  $V_g$  is very large ( $V_1/V_g = 0.9$ ). The right half of the figure represents the more practical case where the relative amplitude of the synchronizing signal is small ( $V_1/V_g = 1/6$ ). The spectrum of the input is shown in part (A), that of the oscillator when synchronized by the first sideband in part (B) and that of the oscillator when synchronized by the second sideband of the input in part (C).

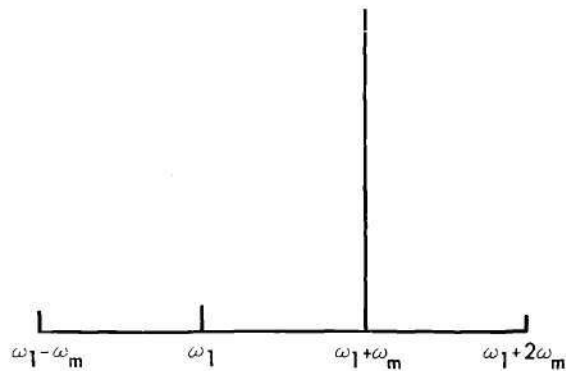
$$K = 9$$

$$0.023 \sin \omega_1 t + 0.99 \sin (\omega_1 + \omega_m) t \\ + 0.01 \sin (\omega_1 - \omega_m) t + 0.01 \sin (\omega_1 + 2\omega_m) t$$

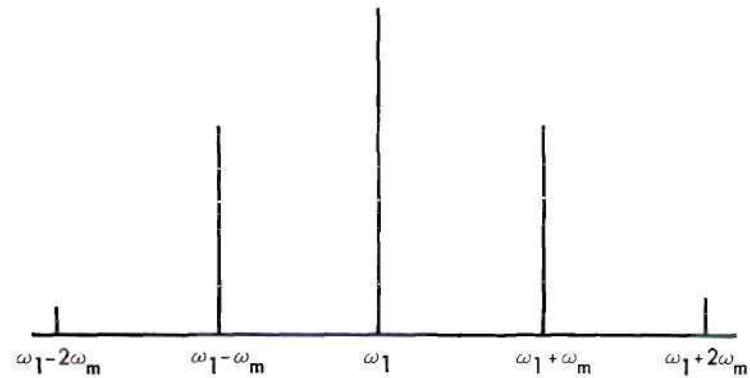


$$K = 3$$

$$0.08 \sin \omega_1 t + 0.99 \sin (\omega_1 + \omega_m) t \\ - 0.06 \sin (\omega_1 - \omega_m) t + 0.05 \sin (\omega_1 + \omega_m) t$$



SPECTRUM OF  
SYNCHRONIZING  
SIGNAL



$$K = 0.7 \text{ (Calculated by numerical analysis).}$$

$$0.316 \sin \omega_1 t + 0.92 \sin (\omega_1 + \omega_m) t \\ + 0.09 \sin (\omega_1 - \omega_m) t + 0.296 \sin (\omega_1 + 2\omega_m) t \\ + 0.05 \sin (\omega_1 - 2\omega_m) t + 0.05 \sin (\omega_1 + 3\omega_m) t$$

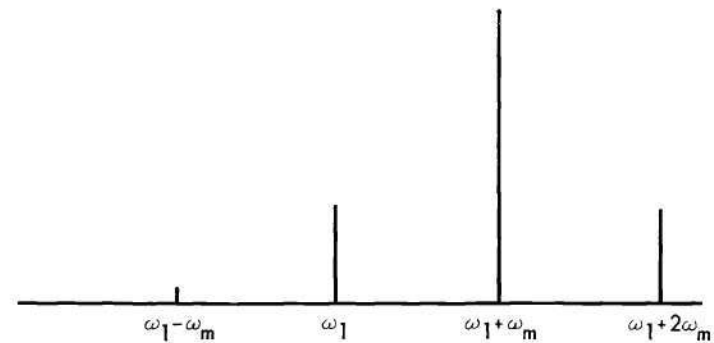


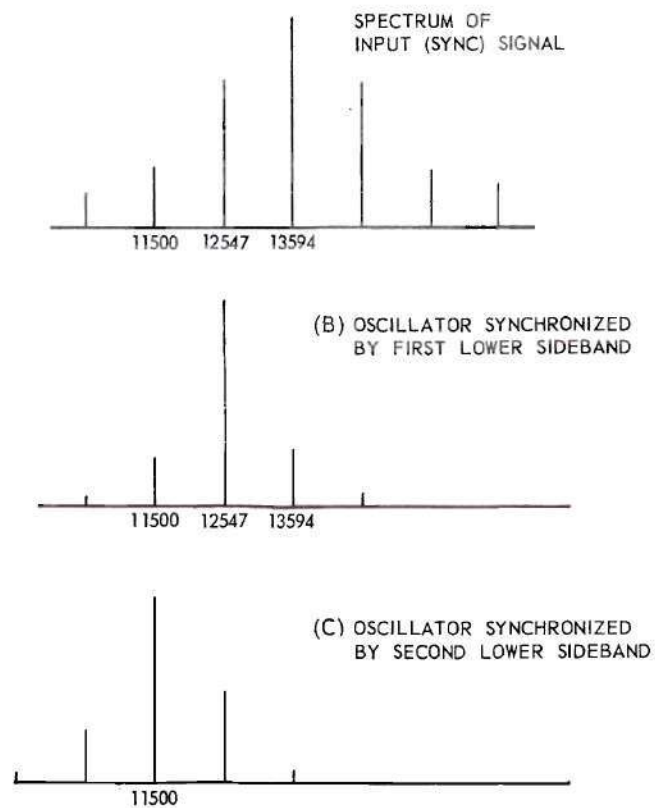
FIGURE 36. SPECTRA OF OSCILLATOR SYNCHRONIZED BY SIDEBANDS OF INTERRUPTED WAVE TRAIN, COMPUTED VALUES.



I. DUTY CYCLE  $k = 1/3$

$$V_1/V_{go} = 0.9$$

$$f_m = 1047 \text{ cps}$$



II. DUTY CYCLE  $k = 1/2$

$$V_1/V_{go} = 1/6$$

$$f_m = 1009 \text{ cps}$$

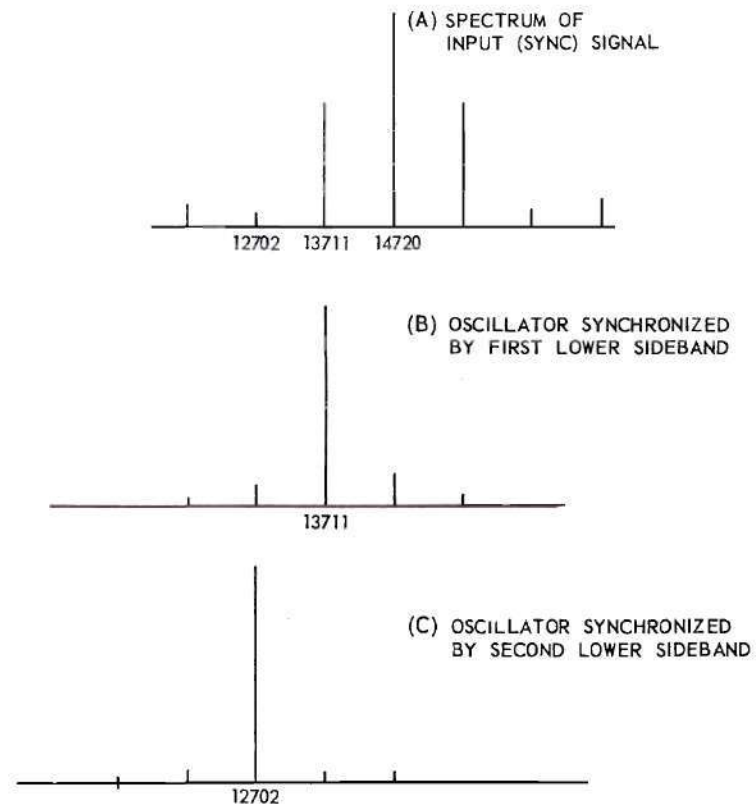


FIGURE 37. SPECTRA OF OSCILLATOR SYNCHRONIZED BY SIDEBANDS, EXPERIMENTAL VALUES.

## CHAPTER VII

### EXPERIMENTAL PROCEDURES AND APPLICATIONS OF THE SYNCHRONIZED OSCILLATOR

#### Details of Experimental Equipment

The test equipment employed and the interconnections between units is illustrated in chapter 3. The basic form of oscillator used as a test vehicle was also shown in that chapter. It is the purpose of this section to give a brief, but more detailed, description of the oscillator and of the method of obtaining and inserting the synchronizing signal.

The actual circuit of the oscillator and associated elements is shown in Figure 38. The circuit is recognized to be that of a simple tuned-plate oscillator with pentode drive, a form which is conveniently used at low frequencies.

The experiments which have formed a basis for most of the discussion and analysis recorded in the previous chapters were conducted at frequencies in the range from 10,000 cps to 30,000 cps. When square-wave modulation was desired the gating (interrupting) device was available in a commercial piece of equipment, a Measurements Corporation square-wave generator which incorporates a square-wave gating circuit. It is controllable in frequency (gating) from about 6 cps to 100,000 cps and utilizes a balance control by which the d-c component of signal can be eliminated. When rectangular-pulse modulation with a different duty cycle was desired a locally-constructed monostable multivibrator of

variable pulse width was employed. A negative-going 50-volt rectangular pulse was applied to one control grid of a mixer which was continuously receiving a c-w signal on the other control grid. The interrupted signal was taken from the plate circuit by means of magnetic coupling to a tuned circuit. This method of coupling is preferred because of its relative insensitivity to change in d-c levels at the anode.

Tests similar to those already described were also conducted at higher frequencies. In this case a Colpitts type oscillator was used and the experiments were conducted in the frequency range centered at 6 megacycles. The input (synchronizing) signal was interrupted at approximately 100,000 cps while the r-f signal was variable in frequency and amplitude. Experiments conducted in this frequency range and with the different form of oscillator produced results which were essentially identical to those obtained at low frequencies. Synchronization was effected in bands centered at 5.7, 5.8, 5.9, 6.0, 6.1, 6.2, and 6.3 Mc. These correspond to the first three lower sidebands, the fundamental, and the three first upper sidebands, respectively, of the synchronizing signal.

Later, tests of similar type were conducted in the three hundred megacycle range but the technical difficulties arising from efforts to gate a signal of this frequency were severe and these tests were terminated. Still later, other means of obtaining the desired synchronizing signal were suggested. One form of gated signal and its application is described in the following pages.

### Limitations of Signals of Small Duty Cycle

The analysis and discussion has thus far been concerned with a signal which is interrupted by a rectangular pulse. The Fourier analysis of the form of modulating signal showed that the envelope of the spectral components of the signal has the familiar  $\sin x/x$  form and that the relative amplitudes of each component of the spectrum due to a rectangular pulse can be predicted by that curve. The analysis also showed that the relative amplitudes of the first several harmonics increase when the duty cycle,  $k$ , is decreased. Now the analysis of synchronization by sidebands has demonstrated that the synchronizing action is essentially the same as that which would be due to c-w signals whose amplitudes were given by the Fourier analysis. Therefore it would appear that a desired signal is one in which the various harmonics (sidebands) of the input are each of large amplitude. An example is found in Figure 39. One might deduce that, since a small duty cycle leads to harmonics of large relative amplitude, a preferred form should be a signal with a very small duty cycle. There is no error in the logic, with the exception that the energy in each of many sidebands, though nearly equal, is small in magnitude. The fundamental component of a signal of amplitude  $E$ , interrupted with a duty cycle  $k$ , has been shown to be equal to the product of the two-- $kE$ .

It is evident that if a small duty cycle is to be employed the original amplitude of the signal to be gated must be very large if the components are to be sufficiently large to be employed as synchronizing signals. In fact, it is this requirement which leads to an immediate



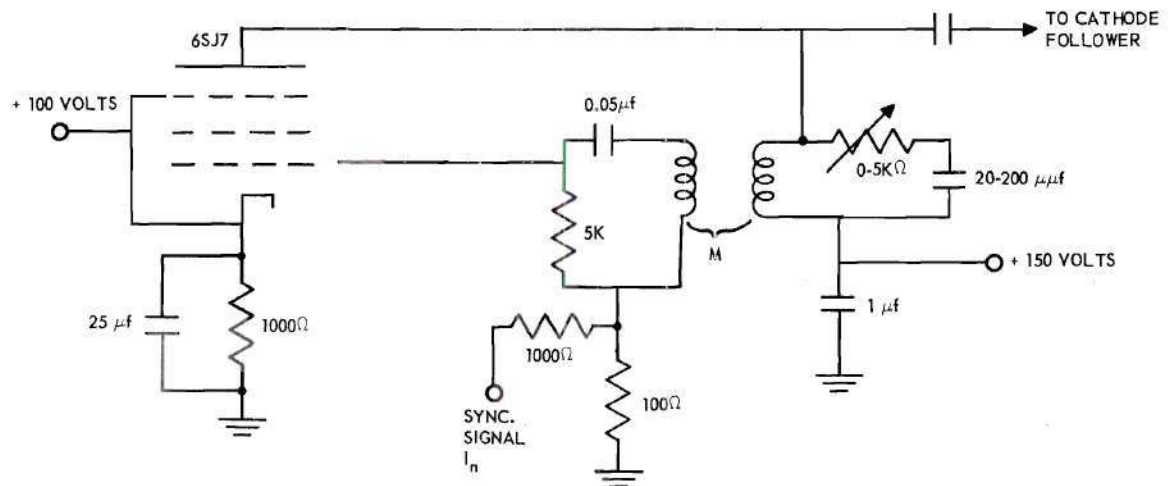


FIGURE 38. CIRCUIT OF OSCILLATOR USED IN BASIC EXPERIMENTS.

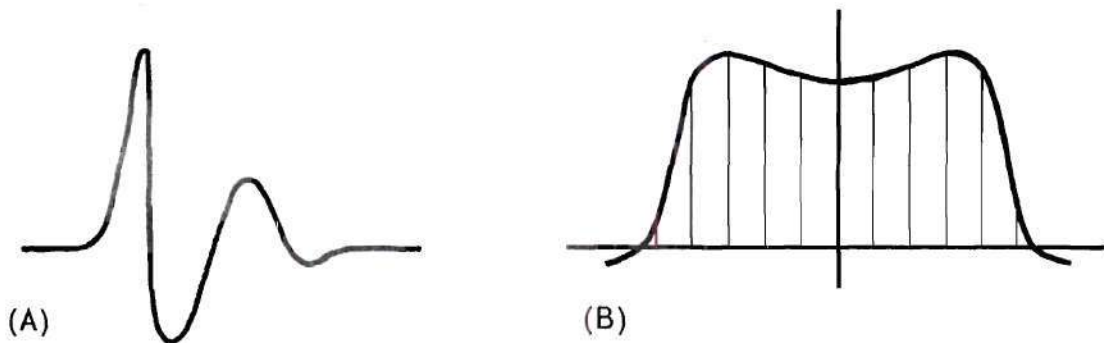


FIGURE 39. SPECTRUM OF WAVE PRODUCING DESIRED FREQUENCY COMPONENTS.

conclusion concerning synchronizing properties of the voltage wave which was discussed in the introduction chapter 1. In that chapter an experiment was described in which a piezoelectric quartz crystal was caused to vibrate at a high mechanical overtone, thereby producing short bursts of high frequency voltage. These "bursts" were of small amplitude and very short duty cycle, therefore it is evident that they would not be adequate for use as synchronizing signals unless they were strongly amplified prior to insertion in another circuit. The difficulties of amplification of this type of signal at frequencies above 300 Mc indicates that synchronization by such signals is probably impractical although theoretically possible.

#### Methods of Increasing the Range of Synchronization

If an oscillator is to be synchronized by the sidebands of an interrupted wave train and if the range of synchronization is to be as large as possible, then a preferred synchronizing signal is one in which the sideband components are of equal amplitude. An ideal envelope of the frequency spectrum is one in which all amplitudes remain constant within the range of interest and all others have zero amplitude. Although a form of this type is not attainable in practice, there does exist an envelope which is a reasonable approximation to the ideal. The interested reader is referred to a volume of the Hewlett-Packard Journal<sup>(18)</sup> which describes numerous waveforms and their respective frequency components. In particular, it is shown that a wave of the type illustrated in Figure 39(A) has a spectrum of the form shown in the (B) part of the same figure. The resulting spectrum approximates the desired ideal to a significant degree.

Two methods of producing a waveform of this type are well known. The first is to shock-excite a tuned circuit whose decrement is sufficiently great to produce the desired damping, the second is to provide plate voltage briefly to an oscillator whose free-running frequency is that within the envelope of Figure 39(A). These methods do not appear to have great promise when the stabilities associated with piezoelectric crystals are desired for it is well known that it is difficult to obtain shock-excited outputs from quartz crystals and also difficult to obtain rapid initiation of oscillations in a crystal-controlled oscillator.

When frequency stabilities of the order associated with crystals are desired the most obvious way of obtaining them is to interrupt the output of a crystal-controlled oscillator by a gating circuit. The gating frequency itself needs to be crystal controlled in order that both fundamental and sidebands have a high order of stability. The technical problems involved with interruption of high frequency signals have been mentioned and certainly must be a factor in the design and construction of an oscillator which is to be synchronized by interrupted wave trains. However, the possible advantages to be gained by utilization of such a synchronizing signal indicate that attempts to solve the application problem at high frequencies may be rewarded by the attainment of considerable flexibility of control. Comments upon various applications of the process appear in the next section.

#### Applications of the Synchronized Oscillator

A number of applications of an oscillator which is synchronized by an interrupted wave train can be cited, but the device which apparently



gains most flexibility from the process is that form which is subject to what is usually referred to in the art as "detent tuning". The latter term usually is taken to signify a process during which a control switch is rotated and drops into "detents". Each semi-fixed position so attained denotes a specific step in the process being controlled. In the present case the steps controlled are steps in frequency and these have a frequency separation roughly equal to the spacing between two sidebands in the spectrum of the synchronizing signal. The action of the switch is then to tune the oscillator, in steps, to free-running frequencies each of which lies within a band of synchronization. The proper sideband of the synchronizing signal, falling within this band, then "locks" the oscillator to its prescribed frequency.

This principle has been successfully applied by a colleague of the author as a means of obtaining several crystal-controlled frequencies from one crystal. He employed a slight modification of the interrupted wave train theory, but achieved a spectrum which had many components of sufficient amplitude to serve as adequate synchronizing signals. The system included a blocking oscillator whose natural frequency was close to 70 kc, a crystal-controlled 70 kc oscillator whose output served to "fire" the blocking oscillator, and such circuitry as was required to inject the output of the blocking oscillator into test vehicles. The blocking oscillator, controlled by the stable 70 kc source, became a spectrum generator whose output consisted of many large amplitude harmonics of 70 kc.

The test vehicle chosen was a Hartley oscillator, free-running in the vicinity of one megacycle and arranged for step tuning in



approximate 70 kc steps. This oscillator was basically no more stable than a normal LC oscillator operating in this range, but the addition of the synchronizing signals from the spectrum generator resulted in crystal-controlled stability at each of the steps. A numerical example will clarify the process. For instance, in absence of the synchronizing signal one of the "steps" might result in a frequency of 981 kc. This would be a nominal quantity because the instability of the free-running oscillator would cause it to drift considerably about the mean figure. Now upon application of the synchronizing signal it is found that the harmonic existing at 980.00 kc "locks" the oscillator to that frequency whereupon a high order of stability results.

Such a device may have promise in the communications field where considerable thought and effort has been directed toward the topic of "crystal saving", a process of obtaining many crystal-controlled frequencies with the use of few crystals. Extensions of the idea of synchronizing by interrupted wave trains might include combinations of oscillators so controlled by which a multiplication of crystal-controlled channels would result.

It will be recalled, and it is important, that phase-modulation is present in the synchronized oscillator. However, experimental and analytical work have shown that the frequency spectrum is simple and that in most cases the sideband rejection is sufficient to permit use of the signal in many applications where a single frequency is desired. However, in those applications where synchronization of both frequency and phase are required such as color television the proposed system would not be satisfactory.

Another possible application of the system may be found in frequency dividers, particularly those in which it might be desired to divide a frequency by other than integral numbers. It is only necessary to choose an interrupting frequency such that the desired output frequency corresponds to a specific sideband of the synchronizing signal. For example, a 28,000 cps signal could be changed to a 17,500 cps signal by interrupting (modulating) the 28,000 cycle signal at a rate of 3,500 per second and synchronizing an oscillator with the third lower sideband of the output.

The various suggestions listed above have been successfully demonstrated, usually at low frequencies, by the author. If the techniques of producing a desired spectrum at high frequencies can be solved it is believed that the process studied may find considerable application in other portions of the frequency spectrum.

## B I B L I O G R A P H Y

1. van der Pol, B., "The Non-Linear Theory of Electric Oscillations," Proc. I.R.E., 22(1934), 1051-1086.
2. Edson, W. A., Vacuum-Tube Oscillators, New York: John Wiley, 1953.
3. Lienard, A., "Etude des oscillations entretenus," Rev. gen. elec., 23(1928), 901-946.
4. le Corbeiller, Ph., "The Nonlinear Theory of the Maintenance of Oscillations," J.I.E.E., 79(1936), 361-368.
5. Hsia, Miss Pei-Su, "A Graphical Analysis for Non-Linear Systems," Proc. I.E.E., (London), 99, Pt. 2 (1952), 125-134.
6. Boland, R. N., "Analysis of Nonlinear Servos by Phase-Plane-Delta Method," Jour. of Franklin Inst., 257(1954), 37-48.
7. Ku, Y. H., "Nonlinear Analysis of Electro-Mechanical Problems," Jour. of Franklin Inst., 255(1953), 9-31.
8. Stoker, J. J., Nonlinear Vibrations, New York: Interscience Publishers, 1950.
9. Adler, R., "Locking Phenomena in Oscillators," Proc. I.R.E., 34(1946), 351-357.
10. Huntoon, R. D., and A. Weiss, "Synchronization of Oscillators," Proc. I.R.E., 34(1947), 1415-1423.
11. van Slooten, J., "Mechanism of the Synchronization of LC Oscillators," Philips Tech. Rev., 14(1953), 292-297.
12. Dwight, H. B., Tables of Integrals, Revised Edition, New York: Macmillan, 1947.
13. Jones, W. B., Jr., Synchronized Oscillators with Frequency Modulated Synchronizing Signals, (Unpublished Thesis), Georgia Institute of Technology, Atlanta, Georgia, 1953.
14. Cuccia, C. L., Harmonics, Sidebands, and Transients in Communications Engineering, New York: McGraw-Hill, 1952.
15. van der Pol, B., "Frequency Modulation," Proc. I.R.E., 18(1930), 1194-1205.
16. Corrington, M. S., "Variation of Bandwidth with Modulation Index in Frequency Modulation," Proc. I.R.E., 35(1947), 1013-1020.
17. Scarborough, J. B., Numerical Mathematical Analysis, Menasha, Wisconsin: George Banta Publishing Co., 1930.
18. Hewlett-Packard Journal, Nos. 3-4, Volume 5, November-December, 1953, Hewlett-Packard Co., Palo Alto, California.



## V I T A

Donald Woodrow Fraser was born in Manchester, Iowa on May 22, 1910. He was educated in the public schools of Montrose, Pennsylvania and was graduated from high school in 1927. He presently resides in Atlanta, Georgia, is married and has one child.

He enlisted in the U. S. Navy in 1928 and in 1930 was appointed from the fleet as a Midshipman in the U. S. Naval Academy. He was graduated from that institution in 1934 with the degree of Bachelor of Science. He served his active Navy affiliations soon thereafter and joined the staff of the Admiral Farragut Academy, Pine Beach, New Jersey. At the outbreak of World War II he was recalled to duty, was trained in electronics at Harvard University and M.I.T. and thereafter served as an electronics field engineer.

Upon release from active duty in 1946 he joined the faculty of the Georgia Institute of Technology, serving as an instructor while procuring the degree of Master of Science in Electrical Engineering and as Assistant Professor of Electrical Engineering and Research Associate at the Engineering Experiment Station thereafter.

In 1950, at the outbreak of the Korean War, he was again called to duty and served with the rank of Commander in the Navy's developmental and testing force, the Operational Development Force. Upon release to inactive duty he resumed his duties and graduate studies at the Georgia Institute of Technology.